CHARACTERIZATION OF MOLECULAR-LEVEL CHANGES DUE TO MICRORNA-125B EXPRESSION IN BREAST CANCER CELLS BY SPECTROSCOPIC AND CHEMOMETRIC ANALYSIS TECHNIQUES

A THESIS SUBMITTED TO
THE GRADUATE SCHOOL OF NATURAL AND APPLIED SCIENCES
OF
MIDDLE EAST TECHNICAL UNIVERSITY

BY

NİHAL ŞİMŞEK ÖZEK

IN PARTIAL FULFILLMENT OF THE REQUIREMENTS
FOR
THE DEGREE OF DOCTOR OF PHILOSOPHY
IN
BIOLOGY

OCTOBER 2015

Approval of the thesis:

CHARACTERIZATION OF MOLECULAR-LEVEL CHANGES DUE TO MICRORNA-125B EXPRESSION IN BREAST CANCER CELLS BY SPECTROSCOPIC AND CHEMOMETRIC ANALYSIS TECHNIQUES

submitted by **NİHAL ŞİMŞEK ÖZEK** in partial fulfillment of the requirements for the degree of **Doctor of Philosophy of in Biological Sciences Department, Middle East Technical University** by,

Prof. Dr. Gülbin Dural Ünver
Dean, Graduate School of **Natural and Applied Sciences** _____

Prof. Dr. Orhan Adalı
Head of Department, **Biological Sciences** _____

Prof. Dr. Feride Severcan
Supervisor, **Biological Sciences Dept., METU** _____

Assoc. Prof. Dr. Ayşe Elif Erson Bensan
Co- Supervisor, **Biological Sciences Dept., METU** _____

Examining Committee Members:

Prof. Dr. Cengiz Yakıcıer
Medical Biology Dept., Acıbadem University _____

Prof. Dr. Feride Severcan
Biological Sciences Dept., METU _____

Assoc. Prof. Dr. Sreeparna Banerjee
Biological Sciences Dept., METU _____

Assoc. Prof. Dr. Mayda Gürsel
Biological Sciences Dept., METU _____

Assist. Prof. Dr. Özgür Şahin
Molecular Biology and Genetics Dept., Bilkent University _____

Date: 15/10/2015

I hereby declare that all information in this document has been obtained and presented in accordance with academic rules and ethical conduct. I also declare that, as required by these rules and conduct, I have fully cited and referenced all material and results that are not original to this work.

Name, Last name: Nihal ŞİMŞEK ÖZEK

Signature :

ABSTRACT

CHARACTERIZATION OF MOLECULAR-LEVEL CHANGES DUE TO MICRORNA-125B EXPRESSION IN BREAST CANCER CELLS BY SPECTROSCOPIC AND CHEMOMETRIC ANALYSIS TECHNIQUES

Şimşek Özek Nihal
Ph.D., Department of Biological Sciences
Supervisor: Prof. Dr. Feride Severcan
Co-Supervisor: Assoc. Prof. Dr. A. Elif Erson Bensan

October 2015, 131 pages

MicroRNAs (miRNAs), are 22 nucleotides long, non-coding RNAs that control gene expression post-transcriptionally by binding to their target mRNA's 3' UTRs (untranslated regions). Due to their crucial roles in various important regulatory processes and pathways, miRNAs have been implicated in disease mechanisms such as tumorigenesis, metastasis and drug resistance when their expression is deregulated. Moreover, the regulatory roles of these micromanagers have been demonstrated in the metabolism of cancer cells. To date, a significant number of miRNAs and their target messenger RNAs (mRNAs) have been identified and verified. Since one miRNA can target many mRNAs, it is hard to delineate the roles of these molecules in etiopathogenesis and metabolism of cancers. Therefore, to uncover the global roles of these molecules in cancer, both experimental and data analysis methods are required. The current thesis study aimed to examine the alterations in the membrane dynamics, content and structure of molecules especially lipids of miR-125b expressing breast cancer cells compared to controls to obtain a more holistic view of how miRNA expression alters cells. miR-125b expression in breast cancer cell line systems was investigated since this is one the most down-regulated miRNAs in breast cancer. MCF7 and T47D cells stably transfected with miR-125b (MCF7-125b, T47D-125b)

and empty vector (MCF7-EV, T47D-EV) were studied. Global molecular changes and specifically the changes in cellular lipids were determined by Attenuated Total Reflectance Fourier Transform Infrared (ATR-FTIR) Spectroscopy. The alterations in membrane dynamics were identified by spin-labelling Electron Spin Resonance (ESR) spectroscopy. In addition to these techniques, to discriminate between EV and miR-125b transfected breast cancer cells, unsupervised chemometric analysis methods including principal component (PCA) and hierarchical cluster analyses (HCA) were applied to the infrared spectra. The spectral results revealed lower saturated and unsaturated lipids, RNA and protein content in both miR-125b transfected breast cancer cells relative to the EV cells. The amount of glycogen, cholesterol ester and triglyceride was found to be decreased in MCF7 cells but opposite results were obtained for T47D cells. The decreased membrane fluidity was acquired in MCF7 cells but for T47D cells an inverse result was obtained. The decline in phospholipid, sphingomyelin, phosphotidyl-choline, sphingolipid and sphingomyelin contents were also observed in both cell lines with miR-125b expression. Based on these alterations, both EV and miR-125b cells lines were discriminated successfully by PCA and HCA methods. Here, a novel approach was proposed to understand the global effects of miRNAs in cells. Potential applications of infrared spectroscopy coupled with chemometric methods are not only limited to research area. This kind of pioneer studies will shed light on the development of future diagnostic tools for deregulated miRNA expression in patient samples.

Keywords: miR-125b, breast cancer, molecular content, cell lipid, ATR-FTIR spectroscopy, ESR spectroscopy, PCA, HCA

ÖZ

MEME KANSERİ HÜCRELERİNDE MİKRORNA-125B İFADESİNİN MOLEKÜLER DÜZEYDE NEDEN OLDUĞU DEĞİŞİMLERİN SPEKTROSKOPİK VE KEMOMETRİK ANALİZ TEKNİKLERİ İLE KARAKTERİZASYONU

Şimşek Özek Nihal
Ph.D., Biyolojik Bilimler Bölümü
Tez Yöneticisi: Prof. Dr. Feride Severcan
Ortak Tez Yöneticisi: Doç. Dr. A. Elif Erson Bensan

Ekim 2015, 131 Sayfa

MikroRNA (miRNA)lar 22 nükleotit uzunluğunda kodlanmayan RNA molekülleridir ve hedef mRNAların 3' UTR (translasyon olmayan bölge) bölgelerine bağlanmak suretiyle post-transkripsiyonel gen ifadesini düzenlerler. Hücrede birçok farklı olayda ve yolakta önemli rolleri olması nedeniyle, ekspresyonlarında bozukluk olduğunda, tümoregenez, metastaz ve ilaç dirençliliği gibi hastalık mekanizmalarıyla ilişkili oldukları belirtilmiştir. Bununla birlikte, söz konusu mikromüdürlerin kanser hücre metabolizmasında düzenleyici rolleri olduğu gösterilmiştir. Bugüne kadar önemli sayıda miRNA ve hedef mRNAları tanımlanmış ve doğrulanmıştır. Tek miRNA bir çok mRNA'ya bağlanabileceğinden dolayı, bu moleküllerin kanser etiopatojenezi ve metabolizmasındaki rollerini açığa çıkarmak oldukça zordur. Bu yüzden, bu moleküllerin kanserdeki global rollerini açığa çıkarmak için hem deneysel hem de data analiz metodları gereklidir. Bu tez çalışmasında miRNA ekspresyonunun hücrelerde nasıl değişikliklere yol açtığını global seviyede belirleyebilmek için, kontrol grubuna göre, miR-125b ekspresyonuna bağlı meme kanseri hücreleri molekülllerinde özellikle lipitlerin içerik ve yapıları ile membran dinamiğinde meydana gelen değişimleri incelemek amaçlandı. miR-125b'nin meme kanserinde en çok ifadesi azalan

miRNAlardan biri olması nedeniyle, söz konusu miRNAnın ifadesi meme kanseri hücre hattı sistemlerinde araştırıldı. miR-125b (MCF7-125b, T47D-125b) ve boş vektörle (MCF7-EV, T47D-EV) transfekte edilmiş MCF7 ve T47D hücreleri ile çalışılmıştır. Global moleküler değişimler ve özellikle hücre lipitlerindeki değişimler Azaltılmış Total Yansıma Fourier Dönüşüm Kızıl Ötesi (ATR-FTIR) Spektroskopisi ile belirlendi. Membran dinamiğindeki değişimler spin etiketleme yöntemi olan Elektron Spin Rezonans (ESR) Spektroskopisi ile elde edildi. Bu tekniklere ilaveten, boş vektör ve miR-125b transfekte edilmiş meme kanseri hücrelerini birbirinden ayırmak amacıyla, hücre spektrumlarına Temel Bileşen Analizi (PCA) ile Hiyerarşik Kümeleme Analizini (HCA) kapsaayan gözetimsiz kemometrik analiz metotları uygulandı. Spektral sonuçlar miR-125b transfekte olmuş hücrelerde boş vektörle transfekte edilen hücrelere göre doymuş ve doymamış lipitler ile RNA ve protein içeriğinde azalma olduğunu gösterdi. MCF7 hücrelerinde glikojen, kolesterol ester ve trigliserit miktarında azalma bulunurken T47D hücrelerinde ise zıt sonuçlar elde edildi. MCF7 hücrelerinde membran akışkanlığında azalma elde edilirken, T47D hücrelerinde artma elde edildi. miR-125b ifadesine bağlı her iki hücre hattında da, fosfolipit, fosfatidilkolin, sifingolipit ve sifingomiyelin içeriklerinde azalış gözlendi. Bu değişimlere bağlı olarak, PCA ve HCA analiz yöntemleri ile boş vektör ve miR-125b transfekte hücreler birbirinden başarılı bir şekilde ayrıldı. Bu çalışma ile, hücrelerde miRNAların global etkilerini anlamak için yenilikçi bir yaklaşım önerildi. Kemometrik analiz yöntemleri ile birlikte kızılötesi spektroskopisinin potansiyel uygulamaları sadece araştırma alanları ile sınırlı değildir. Bu tarz öncü çalışmalar, hasta örneklerinde miRNA ifade bozukluğunun belirlenmesi için diyagnostik metotların geliştirimesine de ışık tutatacaktır.

Anahtar Kelimeler: miR-125b, meme kanseri, moleküler içerik, hücre lipiti, ATR-FTIR spektroskopisi, ESR spektroskopisi, PCA,HCA

Dedicated to my beloved husband and daughter,

Ersin ÖZEK and Bilge Sena ÖZEK

ACKNOWLEDGEMENTS

First and foremost, I would like to express my deepest appreciation to my supervisor Prof. Dr. Feride SEVERCAN for her endless support, patience motivation and immense knowledge. Without her inspiring guidance and encouragement, I couldn't have accomplished this thesis successfully.

I am also grateful to my co-supervisor Assoc. Prof.Dr. Elif ERSON BENSAN for her valuable suggestions and guidance.

I would also like to thank to my PhD Thesis Committee members Prof. Dr. Cengiz YAKICIER, Assoc. Prof. Dr. Sreeparna BANERJEE, Assoc. Prof. Dr. Mayda GÜRSEL and Assist. Prof. Dr. Özgür ŞAHİN.

I would like to express my special thanks to Ferhunde AYSİN, Rafig GURBANOV and Seher GÖK,Aslı ÖZDİLEK for their precious and endless help, concern,support and lovely attitude throughout the progress of my thesis.

I would like to extend my thanks to my friends in Lab-146, Nuri ERGEN, Dilek YONAR, Sherif ABBAS and Fatma KÜÇÜK for their great help, support and considerable advices.

I would like to give my deepest thanks to my husband Ersin ÖZEK and my daughter Bilge Sena ÖZEK for their endless patience, support and love during my all academic life.

Words failed me to express my appreciation to my mother Emine ŞİMŞEK and my sister Fatma ŞİMŞEK for their love, constant support, care and understanding throughout my life. I wouldn't be here without their encouragement. I dedicate this work to my family.

I would like to send my ultimate appreciation to my father, Yaşar ŞİMŞEK for the encouragement to follow my own path, and stipulating that I do my best for anything I should undertake. I believe that he is watching me and so proud of me.

TABLE OF CONTENTS

LIST OF TABLES

TABLES

LIST OF FIGURES

FIGURES

LIST OF ABBREVIATIONS

ATR	Attenuated Total Reflectance
ESR	Electron Spin Resonance
EV	Empty vector
HCA	Hierarchical cluster analysis
miRNA	microRNA
miR-125b	microRNA 125b
PCA	Principal component analysis

CHAPTER I

INTRODUCTION

1.1 MicroRNAs (miRNAs)

miRNAs are small non-coding, 19–24 nucleotide-long, phylogenetically conserved and single stranded RNAs and are reproduced from endogenous hair-pin shaped transcripts. They have crucial roles in many fundamental biological process such as apoptosis, differentiation, development etc. and regulate gene expression by binding to 3' untranslated region (UTR) of a target messenger RNA (mRNA) through limited or extensive their target base-pairing (Erson and Petty, 2008, Erson and Petty, 2009). This may result in the cleavage of target mRNA with subsequent degradation or translation inhibition.

Based on their genomic locations relative to exon and intron positions, they can be divided into four groups (Kim et al., 2009) (Figure 1):

1) Intronic miRNAs in non-coding transcripts: e.g. miR-15a~16-1 cluster-non-coding RNA gene, DLEU2.

2) Exonic miRNAs in non-coding transcripts: e.g. miR-155-non-coding RNA gene, *BIC*198.

3) Intronic miRNAs in protein-coding transcripts: e.g. miR-25~93~106b cluster- the DNA replication licensing factor MCM7 transcript.

4) Exonic miRNAs in protein-coding transcripts: e.g. miR-985 hairpin-exon of *CACNG8* mRNA.

A majority of miRNAs (approximately 80%) are placed in the intronic region of protein coding and/or noncoding transcription units (TU). On the other hand, 10 % are in the exonic region of non-coding TUs.

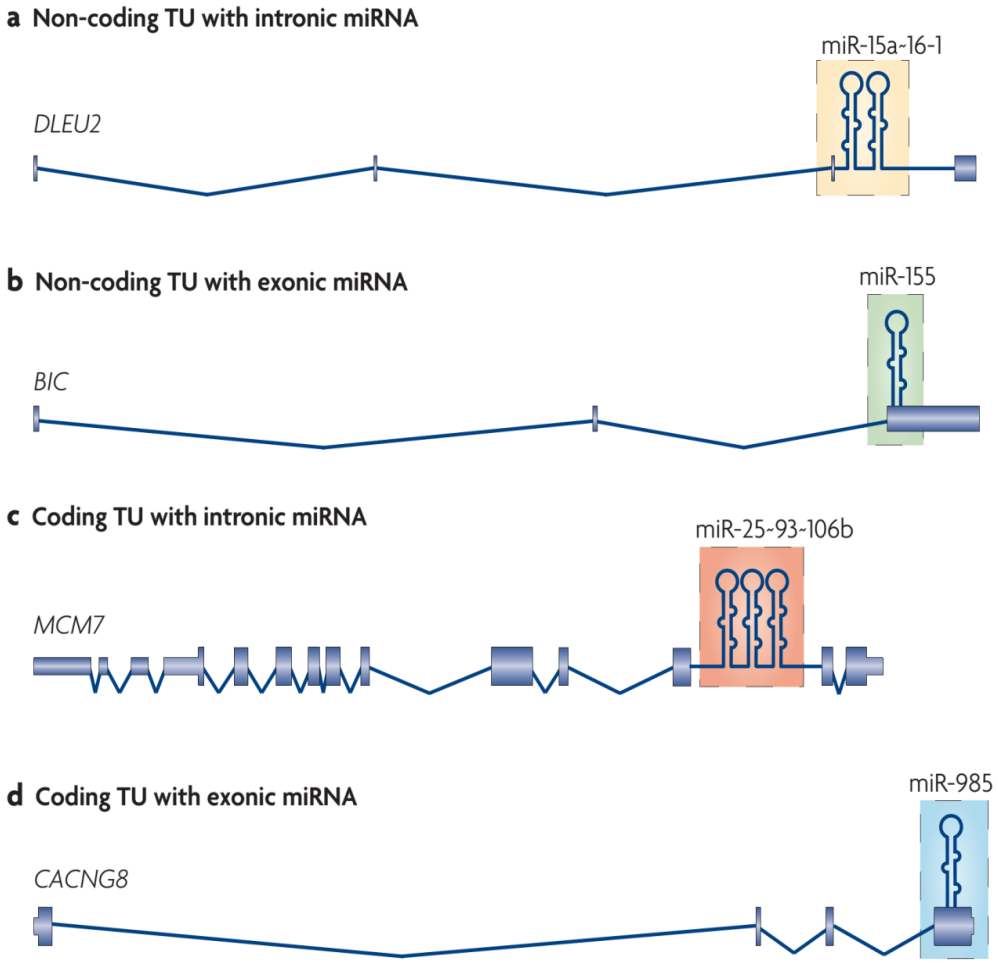

Figure 1 miRNA genomic location and gene structure. The hairpins: miRNA stem-loops. Blue box: protein-coding regions. TU: transcription unit (Taken from Kim et. al., 2009)

1.1.1 Biogenesis of miRNAs

miRNA biogenesis generally initiates with transcription from RNA polymerase II promoters and the mature miRNAs are produced by several processing steps through canonical or non-canonical miRNA biogenesis pathways (Figure 2).

In canonical pathway, miRNA genes are firstly originally transcribed as long primary-miRNA (pri-miRNS) by RNA pol II in the nucleus. The stem-loop portion of the pri-miRNA is cleaved by the microprocessor complex (DROSHA–DiGeorge syndrome critical region gene 8 complex [DGCR8; Pasha in *Drosophila melanogaster* and *Caenorhabditis elegans])* and 70-nucleotide precursor-miRNA (pre-miRNA) sequence is formed. This sequence contains a short stem plus a ~2-nt 3′ overhang. The nuclear export factor, exportin 5 (EXP5) and RanGTP dependent transporter protein, binds this overhang and so pre-miRNA is subsequently transported from nucleus to cytoplasm. In the cytoplasm, the second further cleavage of pre-miRNA occurs with the interaction of DICER-TRBP (TAR RNA-binding protein 2) and miRNA duplexes are formed. This duplex unwinds and one strand of it degraded. The other strand, as a mature miRNA, is loaded into Argonaute 2 (AGO2)-containing RNA-induced silencing complexes (RISCs). The mature miRNA leads RISC to cleavage of the mRNA, translational repression or deadenylation, depending on the degree of complementary sites between the miRNA and its target. Perfect or nearly perfect complementarities between miRNA and its target 3′ UTR induce RISC to cleave the target mRNA. Whereas imperfect base matching induces mainly translational silencing of the target but can also reduce the amount of the mRNA target (Garzon et al., 2006, Kim et al., 2009, Yekta et al., 2004).

Large majority of miRNA biogenesis occurs through canonical pathway, but recently the noncanonical biogenesis pathways have been also discovered; a) Microprocessor (DROSHA-DGRC8) independent, b) DICER independent and c) TUTase-dependent pathway. (Figure 1.3) (Ha and Kim, 2014, Li and Rana, 2014).

In microprocessor independent pathway, in the case of mirtrons, discovered in *Drosophila* and *C. elegans*, mature miRNAs are produced from short intrinsic hairpins with splice sites through mRNA splicing. After processing by the lariat-debranching enzyme, they refold into hairpin secondary (a short stem-loop) structures resembling pre-miRNAs. This structure is recognized by Exp5 protein and is transported cytoplasm and rejoins the canonical miRNA biogenesis pathway (Figure 3).

In the DICER independent pathway, for example, the biogenesis of miR-451, DICER are not required. The pre-miR-451 is directly loaded onto AGO2, cleaved and then it is trimmed by the 3′–5′ exonuclease poly (A)-specific ribonuclease PARN (Figure 3).

In Terminal uridylyl transferase (TUTase) - dependent pathway, the biogenesis of some pre-miRNAs carrying a shorter 3’ overhang(Li and Rana, 2014) (e.g.let-7 family in vertebrates) occurs since this shortness is suboptimal for efficient DICER processing. In this case, this type of pre-miRNAs are extended by one nucleotide monouridylation and then cleaved by DICER (Figure 3).

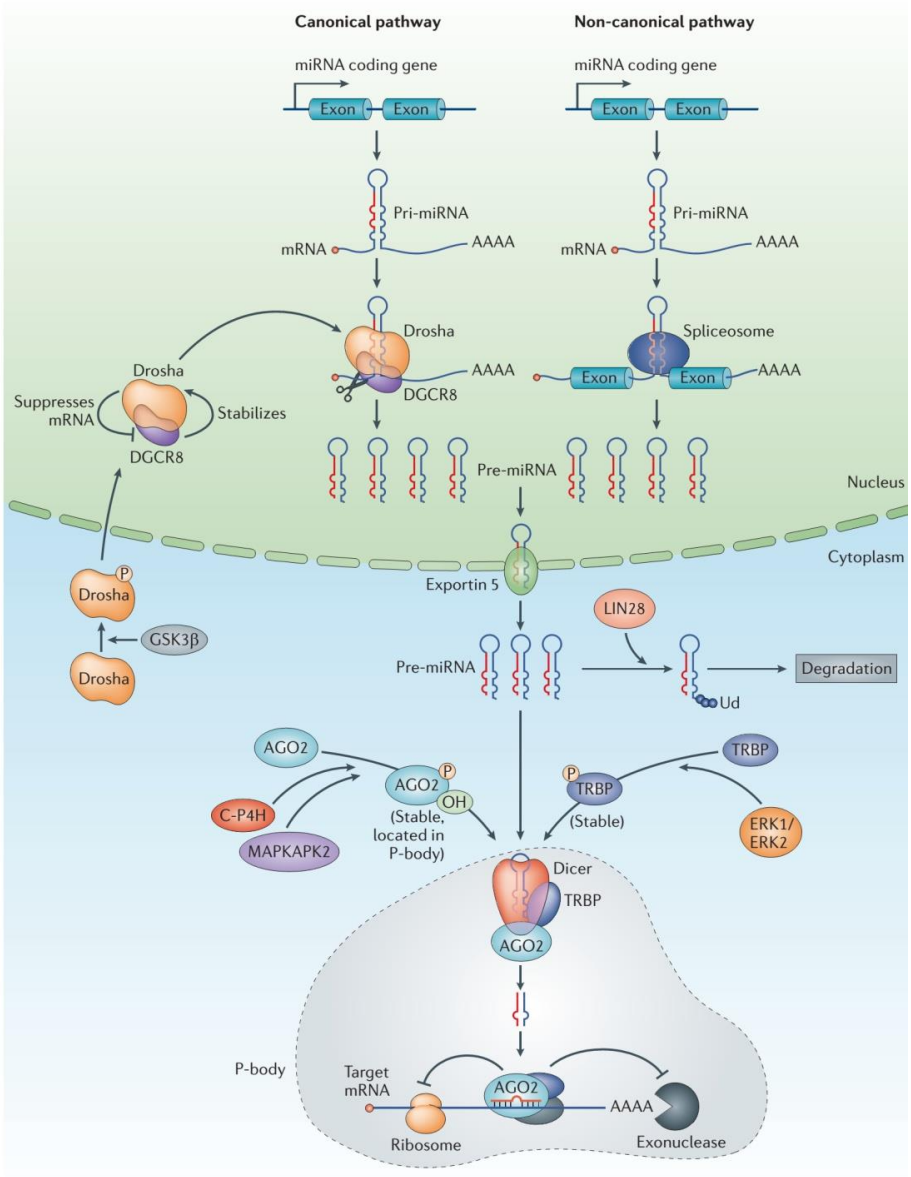

Figure 2 Canonical and non-canonical miRNA biogenesis pathways (Taken from Li and Rana 2014)

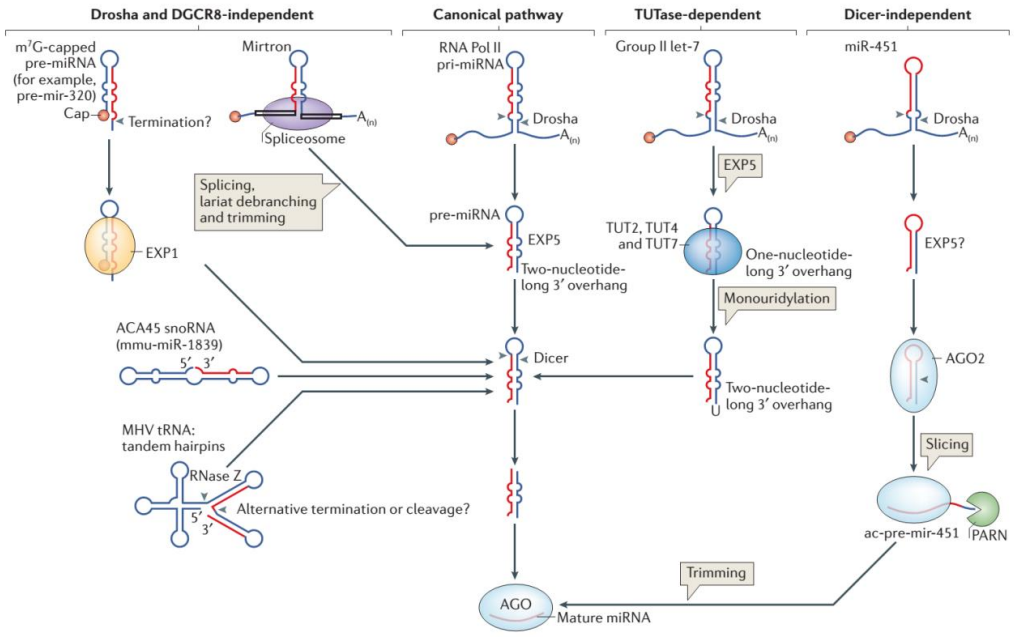

Figure 3 Non-canonical pathways of miRNA biogenesis (Taken from Ha and Kim, 2014).

1.1.2 The Regulation of miRNA Biogenesis

Since miRNAs have crucial roles in many cellular functions, stringent control of miRNA levels are required to keep normal cellular functions. Therefore their biogenesis and functions are tightly/intensely regulated at multiple levels, including their transcription level; their processing by DROSHA and DICER in the nucleus and cytoplasm; their loading onto Argonuate and their turnover (Ha and Kim, 2014, Kim et al., 2009, Krol et al., 2010, Siomi and Siomi, 2010).

Transcription is an important regulatory step in miRNA biogenesis. miRNA and the protein-coding gene promoters contain similar features in terms of CpG islands, TATA boxes, TFIIB recognition elements, initiator elements, and histone modifications so their transcriptions are coordinately regulated by the sets of transcription factors (Ozsolak et al., 2008). For instance, the tumor suppressor p53 activates the miR-34 cluster while oncogenic protein c-myc transcriptionally represses the miR15a clusters. Similar to the protein coding genes, miRNA genes can be regulated epigenetically

through the methylation of CpG islands at the promoter of miRNA genes and histone modifications (Davis-Dusenbery and Hata, 2010).

In addition to transcriptional regulation, miRNA genes can be regulated post-transcriptionally especially by DROSHA processing (cropping), DICER processing (dicing) and slicing events (Han et al., 2009). Cropping/microprocessing step is a crucial point in the regulation and therefore the expression level, activity and specificity of DROSHA and DGRC8 are strictly controlled. There is autoregulation between DROSHA and DGCR8. DGRC8 has stabilizing effect on DROSHA on the protein level while DROSHA destabilizes this protein by cleaving the hairpins in this protein mRNA which leads to its degradation (Han et al., 2009).(Davis et al., 2008, Fukuda et al., 2007) Moreover, the activities of DROSHA and DGCR8 are regulated by posttranslational modifications or association of accessory factors. For example, protein co-factors such as p68 and p72 can affect the Microprocessor activity through the mechanisms that may involve rearrangement of pri-miRNAs to increase DROSHA affinity (Davis et al., 2008, Fukuda et al., 2007).

In addition to the DROSHA cropping, there is a regulation on the nuclear export of miRNA in a cell-type-specific manner. Moreover, miRNA biogenesis can be regulated by dicing or DICER cleavage step through the control of DICER expression level and activity. For instance, depletion of DICER co-factors TRBP and PACT decreases DICER protein levels or the phosphorylation of RNA binding proteins (RBP) leads to an increase in DICER stability and miRNA production. LIN-28 binding to the terminal loop of pre-let-7 leads to block its processing by DICER (Heo et al., 2008).

Mature miRNA levels can further be regulated through the modulation of stability of the miRISC complex, nucleases that degrade miRNAs, and the abundance of their mRNA targets (Wada et al., 2012). The modulation of stability of the complex occurs by the regulation mechanism in the localization, function, and stability of Ago proteins since they are the core component of the miRISC complex. For example, phosphorylation at Ser387 of human AGO2 mediated by MAPK-activated protein kinase or AKT3 leads to its localization to P-bodies or translational repression (Zeng et al., 2008). Moreover, the phosphorylation of AGO2 by EGFR under hypoxia causes

to the dissociation of human AGO2 from DICER and the reduction of premiRNA processing for some miRNAs (Rüdel et al., 2010).

1.1.3 miRNAs in Cancer

Cancer is a multi-factorial, multi-step and complicated disease which can be originated from deregulation of both protein coding genes and non-coding gene expressions. The origin of this disease can be due to the misregulation of miRNA since they are the micromanager of the many cellular processes. Therefore abnormal expression of these molecules can result in the uncontrolled growth of cells, resulting in various kinds of cancers depending upon the type of miRNA or cells involved. The direct role of this molecules in human cancer was firstly demonstrated by Calin and his colleagues in 2002. They indicated that a small region encoding two miRNAs, *miR-15a* and *miR-16-1* (chromosome 13q14) was deleted in chronic lymphocytic leukemia (CLL), which suggested their role as tumor suppressor genes in CLL (Calin et al., 2002). Since then, many studies proved that the abnormal expression of miRNAs are commonly found in almost all types of cancers. According to these studies, miRNA can function as tumor suppressor or oncogenes. The tumor suppressor miRNAs are mainly down-regulated in cancers due to the genetic loss, epigenetic silencing, and defects in their biogenesis pathway or widespread transcriptional repression. They inhibit oncogenes and/or genes that inhibit cell differentiation or apoptosis. However, the oncogenic miRNAs are upregulated as a consequence of amplification or overexpression and they trigger the tumor formation by inhibiting tumor suppressor genes and/or genes that control cell differentiation or apoptosis. Since two decades, tumor suppressor and oncogenic potential of various miRNAs have been determined in different cancers. These studies demonstrated that miRNAs have crucial roles in all of the cancer hallmarks (Pichler and Calin, 2015) . The examples of miRNAs in these hallmarks are given in Figure.4.

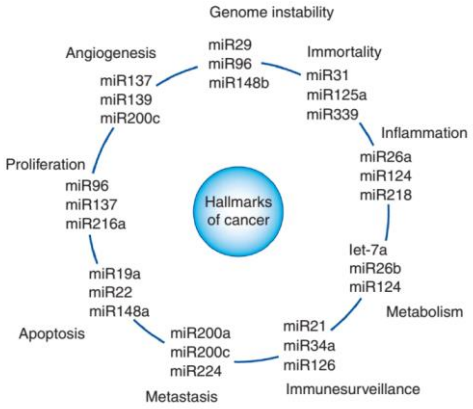

Figure 4 The role miRNAs in the hallmarks of cancer (Taken from Pichler and Calin et al 2015).

Although single miRNAs have tumor suppressor or oncogenic role, recent studies demonstrated the global downregulation of miRNA in tumor cells with respect to the normal tissues. This implies that the deregulation of their expressions may be due to the impairment of miRNA biogenesis especially in the expression miRNA processors (Zhang et al., 2015). The examples of deregulation of these processors in various cancer are summarized in Table 1.

Table 1 Deregulation of miRNA biogenesis machinery in cancers (Adapted from Lin and Gregory, 2015).

Protein	Deregulation	Cancer type	References
DROSHA	Upregulation	Cervical SCC	(Muralidhar et al., 2011)
		Triple-negative breast cancer	(Passon et al., 2012)
		Smooth muscle tumours	(Papachristou et al., 2012)
	Downregulation	Blader cancer	(Catto et al., 2009)
		Endometrial cancer	(Torres et al., 2011)
		Breast cancer	(Yan et al., 2012)
DGCR8	Upregulation	Oesophagel cancer	(Sugito et al., 2006)
		Bladder cancer	(Catto et al., 2009)
		Prostate cancer	(Ambs et al., 2008)
DICER1	Upregulation	Smooth muscle tumours	(Papachristou et al., 2012)
		Gastric cancer	(Tchernitsa et al., 2010)
		Oral cancer	(Jakymiw et al., 2010)
	Downregulation	Triple-negative breast cancer	(Avery-Kiejda et al., 2014)
		Bladder cancer	(Catto et al., 2009)
		BCC	(Sand et al., 2010)
		Nasopharyhgeal carcinoma	(Guo et al., 2012)
		Colorectal cancer	(Faber et al., 2011)
PACT	Upregulation	AK, SCC and BCC	(Sand et al., 2012)
XPO_5	Downregulation	Bladder cancer	(Catto et al., 2009)
AGO_1	Upregulation	AK, SCC and BCC	(Sand et al., 2012)
		Serous ovarian carcinoma	(Vaksman et al., 2012)
AGO_2	Upregulation	AK, SCC and BCC	(Sand et al., 2012)
		Serous ovarian carcinoma	(Vaksman et al., 2012)

AGO, Argonaute; AK, actinic keratoses; BCC, basal cell carcinoma; DGCR8, DiGeorge syndrome critical region 8; miRNA, microRNA; PACT, interferon-inducible double-stranded RNA-dependent protein kinase activator A; SCC, squamous cell carcinoma; XPO5, exportin 5.

The studies on miRNA expression profile in various cancer indicated that each cancer has a distinct miRNA expression profile which suggest the diagnostic and prognostic signatures of these molecules in cancer and even in its classification. For instance, the relationship between miR-135a and the poor prognosis in Hodgkin lymphoma have been reported in Navarro et. al. (2009) (Navarro et al., 2009). Moreover, the correlation between miR-21 expression level and advanced tumor stages in colorectal cancer has been shown (Schetter et al., 2012).

In addition to their diagnostic capability in cancer, the predictability of these molecules in the therapeutic/drug efficacy have been also demonstrated in several studies (Rothschild, 2014, Li and Rana, 2014). For instance, Scholl et. al., (2012) has demonstrated that there is an inverse correlation between miR-451 levels and BCR-ABL rearrangement in the diagnosis and treatment of chronic myeloid leukemia (CML). It was reported that the level of this rearrangement which is the characteristic of this disease, diminished with imatinib treatment (Scholl et al., 2012).

Although most clinical trial studies are based on the usage of miRNAs as biomarkers for patient stratification, prognosis, and drug efficacy, their therapeutic potential in cancer are under investigated(Wang and Wu, 2009, Thorsen et al., 2012). These potential have been established and tested in animals. According to these studies, there are two therapeutic approaches: restoring the expression of tumor suppressor miRNAs and blocking the function of oncogenic miRNAs. These approaches are demonstrated in Figure 5 (Alahari and Alahar, 2013).

In the first approach, to restore miRNA expression, synthetic miRNA mimics or miRNA expression vectors carrying a pre-miRNA sequence or an artificial miRNA hairpin sequence are commonly used. For example, Wiggins and coworkers have indicated that the intravenous delivery of miR-34a using lipid-based delivery vehicle leads to block tumor growth in mouse models of non-small-cell lung cancer (Wiggins et al., 2010).

The second therapeutic approach is based on decreasing the expression level or blocking the function of those oncogenic miRNAs. To block miRNA, there are two approaches: miRNA-sponge/antagomir and miRNA-mask. The sponge function as a

competitive inhibitor of miRNAs while the mask uses chemically modified antisense oligonucleotides perfectly complementary to miRNA binding sites of target mRNAs (Ebert et al., 2007).

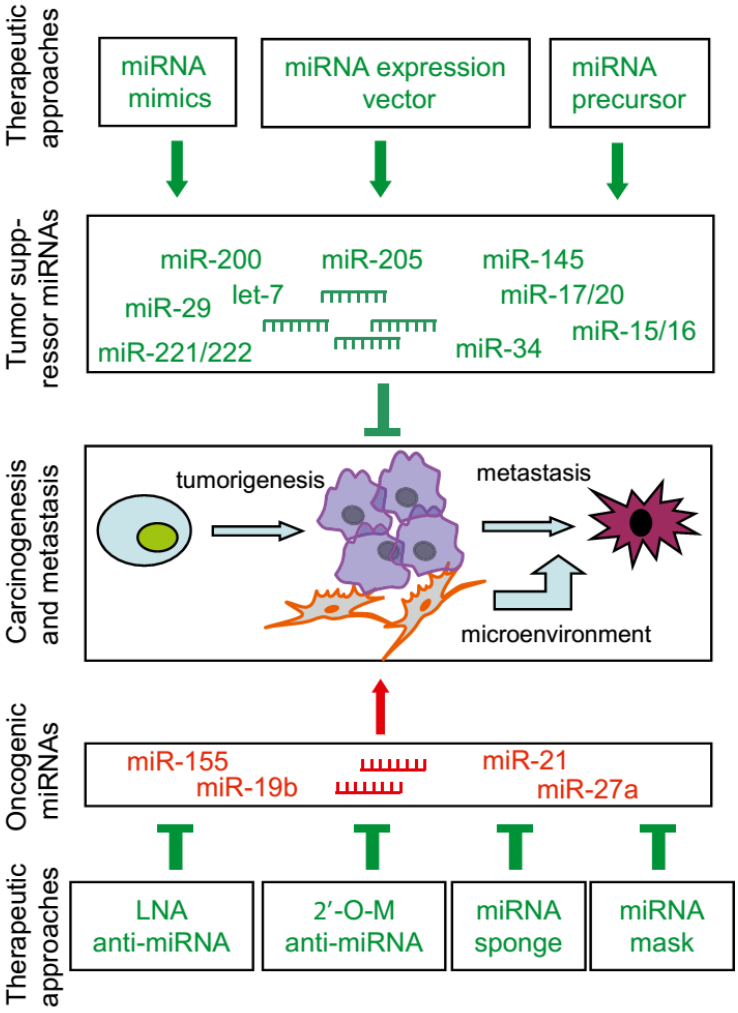

Figure 5 Theurapeutic approaches based on miRNA (Taken from Alahari and Alahar 2013).

1.1.4 miRNAs in Breast Cancers

Breast cancer is a heterogeneous and complex disease that results from the accumulation of various genetic defects. The role of miRNA deregulation in breast cancer have been firstly demonstrated by Iorio et al., (2005) by profiling of 245 miRNAs from76 breast tumor and 10 normal specimens. They indicated that 29 miRNAs were dysregulated in breast cancer as compared to the normal breast tissue. Among them *miR-125b, miR-145,* and *miR-10b* were found to be down-regulated while *miR-21* and *miR-155* were identified as up-regulated suggesting the tumor suppressor or oncogene roles of these miRNAs (Iorio et al., 2005). The later studies also indicated that miRNA profile can be used to classify the subtypes of breast tumors .For example, Blenkiron and colleagues has demonstrated that there is an association between let-7 family members and tumor subtype, ER status, and tumor grade (Blenkiron et al., 2007).

Since 2005, many studies have been performed to understand the role miRNA deregulation in breast cancer pathogenesis. The molecular mechanisms of this deregulation are not very well known yet. Moreover, miRNAs generally are located in cancer-related genomic regions or fragile sites (Calin et al., 2004). Zhang and colleagues proved that 73% of miRNA genes in breast cancer are located in the regions with DNA copy number abnormalities (Zhang et al., 2006).

Up to now, there are various miRNAs that have been identified as biomarkers and/or crucial regulators in both normal mammary and breast cancer development, as demonstrated in Figure 6 (Di Leva and Garofalo, 2014). The plenty of miRNA defined in breast cancer, indicated that they have great potential for development of original miRNA therapeutics.

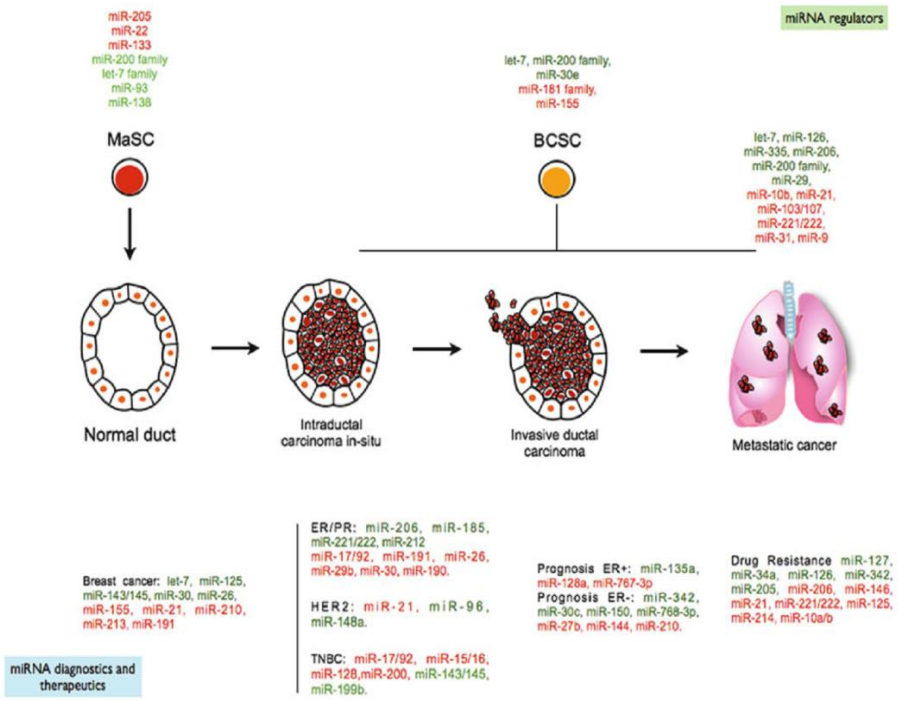

Figure 6 miRNAs involved in breast cancer progression (Taken from Di Leva and Garofalo, 2014).

1.1.5 miR-125 Family

miR-125 is a highly conserved miRNA implicated in cancer. The miR-125 family consists of three homologues: miR-125a, miR-125b-1 and miR-125b-2. miR-125a is placed on chromosome 19q13 which is close by miR-99b and let-7e. There are two mature miRNAs that are denoted as miR- 125a-3p and miR-125a-5p. They are derived from the 3' and 5' end of the pre-miRNA-125a, respectively. However, miRNA-125b is derived from two genes namely miR-125b-1 and miR-125b-2 which are located on chromosome 11q24 and 21q21, respectively. The chromosomal location, stem loop structures and seed sequences of miR-125 homologues are demonstrated in Figure 7 (Tsang, 2010). As can be seen from the figure, they have same seed region and very similar sequences. Therefore, they have same mRNA targets and carry out similar functions. However, their expression is different within different tissues that are abundantly in some endocrine organs and some neuronal tissues. Among these, miR-

125a was found to highly express in the spleen while miR-125b was shown to highly express in brain and ovaries, followed by the thyroid gland, pituitary gland, epididymis, spleen, testes, prostate, uterus, placenta and liver (www.microRNA.org).

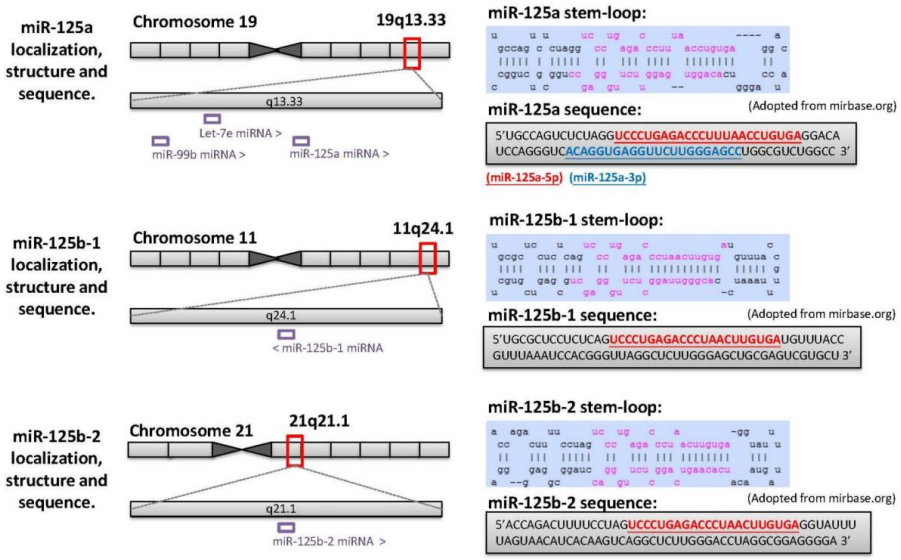

Figure 7 Localization, structure and sequence of miR-125a, miR-125b-1 and miR-125b-2. Red and blue underlined sequences represent seed sequences of miRNA (Taken from Tsang,2010).

Based on the previous studies, miR-125 family have many crucial roles in cellular processes by targeting many different transcription factors and matrix-metalloprotease growth factors. For instance, the regulatory role of both miR-125a and miR-125b were demonstrated in the neuronal differentiation and the pluripotency of embryonic stem cells by targeting lin-28 mRNA(Wu and Belasco, 2005). Moreover, the negative regulatory role of the miR-125b on p53 during embryonic development was shown by Le and colleagues (Le et al., 2009).

The deregulation of miR-125 family in different cancers has been reported in many studies. miR-125a has been reported to be down-regulated in various type of cancers such as colorectal cancer, breast cancer, gastric cancer, etc.(Xie et al., 2013, Nishida et al., 2011). In addition to their downregulation, the upregulation of miR-125b in different cancers such as leukemia, gastric and follicular cancer, pancreatic cancers

have been reported (Vriens et al., 2012, Bloomston et al., 2007, Bousquet et al., 2010). The referred studies imply that this miRNA family have tissue specific oncogenic and tumor suppressor potential which were summarized in detail in Figure 8 and Figure 9, respectively (Banzhaf-Strathmann and Edbauer, 2014).

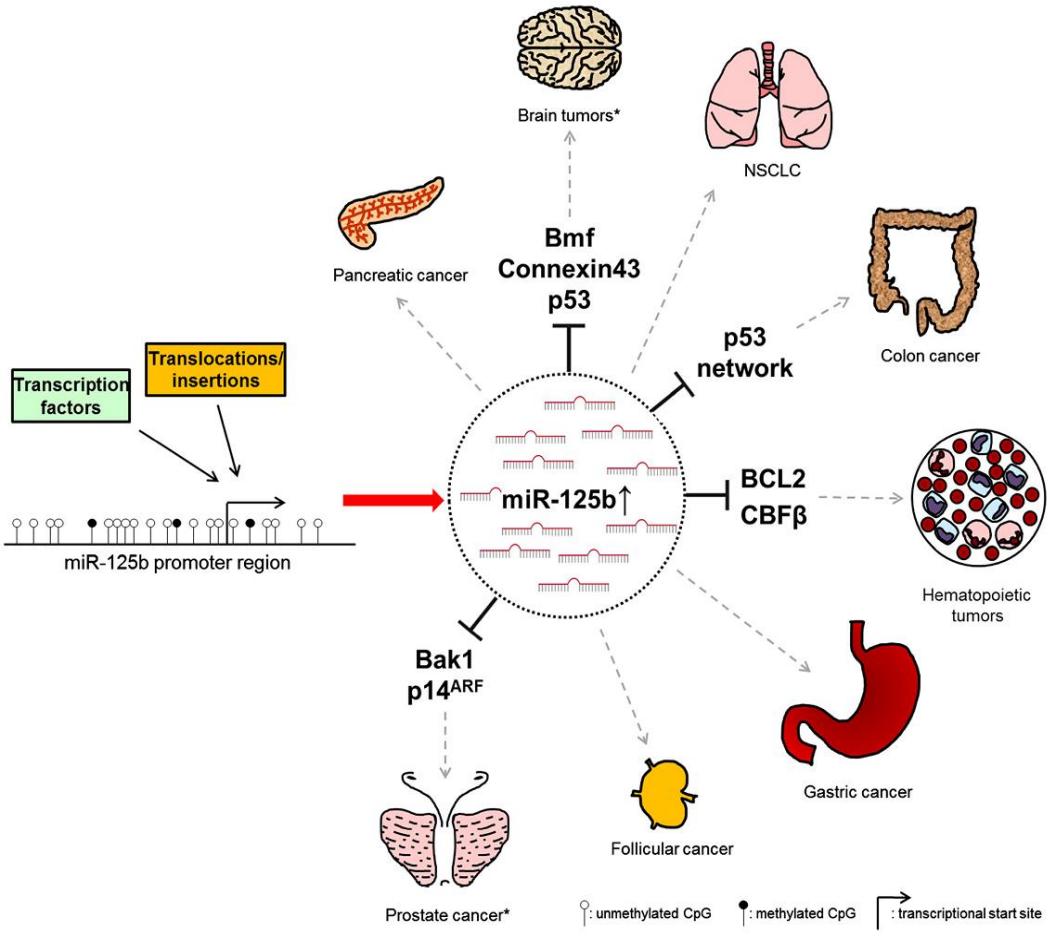

Figure 8 The oncogenic potential of miR-125b in cancer (Taken from Banzhaf-Strathmann and Edbauer, 2014).

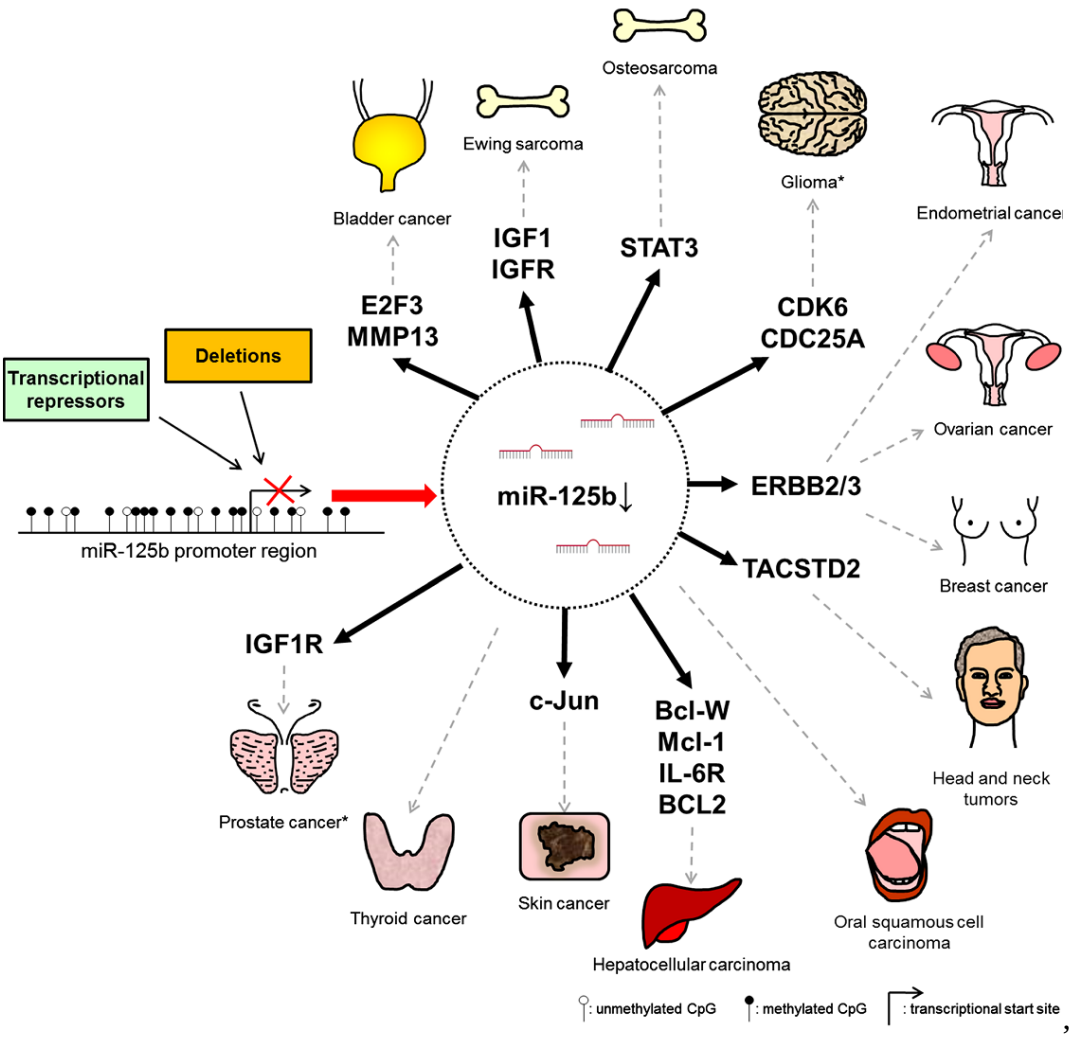

Figure 9 The tumor suppressor potential of miR-125b in cancer (Taken from Banzhaf-Strathmann and Edbauer, 2014).

1.2 Cancer Metabolism

To be able to carry out proliferation, cancer cells has to reprogram their metabolism. The earliest study related to cancer cell metabolism was performed by Otto Warburg indicated that cancer cells have dysregulated metabolism as comparison to the normal tissue. In this study, it has been demonstrated that cancer cells have enhanced aerobic glycolysis under molecular oxygen defect (Warburg, 1956). This theory is known as Warburg Effect. Since this claim, discoveries about cellular metabolism in cancer have

rapidly increased. In 2011, Hanahan and Weinberg suggested that the reprogramming energy metabolism is one of the hallmark of cancer cells (Hanahan and Weinberg, 2011).

During cancer development, to meet their energy requirement, cancer cells has to alter their metabolism. Therefore, they have perturbed metabolism that enables the accumulation metabolic intermediates as sources of cellular building blocks such as nucleic acids, proteins and lipids. For example, uptake of glucose is enhanced in cancer cells even in the abundance of oxygen. Moreover an increased glutamine metabolism/glutaminolysis is emerged in these cells (Dang, 2010). In addition to the glucose and glutamine metabolism, lipid metabolism is altered and enhanced lipid synthesis is observed in cancer cells (Currie et al., 2013). The detailed of this metabolism is demonstrated in Figure 10.

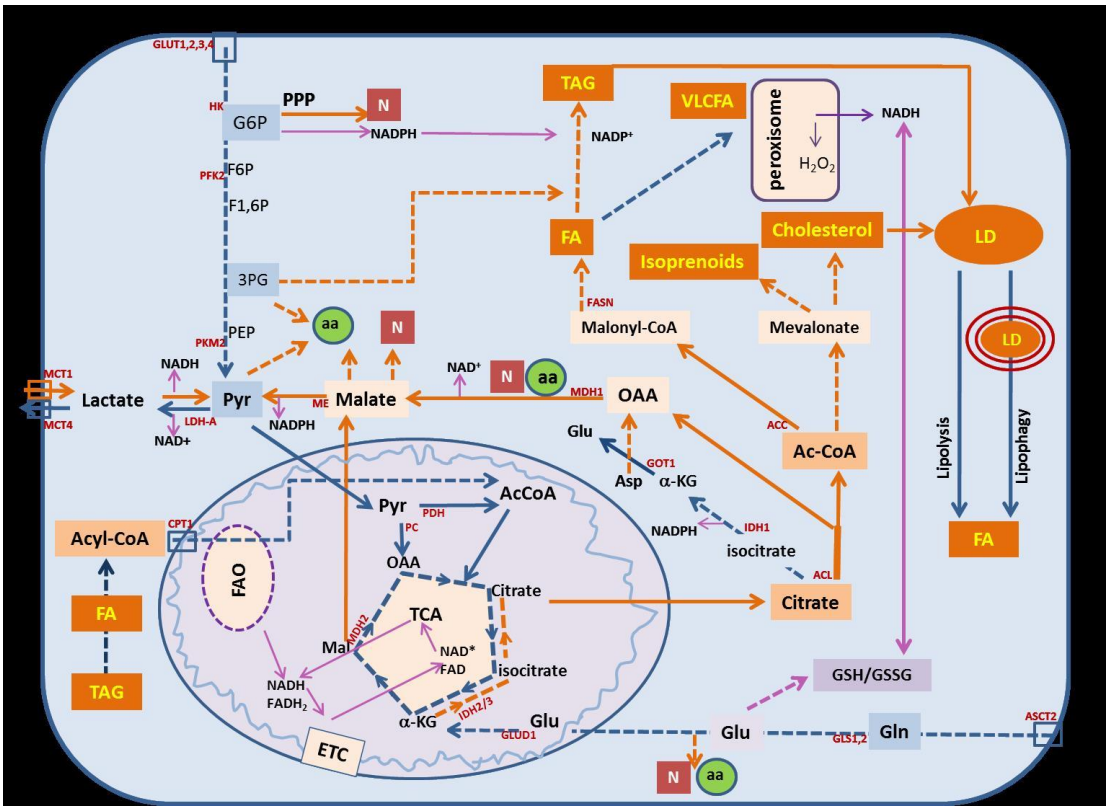

Figure 10 Summary of metabolic pathways altered in cancer: aerobic glycolysis, glutaminolysis, anaplerosis of TCA, mitochondrial oxidative phosphorilation, lipogenesis, cholesteroigenesis, lipolysis, lipophagy, fatty acid oxidation, redox homeostasis **(**Taken from (http://www.food.imdea.org/blog/2015/microtargeting-cancer-metabolism-opening-new-therapeutic-windows-based-lipid-metabolism#sthash.6hpkQQIZ.dpuf), 2015).

1.2.1 Role of miRNAs in Cancer Metabolism

Since miRNAs regulate the expression of many targets in cells, they also have a modulatory role in cellular metabolism.miRNA and metabolism link was recently discussed in (Chan et al., 2015, Chen et al., 2012, Tomasetti et al., 2014).

Many miRNAs have been reported to regulate glucose metabolism through the gene transcription and the expression of glucose transporters (GLUTs) and glycolytic enzymes(Fei et al., 2012, Liu et al., 2012). For example, the direct role of miR-195-5p in the expression of GLUT3 in bladder cancer has been demonstrated by Fei et al., (2012). In addition, transporter regulation, their role in the control essential enzymes

of glycolysis such as hexokinases and glyceraldehyde-3-phosphate dehydrogenase have been reported. For instance, the inhibition of glucose metabolism in breast and lung cancer through downregulation of HK2 by miR-143 has been indicated (Fang et al., 2012, Jiang et al., 2012).

Similar to glucose, miRNAs target the steps in the tricarboxylic acid (TCA) cycle. For instance, it has been demonstrated that miR-183 has a role in the regulation of isocitrate dehydrogenase 1 in glioma cells (Tanaka et al., 2013) and miR-378 also has a role in the regulation of the TCA cycle in breast cancer (Eichner et al., 2010).

The control of glutaminolysis by miRNAs has been also reported (Gao et al., 2009). In 2010, Hu and colleagues have demonstrated that p53 is a target of miR-125b, miR-30 and miR-504 and it has a regulatory role in maintaining glutamine levels (Hu et al., 2010) .

Recent studies have indicated that miRNAs have also essential role in lipid and aminoacid metabolism (Chan et al., 2015, Flowers et al., 2013). Tili et al., (2012) have reported that in chronic lymphocytic leukemia, miR-125b targets several metabolic enzymes such as phosphatidylcholine transfer protein (PCTP), lipase A (LIPA). (Tili et al., 2012).

The regulation of miRNAs in cancer metabolism is also through the regulation of signaling pathways such as p53, c-Myc. The relationship between miRNA and tumor suppressors and oncogenes is shown in Figure 11 (Gao, 2011). For instance, the p53 induced suppression of c-Myc expression by miR-145 has been reported (Sachdeva et al., 2009) and the targets of c-Myc in the glycolysis and oxidative phosphorylation such as LDHA GLUT1, HK2, PFKM, ENO1 expression have been also demonstrated (Shim et al., 1997).

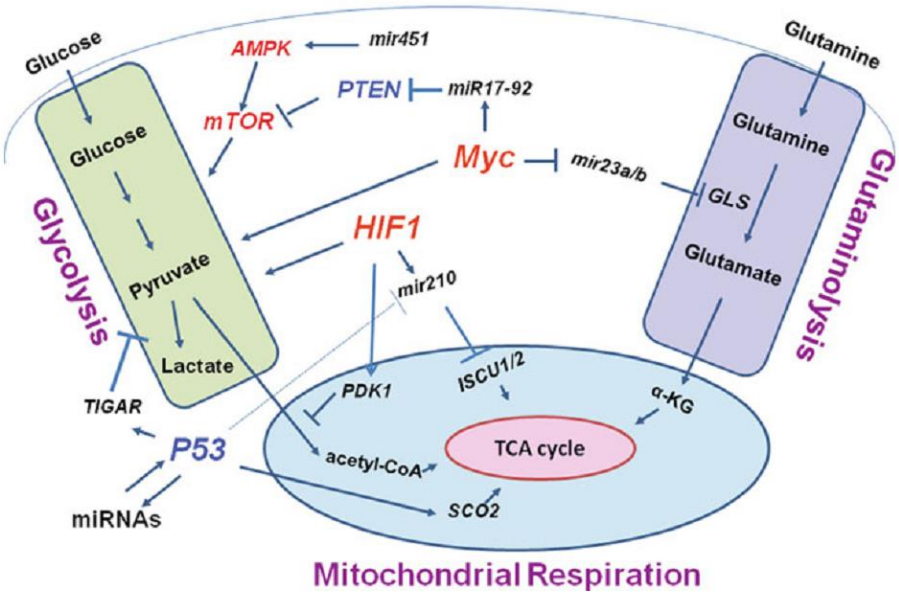

Figure 11 The role of miRNAs in cancer cell metabolism. The relationship between miRNAs and oncogenes (cMyc, HIF-1, mTOR, AMPK, etc, indicated in red), tumor suppressors (P53 and PTEN, indicated in blue) to glycolysis, mitochondrial respiration and glutaminolysis pathways of cancer cells are indicated (Taken from Gao 2011).

1.3 Spectroscopy

Spectroscopy describes the interactions between electromagnetic radiation and matter. This radiations, including light, has characteristics of waves and particles and is categorized due to the frequency of its wave.

Each "particle" of light/photon has a distinct amount of energy that can be transferred to a molecule. When matter interacts with electromagnetic radiation, it can transmit, absorb or reflect this radiations based on the energy levels of them. It has been known that the energy of the photons is related to the frequency (ν) and wavelength (λ) of the light as described in the two equations:

$$E: h\nu \text{ and } \nu = c/\lambda$$

*h:*Plancks's constant

c: speed of light

Therefore high energy radiation (light) will have high frequencies and short wavelengths.

The range of wavelength and frequencies in light is defined as electromagnetic spectrum and this spectrum includes the electromagnetic wave energies having wavelengths from thousands of meters, such as the radio waves, down to size lower than the angstrom for the gamma rays (Figure 12)(http://zebu.uoregon.edu).

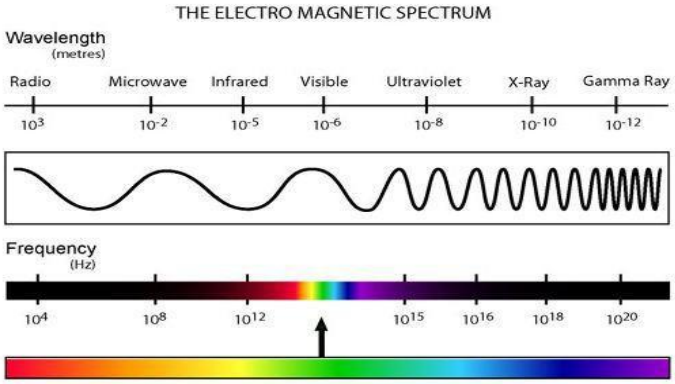

Figure 12 The spectrum of electromagnetic waves ranges from low-frequency radio waves to high-frequency gamma rays (Adapted from http://zebu.uoregon.edu).

Spectroscopy can be occurred due to the enery transfer between the photon and the sample. The samples of these technique and type of energy transfer are shown in Table 2.

Table 2 Examples of spectroscopic techniques (Retrieved from (http://www.asdlib.org/onlineArticles/ecourseware/Analytical%20Chemistry%202.0/Text_Files.html).

Spectroscopic Techniques		
Type of Enery Transfer	**Region of Electromagnetic Spectrum**	**Spectroscopic Technique**
Absorption	γ-ray	Mossbauer spectroscopy
	X-ray	X-ray absorption spectroscopy
	UV/Vis	UV/Vis spectroscopy atomic absorption spectroscopy
	IR	infrared spectroscopy raman spectroscopy
	Microwave	microwave spectroscopy
	Radio wave	electron spin resonance spectroscopy nuclear magnetic resonance spectroscopy
Emission (thermal excitation)	UV/Vis	atomic emission spectroscopy
Photoluminescence	X-ray	X-ray fluorescence
	UV/Vis	fluorescence spectroscopy phosphorescence spectroscopy atomic fluorescence spectroscopy
Chemiluminescence	UV/Vis	chemiluminescence spectroscopy

1.3.1 Infrared Spectroscopy

This spectroscopic techniques use IR light which covers the wavelengths range from approximately 0.7 μm to 1 mm. They can be divided in three regions: the near-, mid- and far- infrared, named after their relation to the visible spectrum (Smith, 1998).

Region	Wavenumber range (cm^{-1})	Wavelength (μm)
Near	14000-4000	0.8–2.5
Middle	4000-400	2.5–25
Far	400-4	25–1000

When infrared radiation interacts with matter, radiation is absorbed and leads to the excitation of molecules into the higher vibrational levels and chemical bonds vibrate at characteristic frequencies and different modes such as the stretching and bending etc. The examples of these mode of are demonstrated CH_2 molecules in Figure 13 (Marcelli et al., 2012). A molecule or a bond must have a dipole moment in order to be IR active.

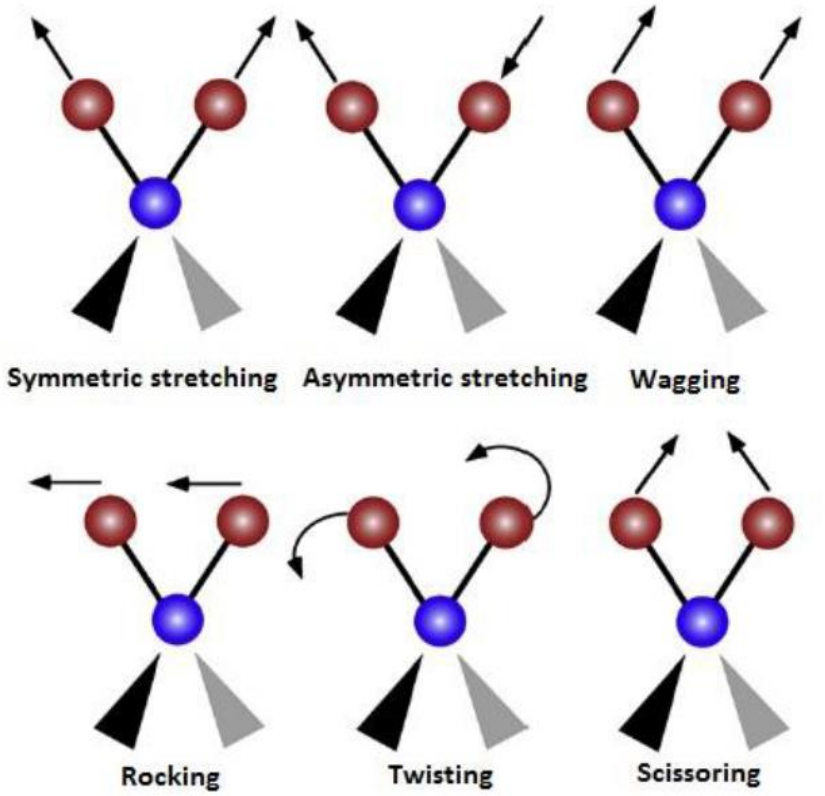

Figure 13 The vibrational modes associated to a molecular dipole moment change detectable in an IR absorption spectrum (Taken from Marcelli et. al., 2012).

Since each sample can absorb specific characteristic infrared wavelength due to its molecular structure, IR spectroscopy can be successfully used to detect subtle changes in biomolecules. Any pathological, physical or physiological changes in the molecule alters biochemical constituents of biological systems. Therefore this technique enables to identify chemical bonds and functional groups of cells or tissues which eventually leads to the monitoring of molecular changes including proteins, carbohydrates, lipids and nucleic acids (Diem et al., 2008).

1.3.1.1 Fourier Transform Infrared Technology

FTIR spectrometer is based on the Michelson Interferometer which uses the beam splitter for taking the incoming IR light and dividing it into two optical beams. Then one beam goes to a fixed flat mirror while the other one goes to a moving flat mirror which moves a few millimeters away from the beam splitter. Two beams recombine at the beam splitter after reflection (Figure 14). These two beams interfere with each other and the resulting signal is called as interferogram. Data points that compose the signal in an interferogram, has information about each infrared frequency from the origin. In other words, when an interferogram is measured, all the frequencies are simultaneously measured, too. By measuring the interferogram, all the frequencies are being measured simultaneously this gives the advantage of highly fast measurements. Fourier transformation is a mathematical function, enables to convert an interferogram into an intensity-versus-frequency spectrum. This conversion is performed by a computer and a plot of intensity against frequency (cm^{-1}) is presented for further analysis (Figure 14).

Prior to collection of sample spectrum, a background spectrum is collected for relative scaling of absorption intensity. Then this background spectrum is compared with the spectrum of the sample of interest to determine the “percent transmittance” and to remove the instrumental characteristics and finally to get pure spectrum where all the signals are due to the sample.

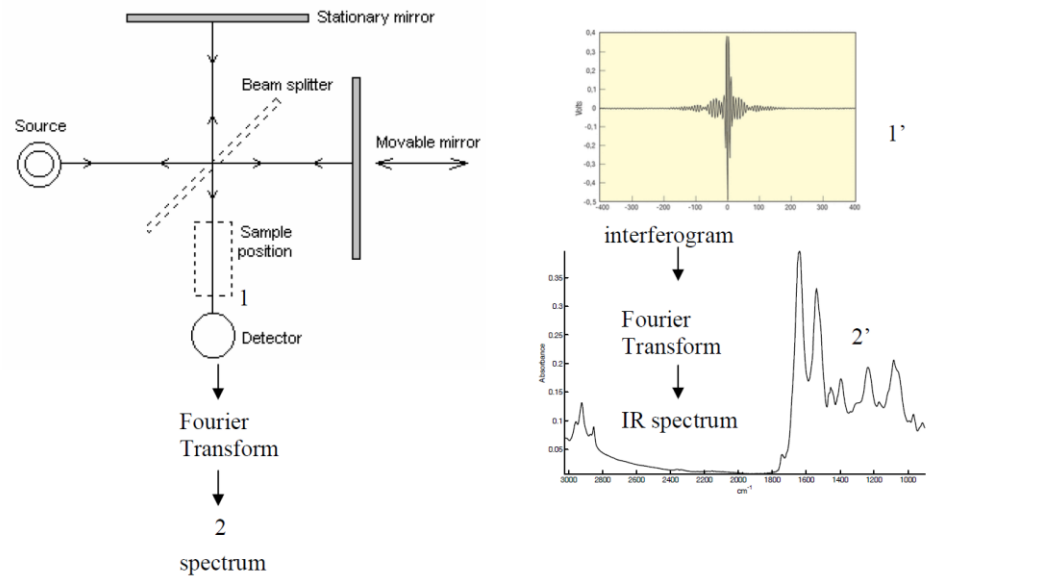

Figure 14 Basic principles of FTIR spectrometer (Taken from Gasper, 2010).

As comparison to the other bioanalytical techniques FTIR spectroscopy have several advantages given in detail Table 3. Due to these advantages, it became a powerful and sensitive tool used by many scientific groups over world to record fingerprints of complex mixtures such as biological samples and to identify biochemical and structural alterations in molecules of different biological systems (Kazarian and Chan, 2006, Goormaghtigh et al., 1999, Baker et al., 2014, Derenne et al., 2011, Gasparri and Muzio, 2003, Di Giambattista et al., 2011, Movasaghi et al., 2008, Levin and Bhargava, 2005, Severcan et al., 2010, Severcan and Haris, 2012, Turker et al., 2014b, Turker et al., 2014a, Ozek et al., 2014, Sen et al., 2015, Severcan et al., 2005, Cakmak et al., 2006, Diem et al., 2008).

Table 3 The advantages of FTIR spectroscopy

Speed	Spectra can be collected in seconds instead of minutes because of the simultaneous measurements of the all frequencies (known as "Felgett Advantage") (Diem et al., 1999).
Sensitivity	FTIR has an improved sensitivity since the higher sensitivity of the detectors and the higher optical throughput (known as "Jacquinot Advantage") that results in lower noise levels (Stuart, 1997)The higher sensitivity allows getting infrared spectra in a high quality from as low as few micrograms sample amounts .Moreover, samples can be investigated in diverse physical states; solids, liquids and gases.
Non-disturbing	It is a non-disturbing technique which provides structural and functional information about the sample (Dogan et al., 2007).
Mechanical simplicity	Mechanical breakdown is a very small possibility since the only moving part of the instrument is the moving mirror.
Internally calibrated	FTIR spectrometer is self-calibrating and uses a HeNe laser which is called as "Connes Advantage".

1.3.1.2 Attenuated Total Reflection Mode in FTIR Spectroscopy

Generally, the spectra of sample are collected in transmission mode. In this mode the IR beam (I0) passes through the sample and the transmitted beam (I) is analyzed. (Figure 15.A). In addition to this, sample spectra are recorded within reflectance mode. However, recently, using the reflection mode has become popular. This technique is called Attenuated Total Reflection (ATR)-IR spectroscopy. One of the basis of this technique is that the refractive index of ATR crystal must be remarkably greater than the index of sample. The second one is that the good contact between the sample and

crystal should be achieved. To able to create higher refractive index, the materials with high refractive index are used for ATR crystal e.g.diamond, amorphous material transmitting infrared (AMTIR), germanium and silicon, zinc selenide (ZnSe) (Kazarian and Chan, 2006).

In ATR mode, IR beam is directed into crystal with high refractive index called also internal reflection element (IRE). In this element, some internal total reflections are occurred depending on its length, until the beam comes out and reaches the detector. When IR beam hits the surface of crystal, electric part of the electromagnetic beam, known as evanescent wave, gets out and interacts with the sample at the crystal-sample surface. This wave extends into the sample which is placed onto the crystal up to 0.5µ to 5µ. Evanescent wave is being attenuated when the sample absorbs the related spectral energy. Then attenuated energy is passed back to the IR beam and leaves the crystal from opposite end and finally reaches the detector to generate the infrared spectrum (Figure 15 B) (Goormaghtigh et al., 1999, Gasper, 2010).

Similar to FTIR spectroscopy, ATR-FTIR provides rapid, sensitive and simultaneous monitoring of different functional groups of molecules in the biological systems. Other advantages, such as small sample size and ease of sample preparation, make this technique a good candidate for biological studies. The samples can be directly investigated without any preparation processes by placing them on the ATR-crystals. In addition, ATR-FTIR studies are not affected by the sample thickness.

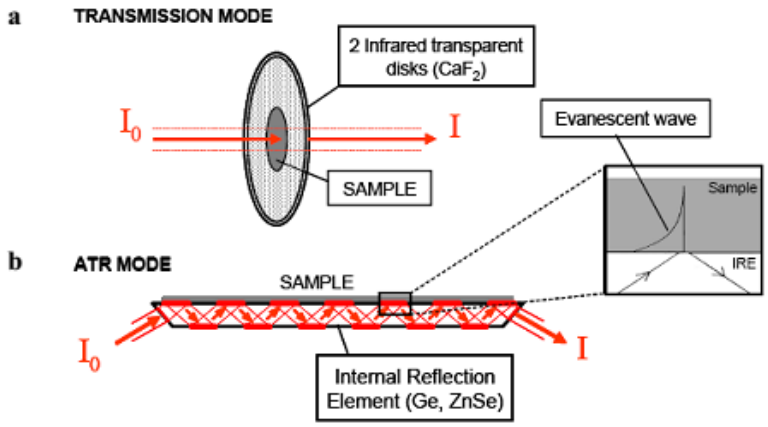

Figure 15 The comparison between transmission and ATR mode in IR spectroscopy (Taken from Gasper et. al., 2010).

1.3.1.3 Infrared Spectroscopy on Cells and Tissues

Since IR spectroscopy has ability to monitor different molecules without causing any perturbation in the systems, it is an excellent method to be applied to biological samples. Therefore its utility for the nondestructive analysis of biological specimens has been continuously and rapidly increasing within recent years. A typical IR spectra of breast tissue section and their spectral bans assignments are demonstrated in Figure 16. As can be seen from the figure, spectra contains many spectral bands arising from different molecules (Baker et al., 2014). By performing qualitative and quantitative analysis of these bands, information related to the biomolecular composition and dynamics of the sample can be obtained easily. For examples, the analysis of spectral bands in the C-H stretching region including saturated and unsaturated lipid associated bands, lipid content, fluidity and order (acyl chain flexibility) information can be obtained at membrane, cell and tissue levels. Moreover, the fingerprint region (1800-650 cm^{-1}) contains sample specific spectral bands arisen from protein, lipid, carbohydrate and nucleic acid (Severcan and Haris, 2012).As can be deduced from the figure, IR cell/tissue spectrum represents the sum of all the individual component spectra, weighted with respect to their abundance in the cell (Baker et al., 2014) .

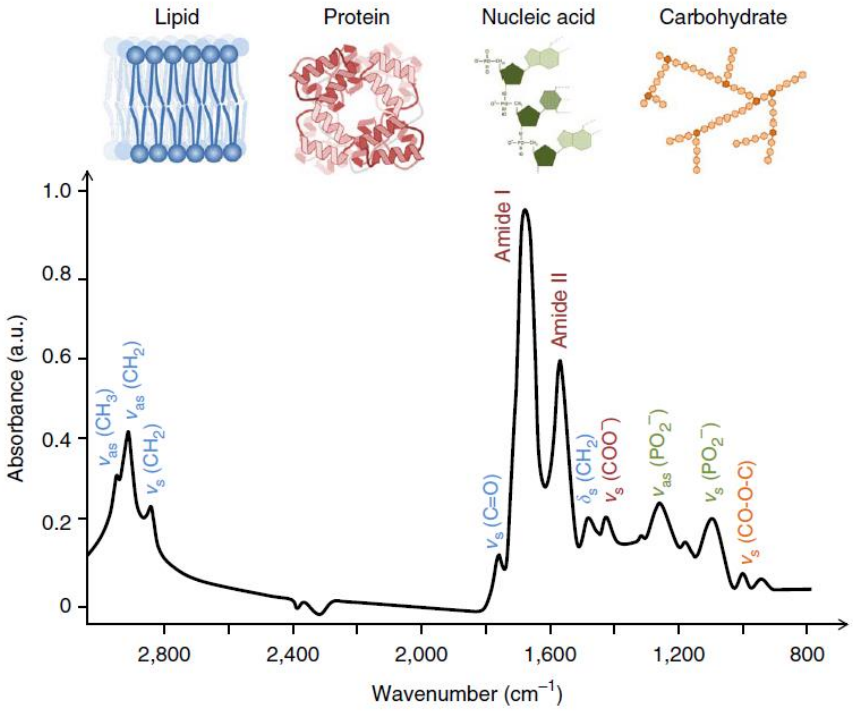

Figure 16 Typical biological spectrum showing biomolecular peak assignments from 3000–800 cm $^{-1}$, where ν = stretching vibrations, δ = bending vibrations, s = symmetric vibrations and as = asymmetric vibrations. The spectrum is a transmission-type micro-spectrum from a human breast carcinoma (Taken from Baker et. al.,2014).

Since more than three decades, IR spectroscopy has been commonly used to extract biochemical information of cells within different conditions These studies indicated that, this method can be used in the discrimination of premalignant cells from malignant cells, the assessment of apoptosis in cancer/other cells after anticancer drug/chemical agent treatment and the monitoring and classification of anticancer drug effects and so on (Derenne et al., 2011, Gasparri and Muzio, 2003, Di Giambattista et al., 2011, Movasaghi et al., 2008).

1.4 Electron Spin Resonance (ESR) Spectroscopy

Electron Spin Resonance (ESR) spectroscopy, also referred to as Electron Paramagnetic Resonance (EPR) spectroscopy, is a versatile, nondestructive and powerful analytical technique based on the absorption of microwave radiation in presence of an applied field by paramagnetic species. The unpaired electrons in any system can be detected which gives information about structure and dynamic of the system occurred during chemical or physical reactions. Therefore it is widely used in different application areas as itself or complementary techniques to other analytical methods.

Most of the biological samples do not contain unpaired electron whose spin transitions does not give rise to an ESR signal. Therefore, the use of extrinsic probes called spin label are required to able to obtain ESR signal in these samples. Most popular labels are nitroxide derivatives with a stable unpaired electron and a functional group for specific attachment to a molecule of the system under study(Severcan and Cannistraro, 1988) and they have been widely used as spin labels in studies of biological membranes and model membrane systems (Thomann et al., 1984). Since these spin labels are specifically incorporated into membranes, the information about the different region of the membrane can be acquired. Among these labels 16 doxyl stearic acid is one of the commonly used spin labels to obtain information about membrane fluidity of the system. This label comprises a nitroxide free radical attached to the 16-carbon position of an 18-carbon fatty acid chain (Fig 17). Perpendicular to the bilayer normal, the nitroxide ring includes an unpaired electron in the nitrogen *p*-orbital parallel to the bilayer normal. Being near the end of the hydrocarbon chain, this spin probe reports dynamics of the inner membrane rather than the headgroup region.

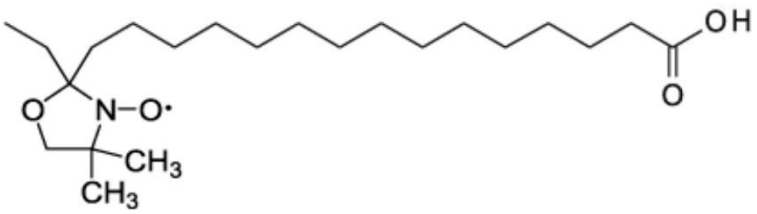

Figure 17 Structure of spin label 16-DSA. The nitroxide spin label (left end) is located at the 16-carbon position of the 18-carbon fatty acid chain.

By analysis of the line positions and line shapes of the bands in ESR spectrum within liquid solutions or liquid crystals, membranes, solids, the information about the rate of motion of the label, the structure, order, viscosity, polarity of the system can be obtained. It has been known that relative anisotropy directly related to the rotational mobility of the spin label which can be correlated with the probe microenvironment under investigation. Therefore the change in its mobility allows to study the membrane fluidity and often yields useful information on the dynamic state of membrane phospholipids in different biological sytems (Deo and Somasundaran, 2002).

1.5 Chemometrics in Biospectroscopy

Chemometrics are the application of statistical and mathematical tools to extract the chemically relevant information from the chemical data of vibrational spectroscopy (Lavine, 2000). Since, vibrational spectra contains many molecular-associated spectral bands, they are very information-rich. Therefore, to able to acquire meaningful data from spectra of different samples, the necessity of multivariate data analysis are inevitable over univariate analyses techniques. Multivariate analysis methods are divided into two groups; unsupervised/supervised chemometric approaches and multivariate calibration methods, respectively. The first approaches are commonly used for qualitative identification/classification of studied groups. The second method is used for quantitative measurements of metabolites in the studied system (Brereton, 2003).

In unsupervised chemometric approaches, there is no need for priori information about studied samples like healthy vs disease while in supervised ones, this information is required. Therefore, clustering pattern of the samples are obtained randomly. However, in supervised approach, this pattern is created based on the training set of samples with known categories. Then the power of method is evaluated by testing the samples with respect their classification predictions (Massart et al., 2003).

Among the unsupervised methods, principal component analysis (PCA) and hierarchical cluster analysis (HCA) are widely used. Principal Component analysis (PCA) are chosen in spectroscopy for decoding the spectra containing overlapping regions (Levin and Bhargava, 2005) enabling the identification of which characteristics or which combinations of characteristics vary most between individuals. It is a powerful dimension-reduction technique Thus, PCA is employed to reduce dimensionality and generate a visualization of data (fairly similar to clustering). In this methods, two types of plots are obtained: score and loading plots. Score plots are used to indicate relationship studied groups while loading plots are used to indicate the degree of contributions of spectral variations among sample groups. Both loading and score plots are created based on the principal components (PCs). PCs can be ranked according to the magnitude of variance captured by each corresponding PCA factor. Usually, the first 3 PCs contain up to 99% variance. The advantage of PCA lies in the fact that it is an unbiased technique in the sense that no information about the classes is inputted into the algorithm, resulting in a representation of the true variability within the data (Severcan and Haris, 2012).

Another unsupervised technique is HCA. Cluster analysis is applied to observe whether there is discrimination or not between sample groups. Samples are grouped based on their characteristic specificities. Similar samples tend to be classified in a same group in the clustering which can be shown as a dendrograms. Ward's algorithm is commonly used and the distances between groups are created by Euclidean Distance value. In dendogram, differences between the clusters are indicated with heterogeneity values. In data analysis, primarily usage of techniques like PCA, can be useful for the determination of general relationship web among data. However, cluster analysis must

be performed if one wants to show grouping of similar data gathered from different samples (Severcan et al., 2010, Severcan and Haris, 2012).

Among supervised approaches, there are several differences. For example, in linear discriminant analysis (LDA) discrimination is focused while in soft independent modelling of class analogy (SIMCA), similarity within a class is emphasized. Another difference is being linear and non-linear methods like neural methods. The last difference is divides the parametric and non-parametric computations (Danzer et al., 2013).

Prior to chemometric analysis, to be able to reproducible and accurate data, spectra are preprocessed. Preprocessing generally composed of baseline correction, normalization and cutting as indicated in Figure 18.

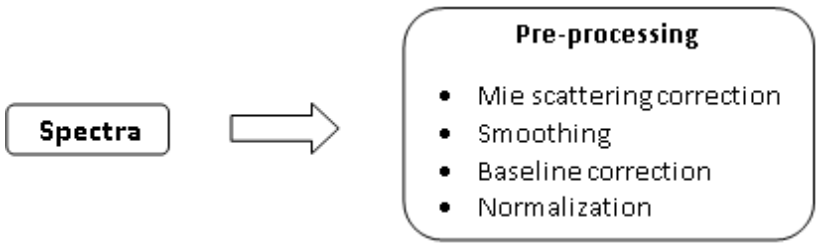

Figure 18 The preprocessing steps applied to spectral data.

1.6 Aim of the Study

Since miRNAs have serious roles in various biological processes, the deregulation of these micromanagers are expected to cause to cancer initiation and progression. Moreover, it has been predicted that single miRNA can target hundreds or thousands of mRNAs on the basis of sequence complementarity. There have been many studies to elucidate the role of these molecules in cancer etiopathogenesis. These studies are based on the individual determination of mRNA targets of miRNA by genetic and bioinformatics approaches. The discovery of the reciprocal action between an mRNA and a corresponding miRNA is of great importance for describing the roles of miRNAs in biological systems. However, more integrated and universal applications are

required to detect the comprehensive alterations in cells originated from miRNA expression. In the current research, the global impacts of miR-125b transfection on MCF7 and T47D cells were investigated since this miRNA is one of the downregulated miRNA in breast cancer .The low expression level of this miRNA was demonstrated in these cell lines in comparison to the other breast cancer cell lines (Tuna, 2010, Akhavantabasi et al., 2012). In the present study, there are three main specific aims:

By the combination use of various spectroscopic, biochemical and unsupervised chemometric analysis approaches,

1- To examine and describe the comprehensive impacts of miR-125b transfection on MCF7 andT47D cells, which are lacking and expressing miR-125b.
2- To determine this miRNA transfection-induced alterations especially in the lipid constituents/composition of these cancer cell lines from their lipid extracts.
3- To discriminate the miR-125b and EV transfected MCF7 and T47D cells based on their spectral variations.

CHAPTER II

MATERIAL AND METHODS

2.1 Cell Culture Experiments

2.1.1 Cell Culture and Growing Conditions

MCF7 and T47D cell lines were a kind gift from Dr. U.H. Tazebay (Gebze Institute of Technology). Both cells were grown as described in detail in the previous study (Ozek et. al., 2010)

2.1.2 Transfection of Mammalian Cells

Empty vector and miR-125b transfected MCF7 and T47D cells were generated by Dr.Ayse Elif ERSON-BENSAN's laboratory (Akhavantabasi et al., 2012, Tuna, 2010). The long term maintenance of transfected cells, 250µg/mL of G418 antibiotic, Gentamycin, from Roche (Cat# 4727878001) was used.

2.2 ATR-FTIR Spectroscopic Study

2.2.1 Sample Preparation

2.2.1.1 Cell Studies

For ATR-FTIR experiments, control (EV) and miR-125b transfected MCF7 and T47D cells were grown in an independent manner and harvested 20 and 10 times, respectively. To obtain a cell pellet, cells were grown until proper confluency (75–80 %), then trypsinized and the number of the cells was determined via a hemacytometer. 2x 10^6 control and transfected cells were taken and centrifuged at 100g for 5 min. Cell pellet was resuspended with 10 µl 0.9% phosphate buffer saline solution (PBS) for ATR-FTIR experiments.

2.2.1.2 Cellular Lipid Experiments

a) Cell Growth: Cells were grown until 80% confluency at 175 cm^2 culture flasks, detached by treatment with trypsin. To be sure about the complete removal of trypsin and culture medium, the cell pellet firstly washed three times in isotonic solution (NaCl, 0.9%) and lastly in pure desalted water by a 2-minute centrifugation (300 g). For each cell group, five 175 cm^2 culture flasks were used to get high quality IR spectra of cellular lipids.

b) Extraction of Cellular Lipids

For cellular lipid extraction, the protocol determined by Bligh and Dyer (Bligh and Dyer, 1959) was used. Firstly, cell pellet were resuspended with 250 µl of

chloroform/500 µl of methanol mixture and vortexed. Secondly, 16.8 µl of hydrochloric acid (6M) and 250µl of chloroform were added to the solution and vortexed again. Thirdly, 250µl of pure desalted water was added into the mixture and vortexed again. Finally, the solution was incubated at 4°C during 24 hrs and then centrifuged at 300g for 10 min. Total lipid content was finally collected in the lower phase and the lower phase was carefully collected for ATR-FTIR measurements.

2.2.2 Data Acquisition

2.2.2.1 Cell Studies

For the collection of the IR spectra of the cells, the one-bounce ATR mode in a Spectrum 100 FTIR spectrometer (Perkin-Elmer Inc., Norwalk, CT, USA) equipped with a Universal ATR accessory were used. Total 20 and 10 independent spectra for control (EV), miR-125b transfected MCF7 and T47D cells were collected, respectively. The collection of the cell spectra were performed as mentioned clearly in our study (Ozek et.al.,2010).

2.2.2.2 Cellular Lipid Studies

All cellular lipid spectra was collected using by the ATR-FTIR spectrometer (Perkin-Elmer Inc., Norwalk, CT, USA) Briefly, 10 µl of lipid extracts for every single measurement was directly put on the ATR crystal and waited at RT to evaporate solvents and thin lipid layer was obtained. The spectra was collected at 4000-650 cm^{-1} spectral region, 200 scans with 2 cm^{-1} spectral resolution. Five cellular lipid extract samples for each group were used for IR measurements. At least 10 lipid spectra was obtained for each group.

2.2.3 Spectral Data Analysis

2.2.3.1 Cell Studies

All spectral data analysis were performed by using OPUS 5.5 software (Bruker Optics, GmbH). To obtain accurate and sensitive spectral changes between EV and miR-125b transfected cells, the second order derivative spectra was used since it enables the correct discrimination and identification of superimposed and unresolved IR spectral bands Absorption maxima appear as minima in the second derivatives. For this reason, minimum positions were used for the comparisons in the second derivative spectra. Therefore, to calculate the wavenumber, intensity and bandwidth values of spectral bands, the second derivative order of the cell spectra was taken and subsequently vector normalized in three IR regions (3050–2800 cm^{-1}, 1800– 480 cm^{-1}, 1480–800 cm^{-1}).

2.2.3.2 Cellular Lipid Studies

To identify the miR-125b transfection induced alterations in the types of breast cancer cells lipids, firstly, the band assignments of the spectral bands in extracted lipid IR spectra was determined based on the studies of FTIR spectroscopy and tissue/or cell lipids. Then the band area of these bands are from the baseline corrected spectra by Spectrum 100 software (PerkinElmer Inc., Norwalk, CT, USA).

2.2.4 Chemometric Analysis

To discriminate the EV and miR-125b transfected MCF7 and T47D cells and cellular lipids based on spectral alterations, Hierarchical cluster analysis (HCA) and Principal Component analysis (PCA) were performed as an exploratory analysis.

For HCA, OPUS 5.5 software (Bruker Optics, GmbH) was used. For cell studies, the second derivative vector normalized spectra at 3050–900 cm^{-1} and 3800-800 cm^{-1} spectral regions were used for MCF7 and T47D cells, respectively. For cellular lipid studies, the mean centered absorbance spectra at 4000-650 cm^{-1} spectral region were used. In both analysis, Pearson's correlation coefficients was used to calculate spectral distance between pairs of spectra. To construct the dendrogram, Ward's algorithm was used. The separation of EV and miR-125b clusters was based on the Euclidean distances as described in detail (Severcan et al., 2010).

PCA was performed using *Unscrambler X* 10.3 (*Camo Software AS)* multivariate analysis (MVA) software .The mean centered absorbance spectra at 4000-650 cm^{-1} spectral region were used for both EV and miR-125b MCF7 and T47D cells and cellular lipids the loading plots constructed to find the contribution of spectral bands in the discrimination of EV and miR-125b transfected groups. Discrimination between the groups was shown as score plots.

2.3 Measurement of lipid peroxidation (TBAR assay)

To determine lipid peroxidation level, malondialdehyde (MDA) levels were measured by using Abcam's Lipid Peroxidation Assay Kit (Abcam, Cat.-No. ab118970, Cambridge, UK) For standard solution, 0,2,4,6,8 and 10 µM MDA solution were prepared. For cell samples, both control and miR-125b transfected cells were grown at 80 % confluency, harvested with trypsin and then washed with cold PBS buffer. The cells were homogenized with lysis solution (buffer + buthylatedhydroxytoluene

(BHT)) using sonicator and were centrifuged at 13,000 x g for 10 minutes and supernatant was collected. 600 µL of TBA reagent was added into both 200 µL standard and 200 µL sample and incubated at 95°C for 60 minutes. After cooling them down to the room temperature in an ice bath for 10 minutes, the absorbance of mixture was measured at 532 nm. MDA values were calculated and expressed as nmol.

2.4 Electron Spin Resonance Spectroscopic Study

ESR spectroscopy was used to identify the alterations in the membrane dynamics in EV and miR-125b transfected MCF7 and T47D cells, as it has been commonly used in previous cell culture studies (Ogura et al., 1988, Rossi et al., 1999). 16-doxyl-stearic acid (16-DSA) spin label was used to label lower part of the acyl chain of membrane lipids. The labelling of the cells and the collection of their ESR spectra were performed as explained clearly in a previous study (Ozek et. al.,2010) .The results of ESR spectra for control MCF7 and T47D cells was demonstrated in Figure 19. The membrane fluidity information was obtained from the calculation of the rotational correlation time (τ_c) from spectra which monitor the lower part of the acyl chain of membrane lipids using 16-doxyl stearic acid spin label based on using the formula given below;

$$\tau c = 6.5 \times 10^{-10} W_0 \left[\left(\frac{h_0}{h_{-1}} \right)^{1/2} - 1 \right]$$

where $K = 6.5 \times 10^{-10}$ s G^{-1} is a constant depending on microwave frequency and the magnetic anisotropy of the spin label, W_0 is the peak-to-peak width of the central line, and $\frac{h_0}{h_{-1}}$ is the ratio of the heights of the central and high field lines, respectively (Severcan and Cannistraro, 1990).

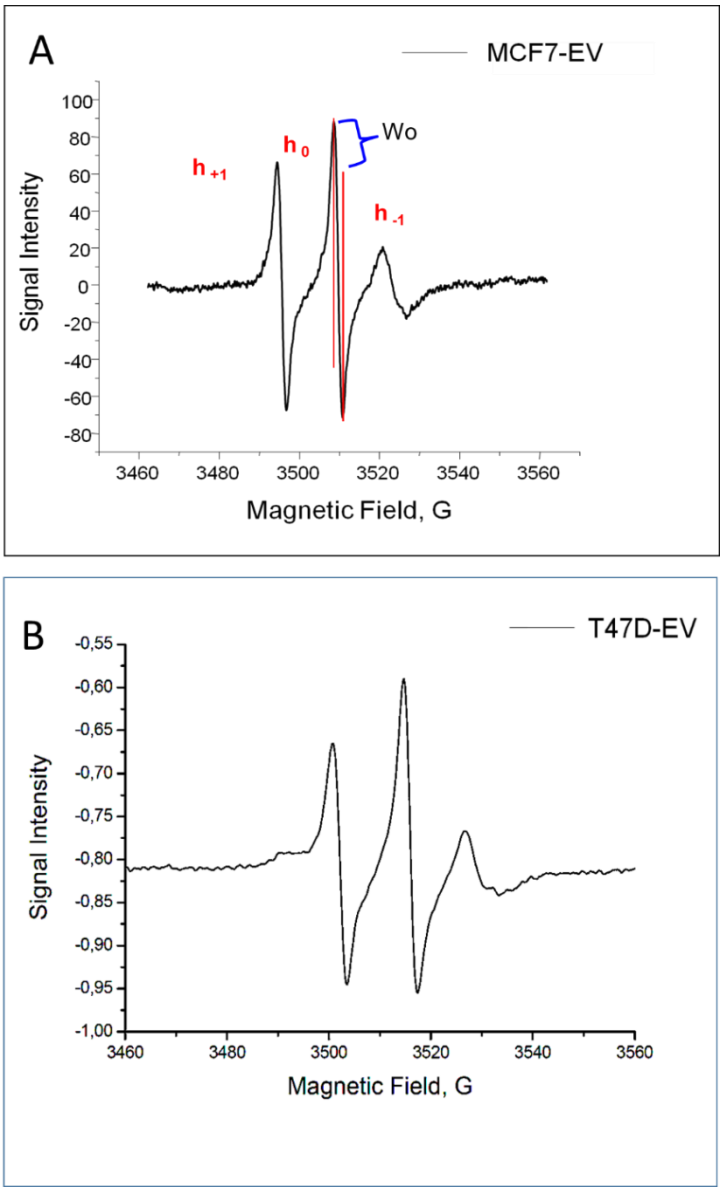

Figure 19 Representative ESR spectra of 16DSA labelled MCF7-EV (A) and T47D-EV (B) cells.

2.5 Statistical Data Analysis.

For MCF7 cells, the mean was calculated from 20 independent FTIR spectra while for T47D cells, the mean was calculated from 10 independent FTIR spectra. All the results in figures were demonstrated as mean± standard error of mean. To assess the statistical

significance of data for control and miR-125b transfected cells, Student-t test was performed. p values equal to or less than 0.05 were considered as significantly different from the control group. The degree of significance was denoted as: *$p < 0.05$, **$p < 0.01$, ***$p < 0.001$, ****$p < 0.0001$.

CHAPTER III

RESULTS AND DISCUSSION

miR-125b is one of the most consistently down-regulated miRNA in breast cancer compared to normal tissue (Iorio et al., 2005). One reason of this downregulation is hypermethylation of the miR-125b promoter regions as demonstrated in breast cancer cells and tissues (Zhang et al., 2011). The other reason is the deletion of the miR-125b loci (Calin et al., 2004). Similarly, miR-125b-1 and miR-125b-2 were shown to be down-regulated in breast tumors, as compared to normal tissues (Volinia et al., 2006). Several studies have been conducted to determine the role of the miR-125b in breast cancer etiopathogenesis (Scott et al., 2007, Iorio et al., 2005, Zhang et al., 2011). For instance, Scot and his colleagues demonstrated that the miR-125b reexpression led to the inhibition of ERBB2 and ERBB3 expression and signaling thus inhibiting the proliferation of human breast cancer cells (Scott et al., 2007).

It has been demonstrated that the down-regulation of miR-125b induced the activation of the ERBB2 pathway and thus stimulated promoting cell survival in metastasis of breast cancer (Banzhaf-Strathmann and Edbauer, 2014, Ferracin et al., 2013). Hence, down-regulation of miR-125b correlates with the aggressiveness and metastatic property of the breast cancers which is ERBB2 positive (Scott et al., 2007). The reduced expression of this miRNA stimulates the expression ETS1 gene, which has a role in cell cycle transition, cell growth and proliferation (Zhang et al., 2011). In addition to these studies, Akhavantabasi et. al., (2012) demonstrated that ARID3B, which has role in cell motility, is the target of miR-125b in breast cancer cells. Akman et al., (2015) has also demonstrated the miR-125b reexpression led to increase in the

expression of activated leukocyte antigen molecule (ALCAM) mRNA and protein levels (Akhavantabasi et al., 2012, Akman et al., 2015).

Most of the studies, that performed to clarify the roles of miR-125b in breast cancer, are based on the determination of single mRNA target of miR-125b. To uncover this miRNA in the tumorigenesis and progression of breast cancer cells, comprehensive/ holistic approaches are required. Therefore, this study was conducted to clarify the miR-125b transfection induced alterations in the molecular profile of MCF7 and T47D cell lines since low/no expression of miR-125b was demonstrated in these cell lines (Akhavantabasi et al., 2012, Tuna, 2010). In addition to whole cell studies, we investigated whether this miRNA reexpression lead to the changes in the constituents of cellular lipids. Moreover, we explored whether miR-125b reexpression induced alterations lead to distinguish miRNA transfected cells from EV cells or not.

3.1 Characterization of miR-125b Reexpression Induced-Molecular Alterations in Breast Cancer Cells

3.1.1 ATR-FTIR Spectroscopy

3.1.1.1 Spectral Analysis

Second derivative ATR-FTIR spectra of EV transfected MCF7 and T47Dcells in the 3050-2800 cm^{1}, 1800-1480 cm^{-1} and 1480-900 cm^{-1} regions were given in Figure 20 A, B and C, respectively. The characteristic frequency values and detailed assignments of these bands were given in Table 4. Since the infrared spectra of MCF7 and T47D cells consists of many spectral bands arisen from the lipids, proteins, polysaccharides and nucleic acids, the detailed spectral analysis was performed in three different spectral regions: 3030–2800, 1800–1480 and 1480–900 cm^{-1}.

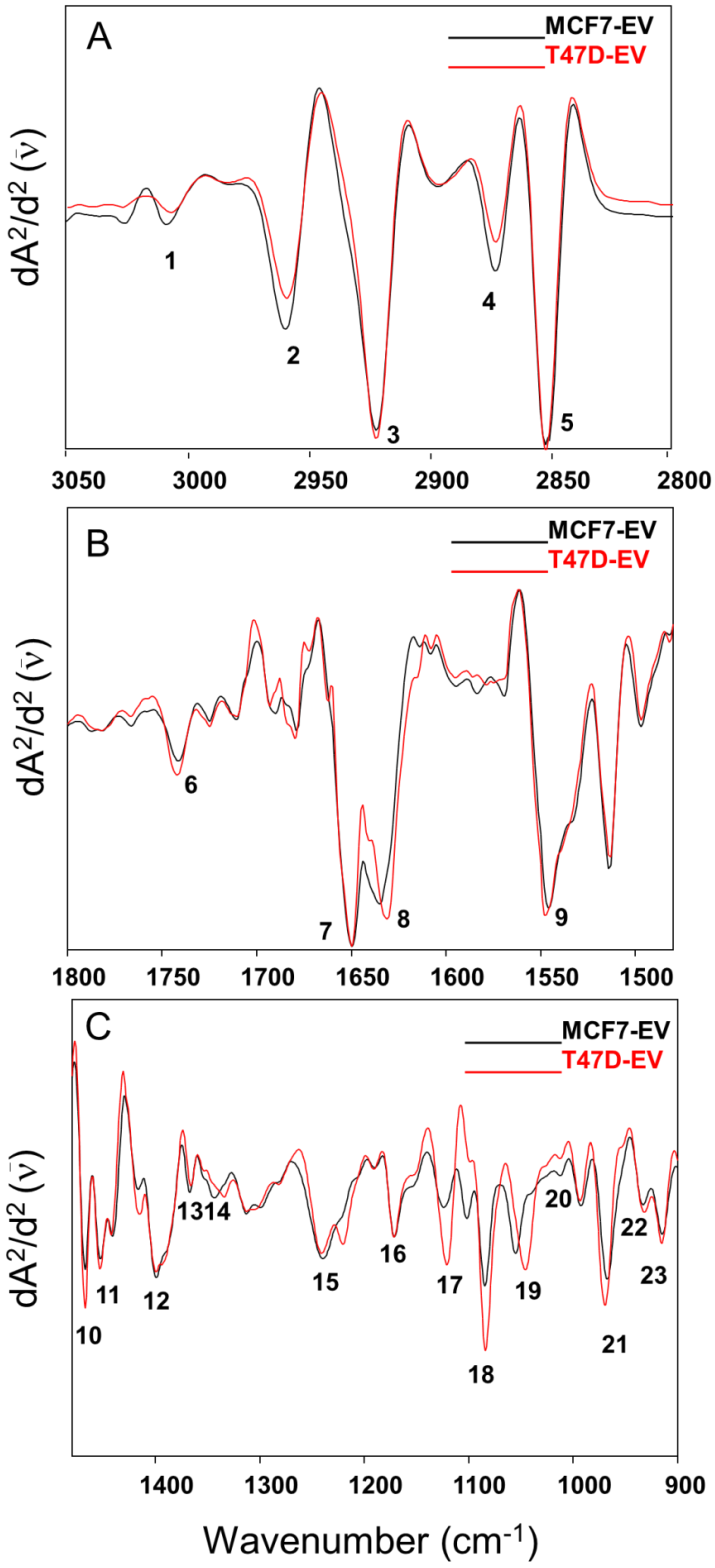

Figure 20 Representative second derivative spectra of EV transfected MCF7 and T47D cells in the 3050-2800 cm^{-1} (A), 1800-1480 cm^{-1} (B) and 1480-900 cm^{-1}(C) regions (Adapted from Ozek et. al.,2010).

Table 4 Band assignments of major absorptions in IR spectra of breast cancer cell in the 3030–900 cm^{-1} region based on literature (Choo et al., 1995, Jackson et al., 1998, Banyay et al., 2003, Ramesh et al., 2002, Mourant et al., 2003, Salman et al., 2001, Diem et al., 1999, Gasper, 2010, Kazarian and Chan, 2006, Baker et al., 2014, Derenne et al., 2011, Severcan et al., 2010, Severcan and Haris, 2012, Turker et al., 2014b, Ozek et al., 2014, Severcan et al., 2005, Cakmak et al., 2006) (Taken from Ozek et. al.,2010).

Peak no.	Wavenumber (cm^{-1})	Definition of the spectral assignment
1	3008	Olefinic=CH stretching vibration: unsaturated lipids, cholesterol esters
2	2958	CH_3 antisymmetric stretching: lipids, protein side chains, with some contribution from carbohydrates and nucleic acids
3	2921	CH_2 antisymmetric stretching: mainly lipids, with the little contribution from proteins, carbohydrates, nucleic acids
4	2870	CH_3 symmetric stretching: protein side chains, lipids, with some contribution from carbohydrates and nucleic acids
5	2851	CH_2 symmetric stretching: mainly lipids, with the little contribution from proteins, carbohydrates, nucleic acids
6	1740-1744	Ester C=O stretch: triglycerides, cholesterol esters
7	1651	Amide I: (mainly protein C=O stretching), α-helical structure
8	1631	Amide I: β-sheet
9	1546	Amide II: (protein N–H bending, C–N stretching),α-helical structure
10	1468	CH_2 scissoring: lipids
11	1453	CH_2 bending: mainly lipids, with the little contribution from proteins
12	1400	COO^- symmetric stretching: fatty acids
13	1367	CH_3 symmetric bending:lipids
14	1343	CH_2 wagging: phospholipid, fatty acid, triglyceride , amino acid side chains
15	1238	PO^-_2 antisymmetric stretching, fully hydrogen-bonded: mainly nucleic acids with the little contribution from phospholipids
16	1171	CO–O–C asymmetric stretching: ester bonds in cholesteryl esters
17	1121	Ribose ring vibrations:RNA
18	1084	PO^-_2 symmetric stretching: nucleic acids and phospholipids C-O stretch: glycogen, polysaccharides, glycolipids
19	1045	C-O stretching: polysaccharides (glycogen)
20	1020	DNA
21	968	$C\text{-}N^{\pm}\text{-}C$ stretch: nucleic acids, ribose-phosphate main chain vibrations of RNA-DNA
22	933	Z type DNA
23	915	Ribose ring vibrations:RNA/DNA

3.1.1.1.1 Lipids

To monitor the alterations in the lipid content of the biological systems the C–H stretching region are commonly used. This region is located between 3030–2800 cm^{-1} spectral region and contains several spectral bands which are due to the olefinic (=CH), CH_2 and CH_3 stretching groups. To determine the changes in unsaturated lipids and unsaturation index, the olefinic band (3008 cm^{-1}) is commonly used (Krishnakumar et al., 2009, Gasper et al., 2009, Severcan et al., 2005). A significant diminish in the intenstiy of this band was found in miR-125b transfected MCF7 and T47D cells as comparison to the their EV transfected cells (Figure 21 and 22, A,B). This reduction revealed the decline in unsaturated lipid content. In addition to the olefinic band, the $CH{=}CH/CH_2$ ratio is also used to determine unsaturation index (Kinder and JM Wessels, 1997). This ratio was also significantly decreased (Figure 21 and 22 C) in MCF7-125b and T47D-125b cells, which also indicates a decrease in the amount of unsaturated bonds in the structures of the lipids. It has been demonstrated that the olefinic band can be used to identify lipid peroxidation Krishnakumar et al., 2009, Leskovjan et al., 2010, Kinder and JM Wessels, 1997, Gasper et al., 2009, Severcan et al., 2005). For that reason, the decrease in the unsaturated lipid content may be arisen from a diminish in the synthesis of unsaturated lipids or an increment in the oxidative degradation of lipids. To prove the increase in lipid peroxidation in miR-125b transfected cells, we measured the malondialdehyde level, which is the indicator of lipid peroxidation by Lipid Peroxidation Assay Kit. Their results are demonstrated in Figure 23. As can be seen from the figure, MDA levels were significantly increased for both miR-125b transfected breast cancer cells, which is in accordance with our FTIR results. Previous reports proposed that polyunsaturated fats encourage proliferation and alter attachment properties of the cells (Kasayama et al., 1994,Johanning, 1996, Rose and Connolly, 1990). Moreover, recent spectroscopic study showed that the metastatic characteristics of breast cancer cells has been linked to elevated polyunsaturated lipid composition (Hedegaard et al., 2010). Cell growth is also inhibited by lipid peroxidation (Morisaki et al., 1982).As a result, the decrease in the composition of unsaturated lipids and higher amount of lipid peroxidation induced by the transfection of miR-125b can alter the growth profile of MCF7 and T47D breast cancer cell lines.

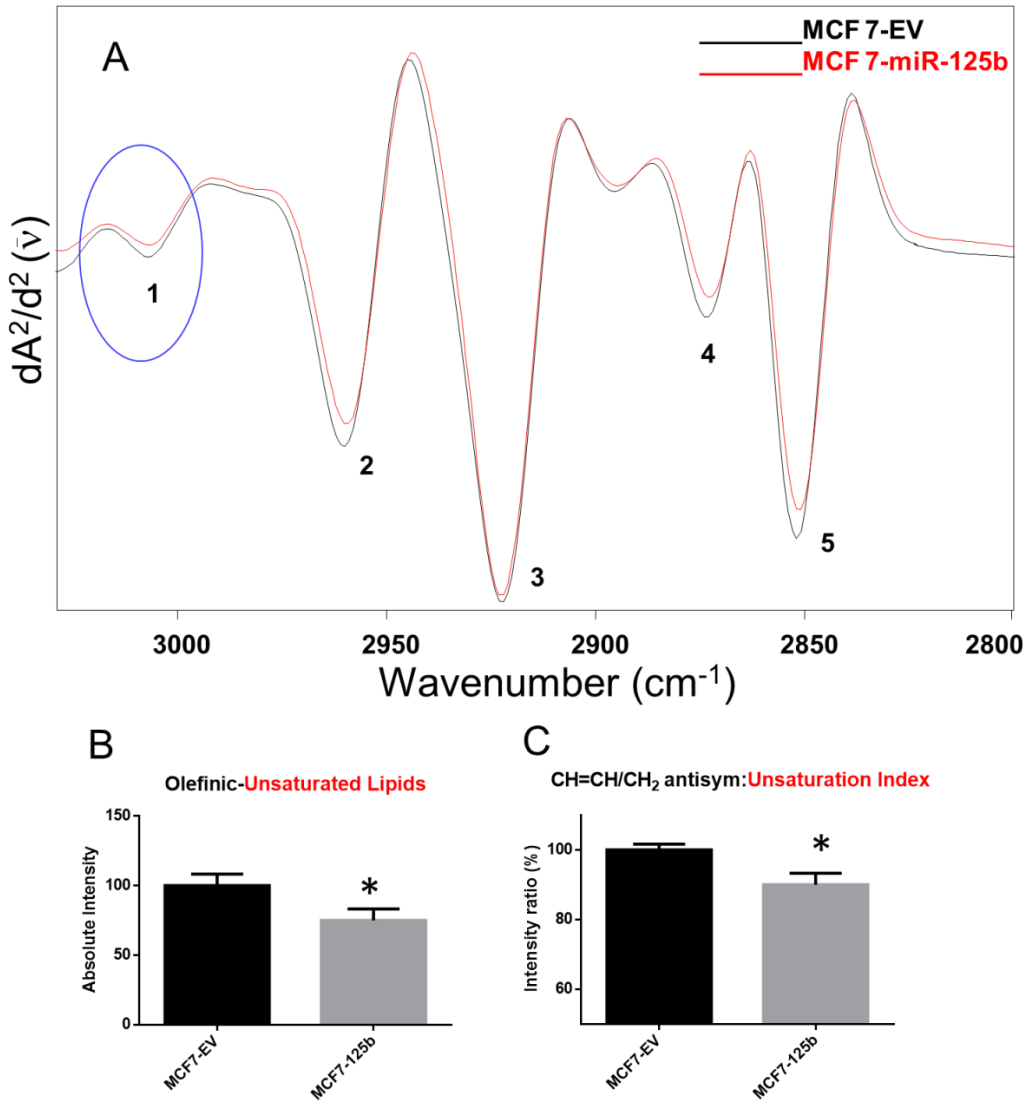

Figure 21 A) Representative second derivative spectra of EV and miR-125b transfected MCF7 cells in the 3030-2800 cm^{-1} region B) The absolute intensity of olefinic (CH=CH) band and C) the intensity ratio of olefinic/CH_2 antisymmetric stretching bands in these groups (Adapted from Ozek et. al.,2010).

.

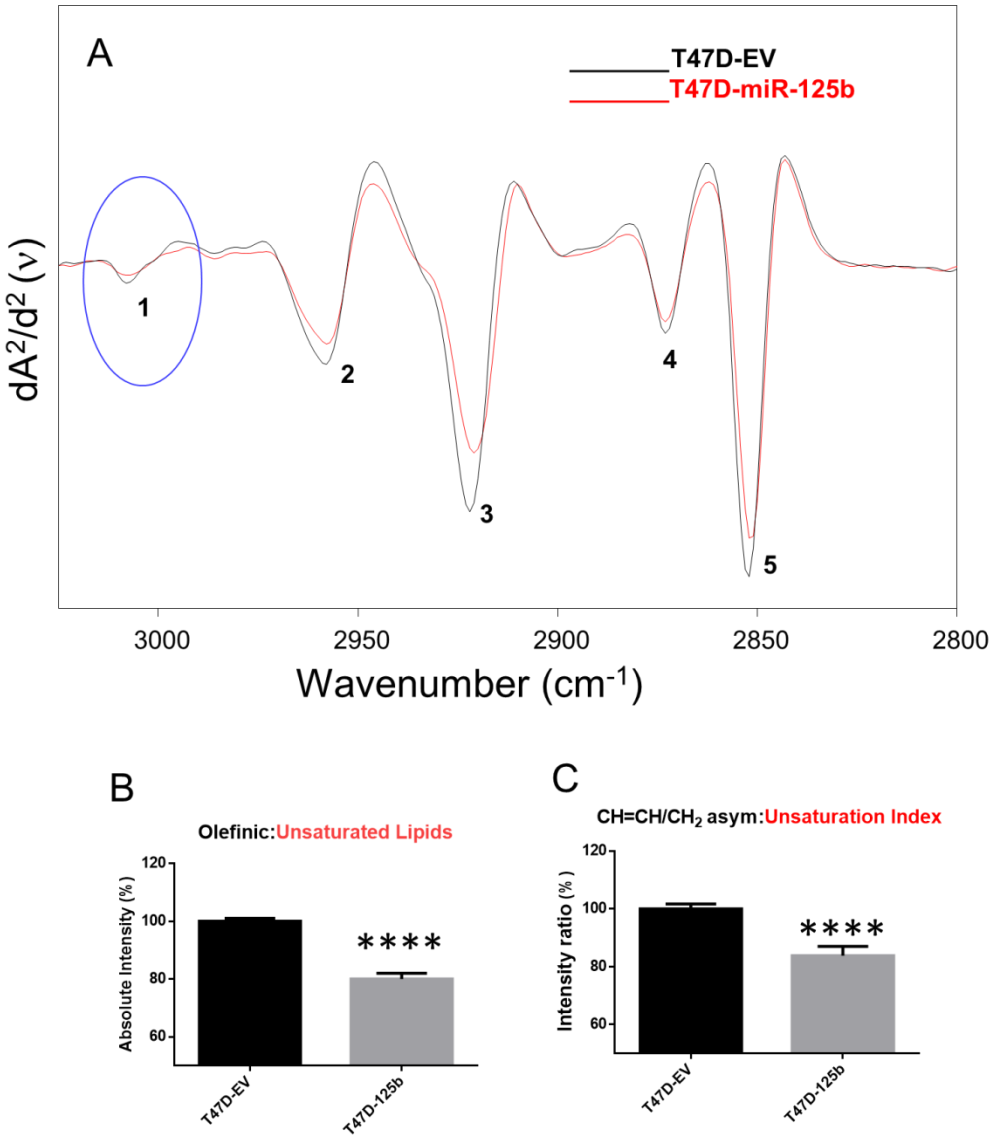

Figure 22 A) Representative second derivative spectra of EV and miR-125b transfected T47D cells in the 3030-2800 cm^{-1} region B) The absolute intensity of olefinic (CH=CH) band and C) the intensity ratio of olefinic/CH_2 antisymmetric stretching bands in these groups.

.

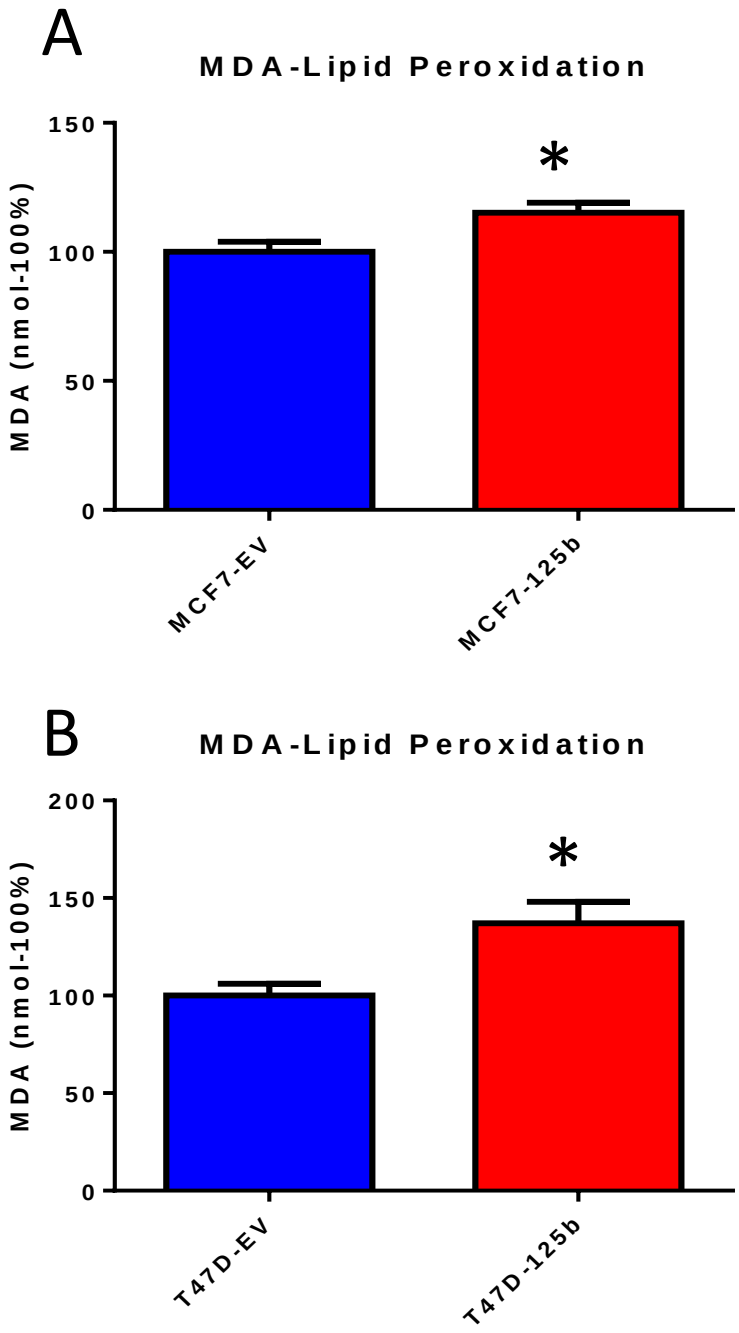

Figure 23 Malondialdehyde amount (nmol) in EV and miR-125b transfected MCF7 (A) and T47D (B) cancer cells.

.

To clarify miR-125b reexpression-induced alterations in the structure and concentration of cancer cell lipids, the CH_2 asymmetric and symmetric stretching bands were analyzed since these bands are arisen from lipid acyl chains (Table 4) (Gasper et al., 2009, Severcan et al., 2005, Turker et al., 2014a, Ozek et al., 2014). Significant decline in the intensity values of these bands were obtained in miR-125b transfected MCF7 and T47D cells , which implies the diminish in saturated lipid content of these breast cancer cells.(Figures 24 B, C and 25 B, C). In addition to these bands, the diminish in the intensity values of the CH_2 scissoring (1468 cm^{-1}) and COO^- symmetric stretching (1400 cm^{-1}) bands was acquired, which also supports the decrease in the saturated lipid content of MCF7-125b and T47D-125b cells (Figures 26 B,C and 27 B,C) (Jackson et al., 1998, Ozek et al., 2014, Sen et al., 2015, Cakmak et al., 2006)The reduction in the saturated lipid amount may be originated from the decline in the biosynthesis of the lipids or elevation in the lipid degradation arising from the increase in the lipid peroxidation (Ozek et al., 2014). . The reduction in the saturated lipid composition detected in the miR-125b transfected MCF7 and T47D cells also denoted to reduced cell growth /metabolic rate. The synthesis of the lipids is high in actively dividing cells. (Gillies et al., 2008, Jackowski et al., 2000).

To detect miR-125b rerexpression induced changes in the membrane dynamics of the breast cancer cells, the bandwidths of the CH_2 asymmetric and symmetric stretching bands were calculated. (Turker et al., 2014a, Ozek et al., 2014, Cakmak et al., 2006). A significant decrease in this parameter was obtained in miR-125b transfected MCF7 cells while a meaningful increased in the same parameter was acquired in T47D-125b cells (Figure 24 and 25D). The decreased and increased in the bandwidth values of the CH_2 asymmetric stretching band implied the decrease and increase in the membrane fluidity of miR-125b transfected MCF7 and T47D cells, respectively. To prove these results, the membrane fluidity was also measured by ESR spectroscopy. To obtain information about membrane fluidity, the cells were labeled with 16-doxyl stearic acid that provides information on the motion of the lower portion of the chain towards the center of the membrane. Then, the rotational correlation time (τ_c) of the spin label was calculated from the ESR spectra of the cells. The significant rise and decline in this parameter was obtained in miR-125b transfected-MCF-7 and T47D cells, respectively (Figure 28A and B) which indicated the decreased and increased the membrane fluidity

of the cells. These results support the IR results about membrane dynamics. The differences in membrane fluidity of MCF7-125b and T47D-125b cells may be due to the distinctions in the alterations of ratio of membrane lipids and membrane lipid microdomains such as rafts and caveolae. It has been known that these domains are all enriched in the sphingolipids, and cholesterol and affects membrane fluidity (Mattson, 2005). The correlation between the lipid order and the membrane fluidity is quite important for regulating the proper functioning of the cells (Boesze-Battaglia and Schimmel, 1997). Furthermore, any alterations in the membrane fluidity in cancer cells have negative impacts on membrane receptor functions and the migratory characteristics of cancer cells (Taraboletti et al., 1989, Daefler et al., 1986). Membrane fluidity has also been increased in the course of cancer cell metastasis (Gonda et al., 2010, Zeisig et al., 2007). For that reason, miRNA-125b reexpression -induced alterations in membrane fluidity of breast cancer cell may affect their migration abilities.(Liang et al., 2010).

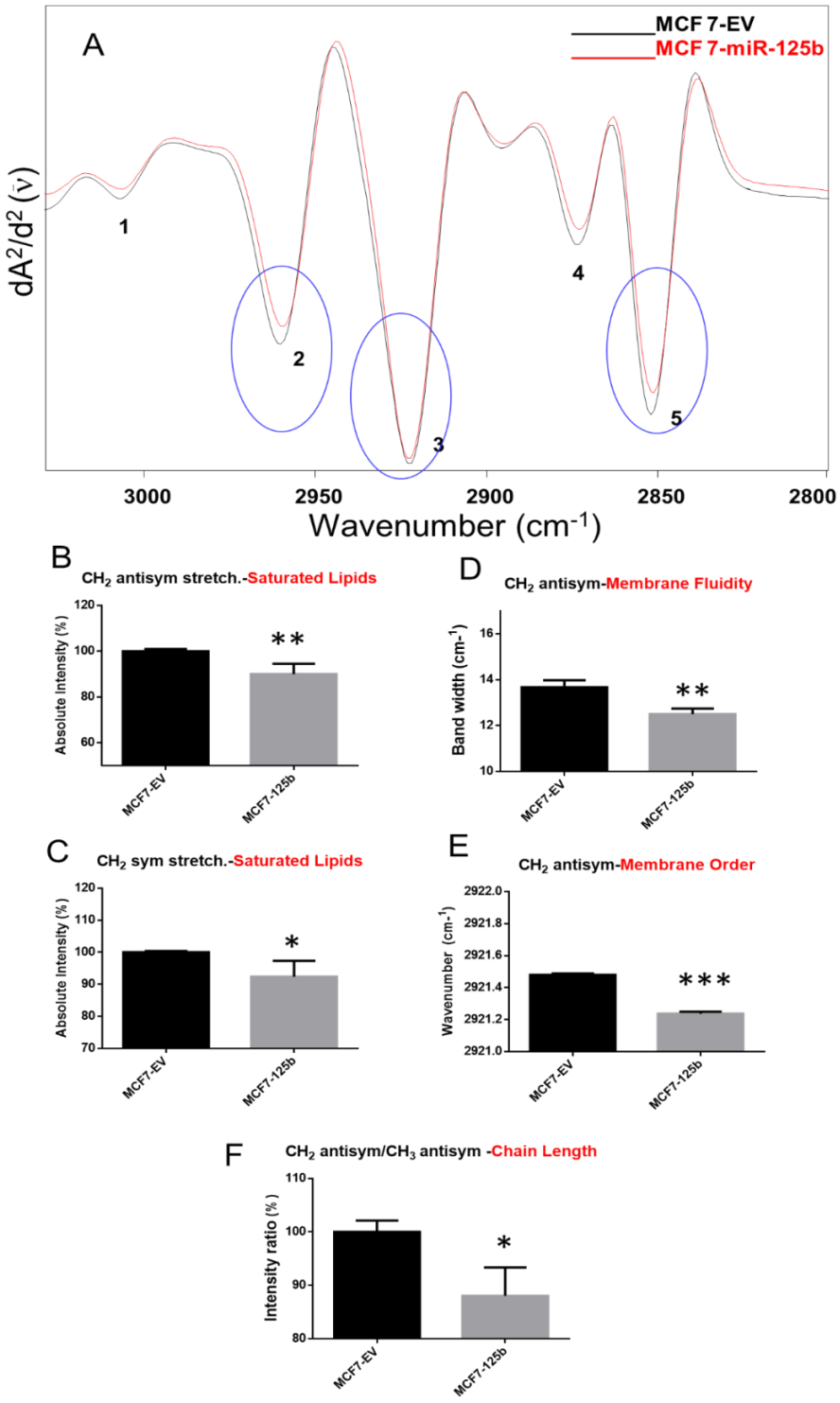

Figure 24 A) Representative second derivative spectra of EV and miR-125b transfected MCF7 cells in the 3030-2800 cm^{-1} region. B) and C) The absolute intensities of CH_2 antisymmetric and symmetric stretching bands, respectively. D) and E) The bandwidth and wavenumber of CH_2 antisymmetric and symmetric stretching bands, respectively. F) The intensity ratio of CH_2 antisymmetric/ CH_2 antisymmetric stretching bands in these cells (Adapted from Ozek et. al.,2010).

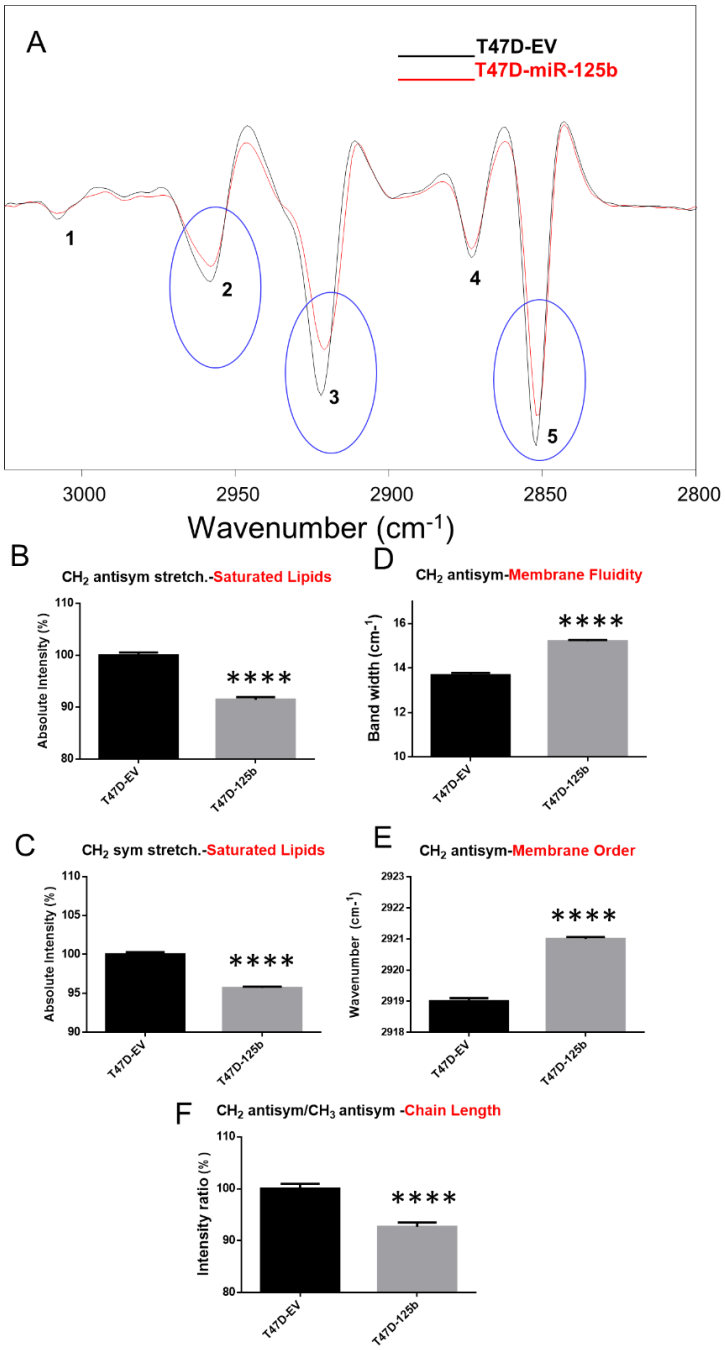

Figure 25 A) Representative second derivative spectra of EV and miR-125b transfected T47D cells in the 3030-2800 cm^{-1} region. B) and C) The absolute intensities of CH_2 antisymmetric and symmetric stretching bands, respectively. D) and E) The bandwidth and wavenumber of CH_2 antisymmetric and symmetric stretching bands, respectively. F) The intensity ratio of CH_2 antisymmetric/ CH_2 antisymmetric stretching bands in these cells.

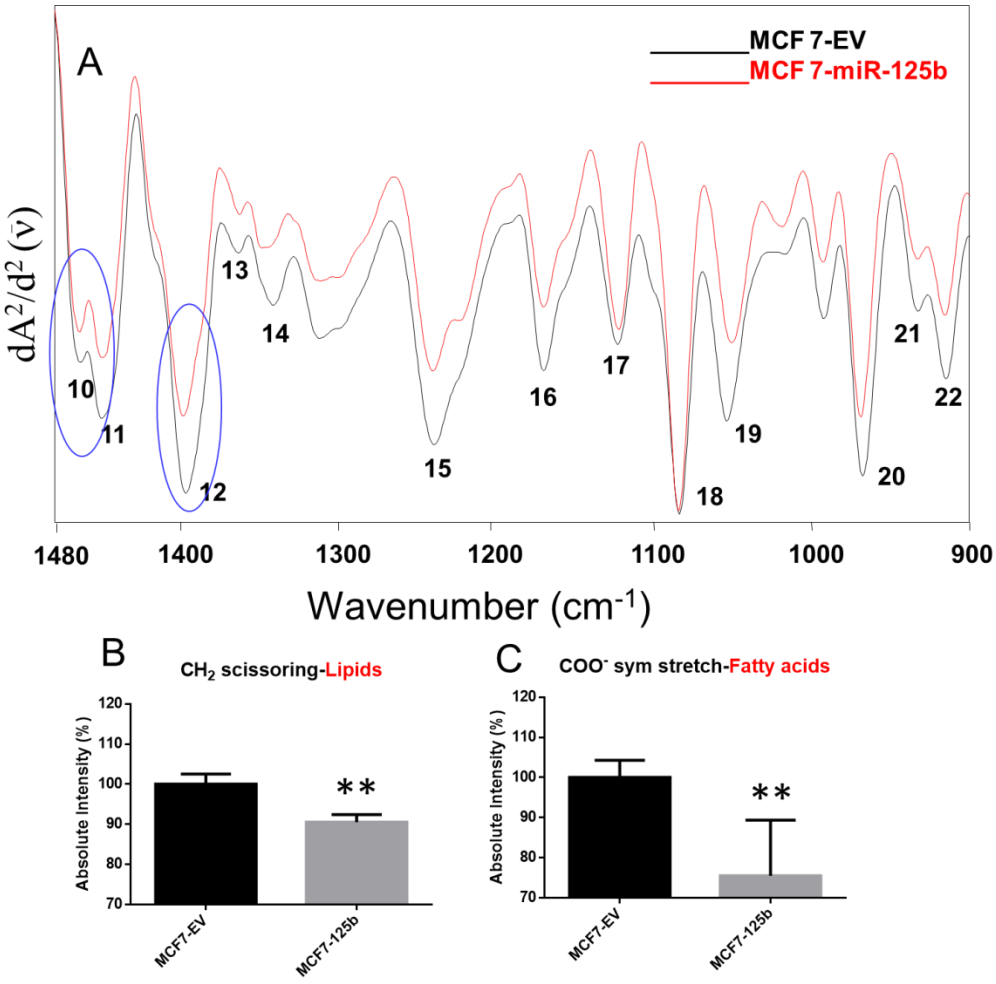

Figure 26 A) Representative second derivative spectra of EV and miR-125b transfected MCF7 cells in the 1480-900 cm^{-1} region, B) and C) The absolute intensities of CH_2 scissoring and COO^- symmetric stretching bands, respectively (Adapted from Ozek et. al.,2010).

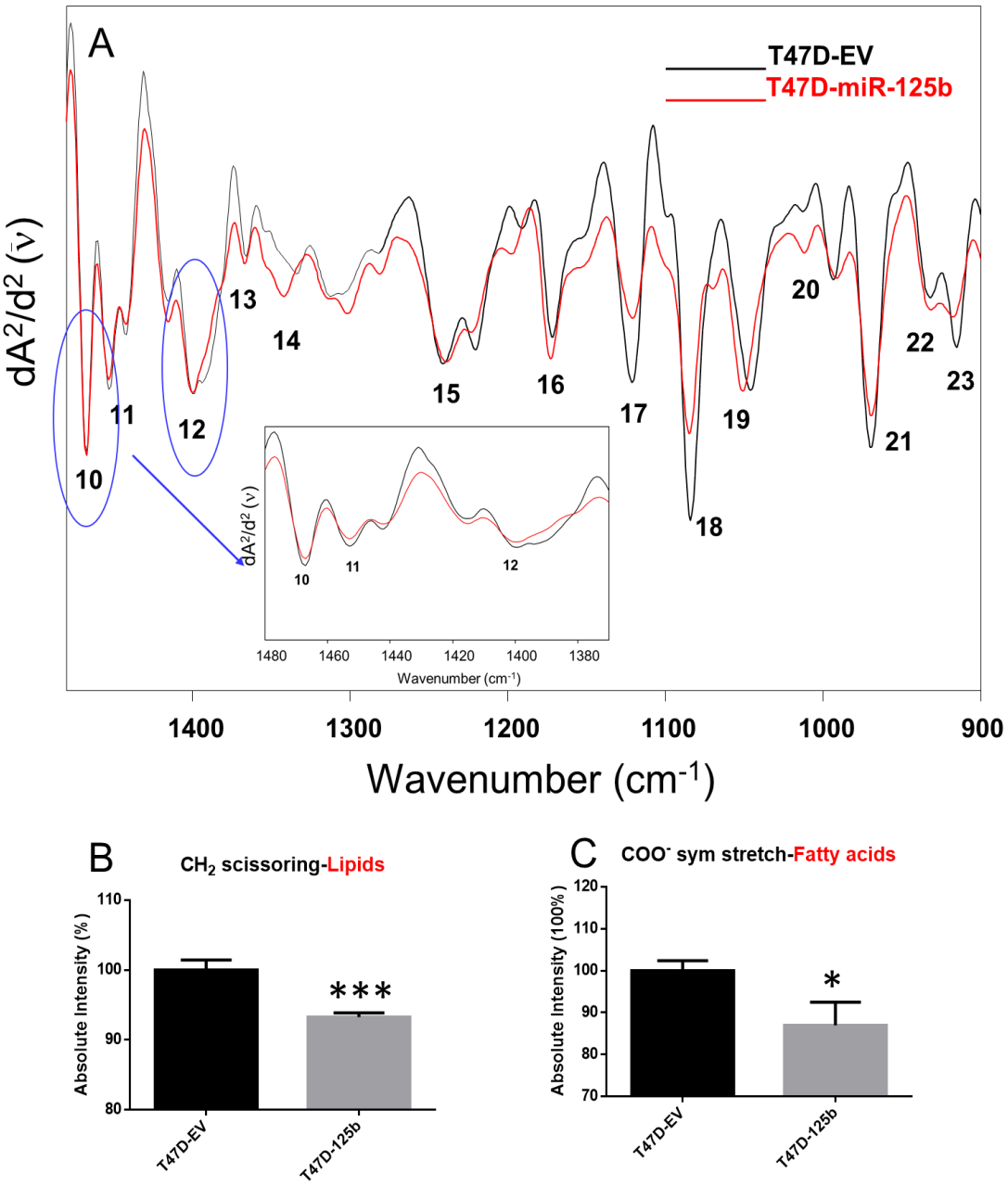

Figure 27 A) Representative second derivative spectra of EV and miR-125b transfected T47D cells in the 1800-1480 cm^{-1} region, B) and C) The absolute intensities of CH_2 scissoring and COO^- symmetric stretching bands, respectively.

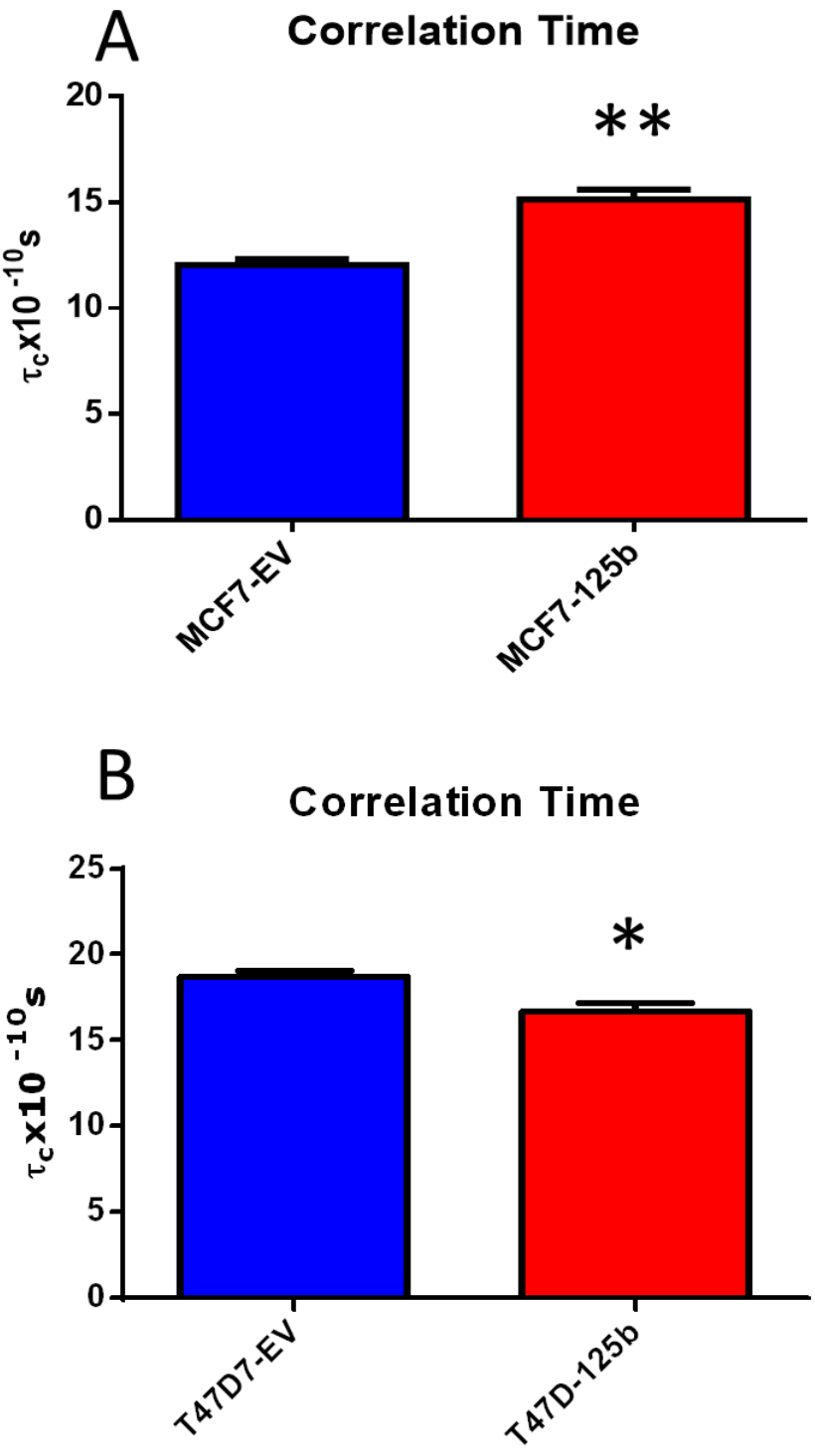

Figure 28 Correlation times of 16-doxyl stearic acid labelled EV and miR-125b transfected MCF7 (A) and T47D (B) cancer cells.

To determine miR-125b rerexpression induced alterations in membrane-lipid order (acyl chain flexibility) of cancer cells, the shifts in the frequencies of the CH_2 antisymmetric and symmetric stretching bands were measured (Turker et al., 2014a, Ozek et al., 2014). The shift in the frequency of CH_2 antisymmetric band to lower value show an increase in the number of trans conformers of lipid molecules which imply an increase in lipid order. On the contrary, the shift in the frequency of this band to and higher values indicates an increase in the number gauche conformers of lipid molecules which reveals a decrease in lipid order (Severcan, 1997) A significant slight shift to lower values in the frequency of CH_2 antisymmetric band was found in miR-125b transfected MCF7 cells. (Figure 24 E). On the other hand, the frequency shift to higher values was obtained for T47D-125b cells (Figure 25E).These shifts suggested that an increase and decrease in lipid order were observed in miR-125b transfected MCF7 and T47D cells. In earlier studies, it has been demonstrated that changes in lipid order affects cellular shape and these changes alters the intake of drugs (Moore et al., 1997) (Ramu et al., 1983). Therefore, miR-125b rerexpression in MCF7 and T47D cells may lead to alteration in diverse cell functions through the changes in the cell shape and thickness of the cell membrane s (Spector and Yorek, 1985).

The band intensity ratio of CH_2 antisym/CH_3 antisym bands are used to obtain information about the hydrocarbon chain length of the lipids. The lower ratio of these bands suggests the presence of shorter chained lipids and lower lipid content (Wang et al., 2005). As can be seen from both the Figures 24F and 25F, this ratio was lowered in both cell lines which might be due to miR-125b transfection. This indicates which may be due to the synthesis of this kind of lipids and/or shorter-chained lipids which is due the degradation of lipids by free radicals.

To monitor the miR-125b transfection induced alterations in the cholesterol esters and triacylglycerols amount, the band located at 1744 cm^{-1} was analyzed. (Table 4). The intensity of this band declined in miR-125b transfected MCF7 cells and increased in miR-125b transfected T47D-cells, respectively (Figure 29 and 30) indicating a low and high abundance of ester groups of triacylglycerols and cholesterol (Figure (Nara et al., 2002). The decrease in the intensity of the other cholesterol ester bands in

MCF7-125b cells was also contributed to previous results. Moreover, this increased cholesterol esters and triacylglycerols for T47D-125b cells was confirmed by the increment of the intensity of this cholesterol ester band. This band is named as CO–O–C asymmetric stretching band which is located at 1171 cm^{-1}. The reduced level of these lipids in MCF7-125b and the increased concentration of same lipids for T47D-125b may be due to the decrease and increase in their biosynthesis.

Cholesterol is indispensable for life due to its critical roles in cells for the synthesis of steroid hormones and in cell membranes for the fluidity of the membranes. High levels of cholesterol requirement is a characteristic feature of pre-malignant and malignant cells. For this reason, elevated LDL receptor activity and high amount of the synthesis of the cholesterol were discovered in these cells (Vitols et al., 1996). Additionally, there was a correlation between triglyceride, cholesterol composition and drug resistance of cancer cells (Santini et al., 2001). Therefore, the alteration in the cholesterol ester and triglyceride amount of the miR-125b transfected cells is crucial for further confirmation of the tumor suppressor function of miR-125b.

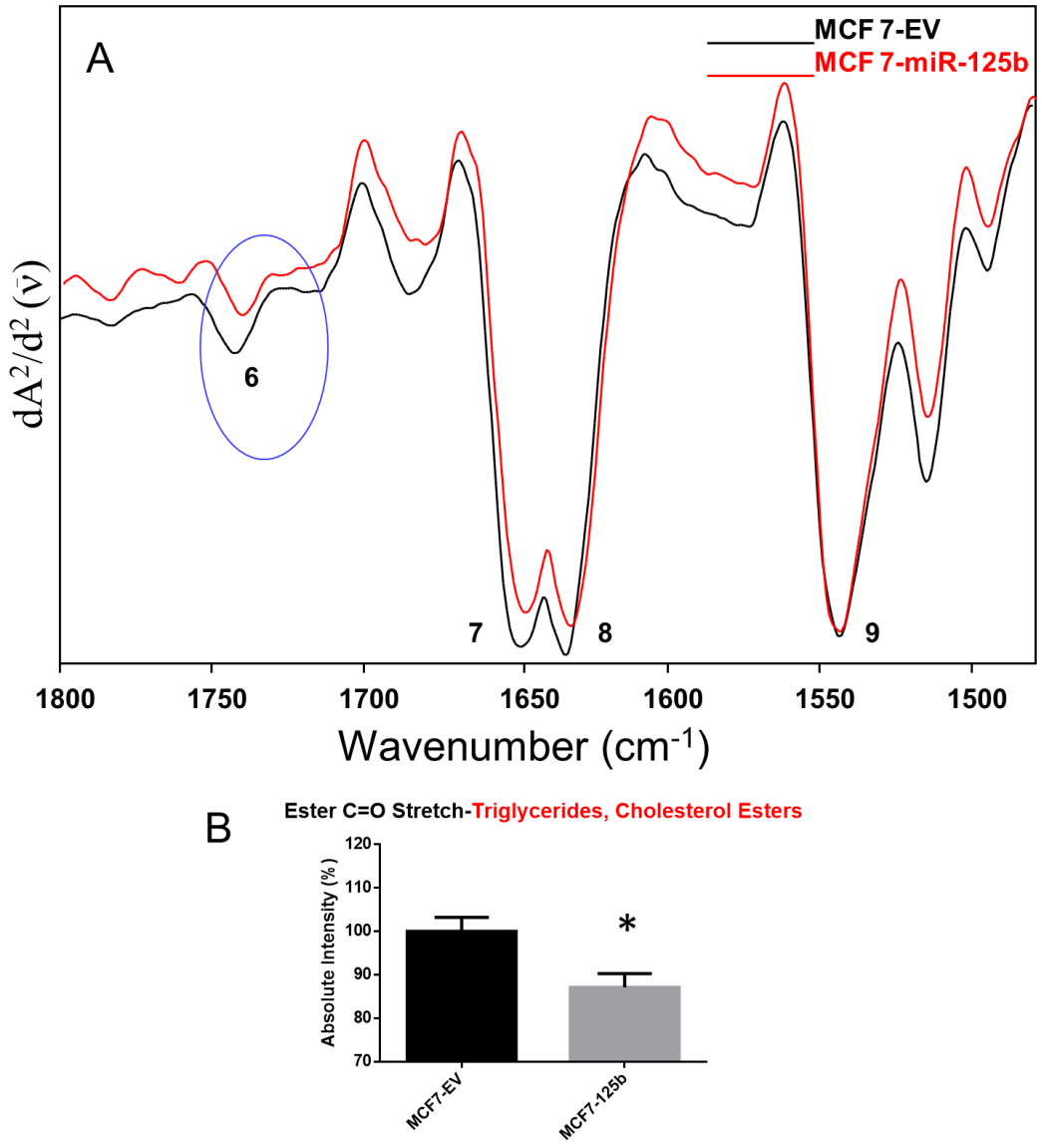

Figure 29 A) Representative second derivative spectra of EV and miR-125b transfected MCF7 cells in the 1800-1480 cm^{-1} region.B)The absolute intensity of Ester C=O stretching band in these cells (Adapted from Ozek et. al.,2010).

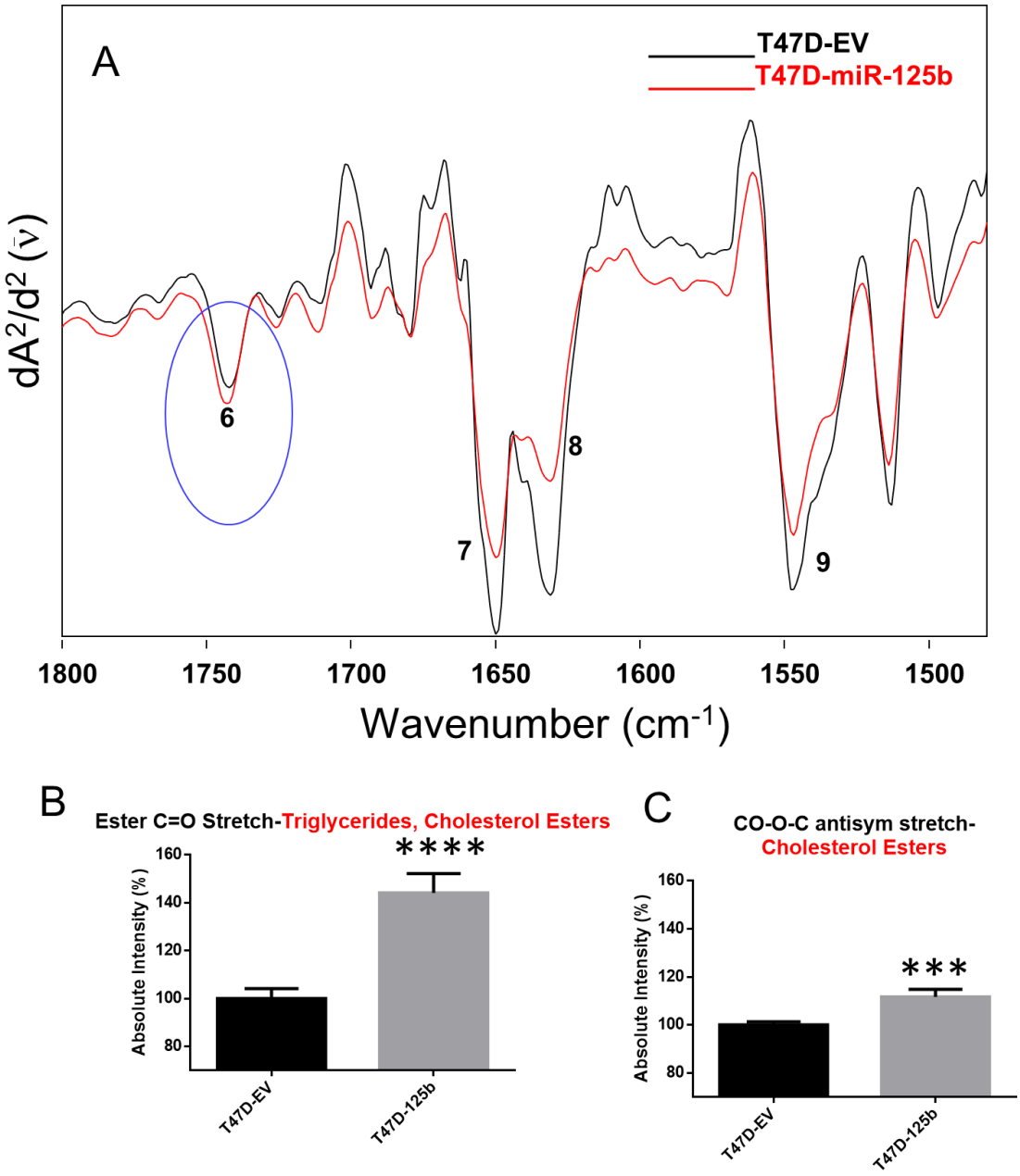

Figure 30 A) Representative second derivative spectra EV and miR-125b transfectedT47D cells in the 1800-1480 cm^{-1} region. The absolute intensity of Ester C=O stretching (B) and CO-O-C antisymmetric bands (C) in these cells.

3.1.1.1.2 Proteins

Amide I and amide II bands are generally used to determine about the changes in protein concentration and structure. (Severcan and Haris, 2012, Turker et al., 2014b, Turker et al., 2014a, Ozek et al., 2014, Cakmak et al., 2006). In the current study, the intensity values of the amide I (1651 cm^{-1}: of α-helix, 1631 cm^{-1}: β-sheet) and amide II (1546 cm^{-1}: α-helix) were measured to identify miR-125b reexpression caused alterations in protein amount of cancer cells. (Liu et al., 1996). Figures 31 B, C, D and 32 B, C and D indicated the significant diminish in the amount of α-helical and β-sheet structures in miR-125b transfected MCF7 and T47D cells. This decrease may be arisen from the decline in the protein synthesis which can be inferred from the decrease in the RNA content in miR-125b transfected breast cancer cells. Guo and his colleagues demonstrated the decreased target mRNA and thus protein levels induced by miRNA transfection which also supports our results (Guo et al., 2010).

To determine which metabolism (lipid or protein metabolism) is more profoundly affected from miR-125b reexression, the lipid-to-protein ratio was calculated by deriving from the ratio of the total band intensities of the CH_2 asymmetric and symmetric stretching bands to the total band intensities of the amide I band (Turker et al., 2014a, Ozek et al., 2014, Cakmak et al., 2006). Significant decline in the ratio of these bands was obtained in the miR-125b transfected MCF7 cells while the significant increased the same ratio was acquired in T47D-125b cells (Figure 31F and 32F). The decrease implies more reduction in the lipid amount relative to protein amount in the MCF7-125b cells. However, the increase demonstrates more decrease in protein content relative to the lipid content in the T47D-125b cells. More decrease lipid content of MCF7-125b cells means that miRNA-125b reexpression caused more profound alterations in lipid metabolism than protein metabolism. On the other hand, more decrease in protein content of T47D-125b cells suggests that miR-125b transfection to breast cancer cells led to great changes in protein metabolism with respect to lipid metabolism.

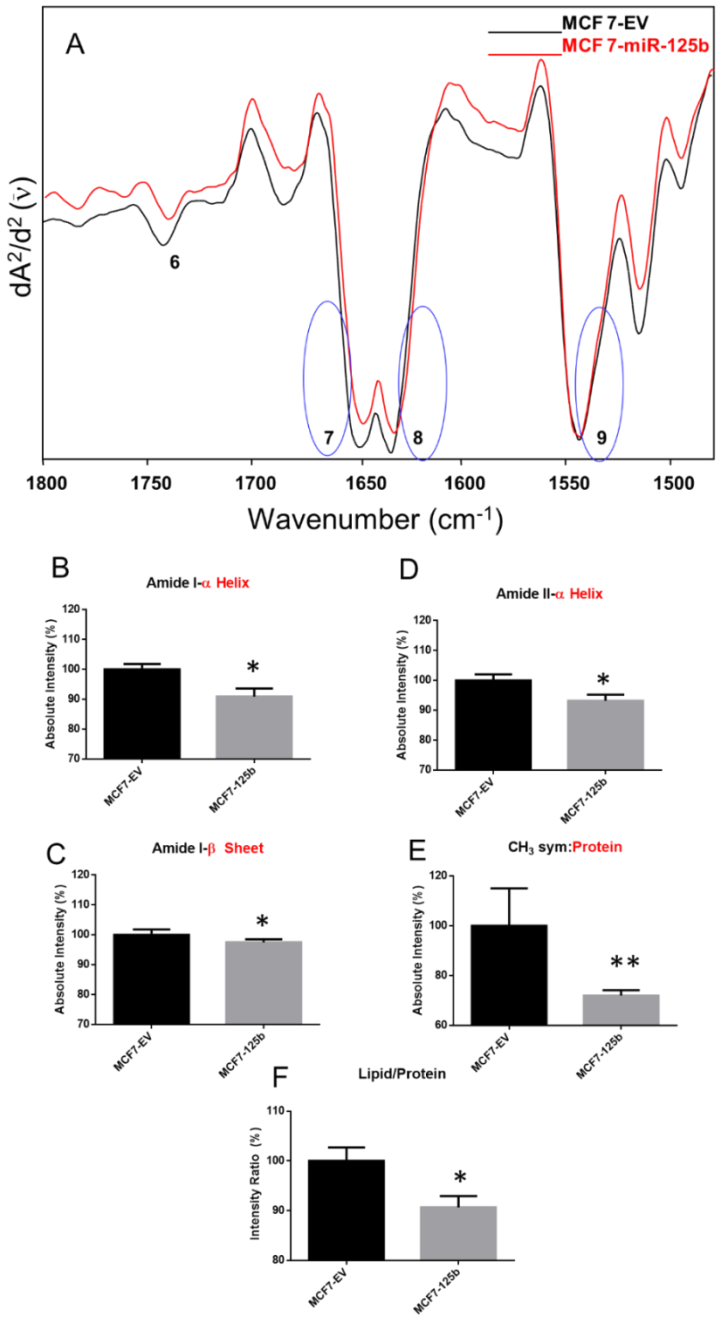

Figure 31 A) Representative second derivative spectra of EV and miR-125b transfected MCF7cells in the 1800-1480 cm^{-1} region (A), B) and C) the absolute intensities of Amide I -α helix and β sheet, respectively D) Amide II and E) CH_3 asymmetric bands and F) the intensity ratio of lipid and protein bands in these cells (Adapted from Ozek et. al.,2010).

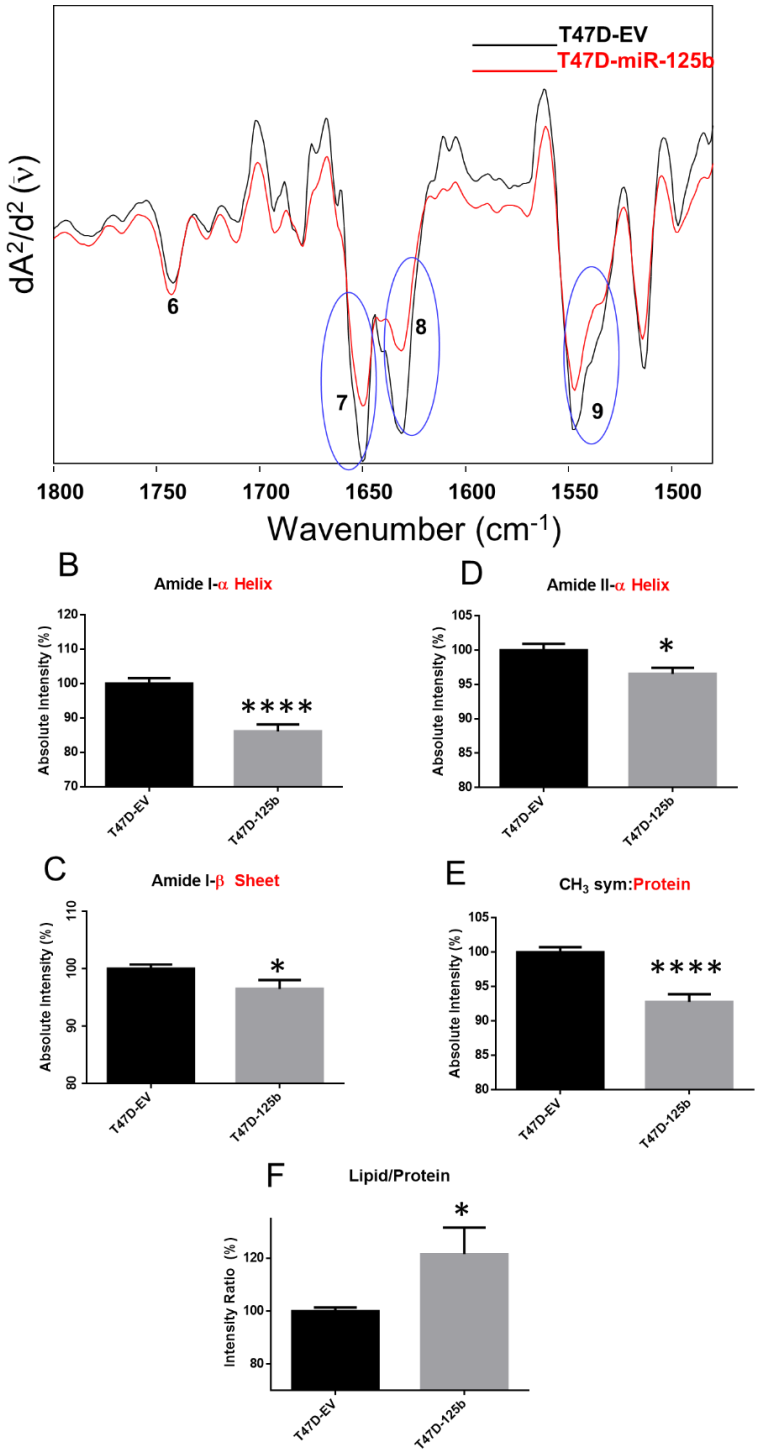

Figure 32 A) Representative second derivative spectra of EV and miR-125b transfected T47Dcells in the 1800-1480 cm-1 region (A), B) and C) the absolute intensities of Amide I -α helix and β sheet, respectively D) Amide II and E) CH3 asymmetric bands and F) the intensity ratio of lipid and protein bands in these cells.

3.1.1.1.3 Nucleic Acids and Polysaccharides

To detect miR-125b rexpression induced alterations in nucleic acid content, the bands at 1238 cm^{-1} and 1084 cm^{-1} originating from PO^{-}_{2} antisymmetric and symmetric vibarions of nucleic acids were analyzed. Significant reduction in the intensity values of these bands was found in the miR-125b transfected MCF7 and T47Dcells (Figure 33 & 34 B, C), implying a decline in nucleic acid content in miR-125b transfected cells. This decline may be due a decrease in the synthesis of nucleic acids. Both 5'-AMP and 5'- GMP levels for DNA synthesis have been found to be increased in CLL patients with a corresponding low miR-125b expression upon metabolon study of cancer cells (Tili et al., 2012). The increased synthesis can be due to increased the expression level of phosphoribosyl pyrophosphate amidotransferase (PPAT). This enzyme catalyzes the first step of denovo purine nucleotide biosythetic pathway and provides purines for FAD(H2), NAD(H), NADP(H), coenzyme A, DNA and RNA biosynthesis. Moreover, it is one of the putative targets of miR-125b (Tili et al., 2012, www.targetscan.org). Ozen et. al., disclosed that the upregulation of PPAT was found in prostate cancer with down-regulated miRNA-125b level (Ozen et al., 2008).In addition to this, the increase in this protein expression have been also demonstrated in breats and prostate cancer tissues by immunostaining method (http://www.proteinatlas.org/ENSG00000128059-PPAT/cancer). According to these results, we can infer that miR-125b reexpression may suppress this target which lead to decreased purine synthesis.

To identify the alteration in RNA amount of miR-125b transfected cells, the band intensity values of t 1121 and 915 cm^{-1} bands were calculated. The significant decrease in the intensity of these bands were in both cell lines, suggesting the diminish in RNA concentration with miR-125b reexpression (Figure 33 & 34 D, E). These reductions may be due to to the decrease in its synthesis or the miR-125b caused degradation of mRNAs. The decreased RNA biosynthesis might be due to the downregulation of PPAT which is induced by miR-125b reexpression in breast cancer cells (Tili et al., 2012)(Tili et. al., 2012).

To determine miR-125b reexpression caused changes in the glycogen amount of MCF7 and T47D cells, the the intensity of glycogen band (1045 cm^{-1}) was calculated. Significant reduction in this band intensity was obtained in the miR-125b transfected MCF7 cells while it significantly increased in the miR-125b transfected T47D cells (Figure 33 and 34 F), indicating the diminish in the in the glycogen amount of the miR-125b transfected MCF7 cells, while an increase in T47D cells. The opposite results related to glycogen content may be due to the differences expression level of enyzmes within glycolytic and gluconeogenesis pathway. These differences has been shown in the study of functional proteome analysis of MCF7 and T47D cells (Adjo Aka et al., 2012). The difference in glycogen content of miR-125b transfected MCF7 and T47D cells can be due to the differences in bioenergetic profile of them since it has been reported that MCF7 cells are more energetic and glycolytic than T47D cells (Brandie et al., 2015).

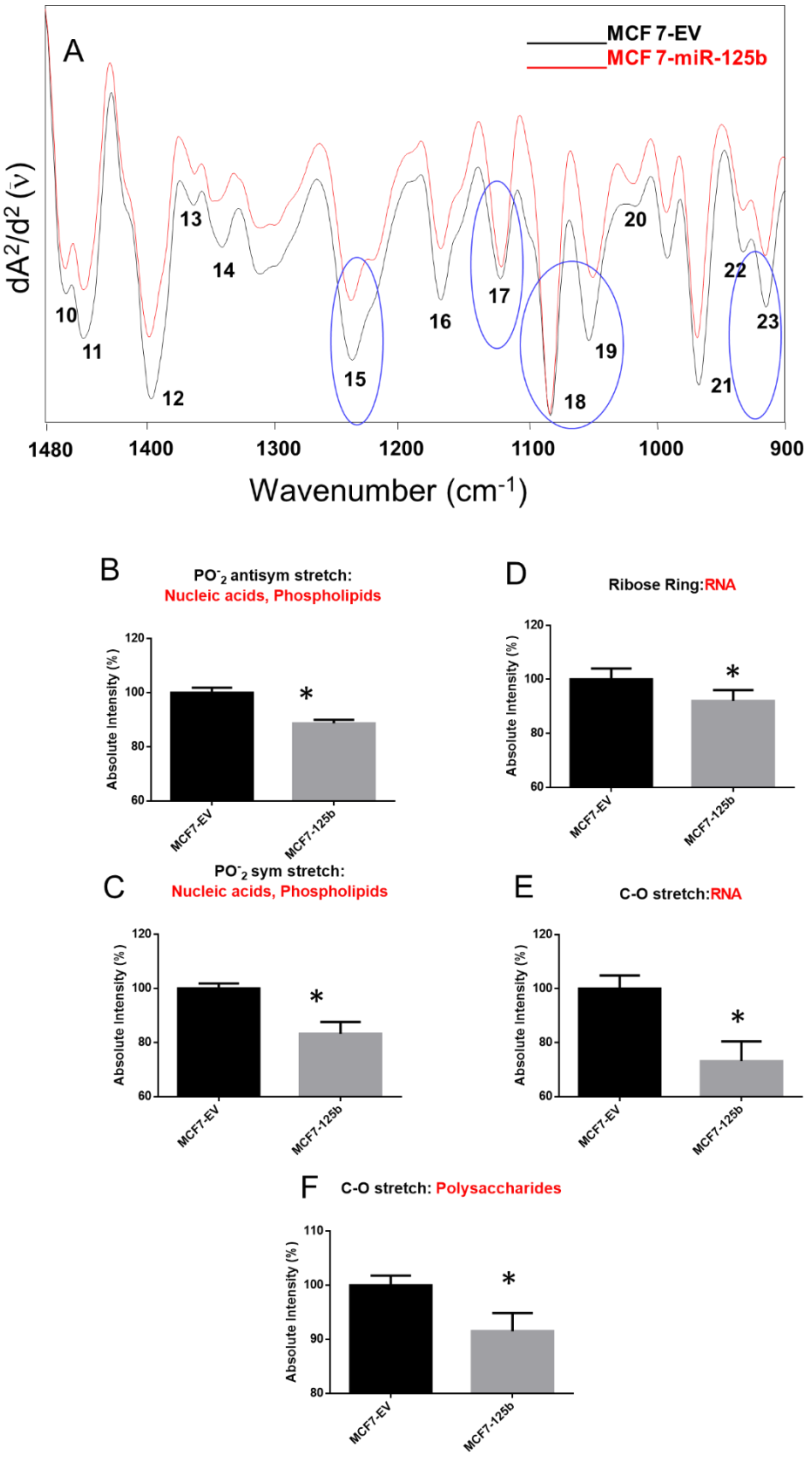

Figure 33 Representative second derivative spectra of EV and miR-125b transfected MCF7 cells in the 1480-900 cm^{-1} region. The absolute intensities of B and C) PO^{-}_{2} antisymmetric and symmetric bands, respectively, D) Ribose Ring, E) C-O stretching:RNAand F) C-O stretching:Polysachharides bands in these cells (Adapted from Ozek et. al.,2010).

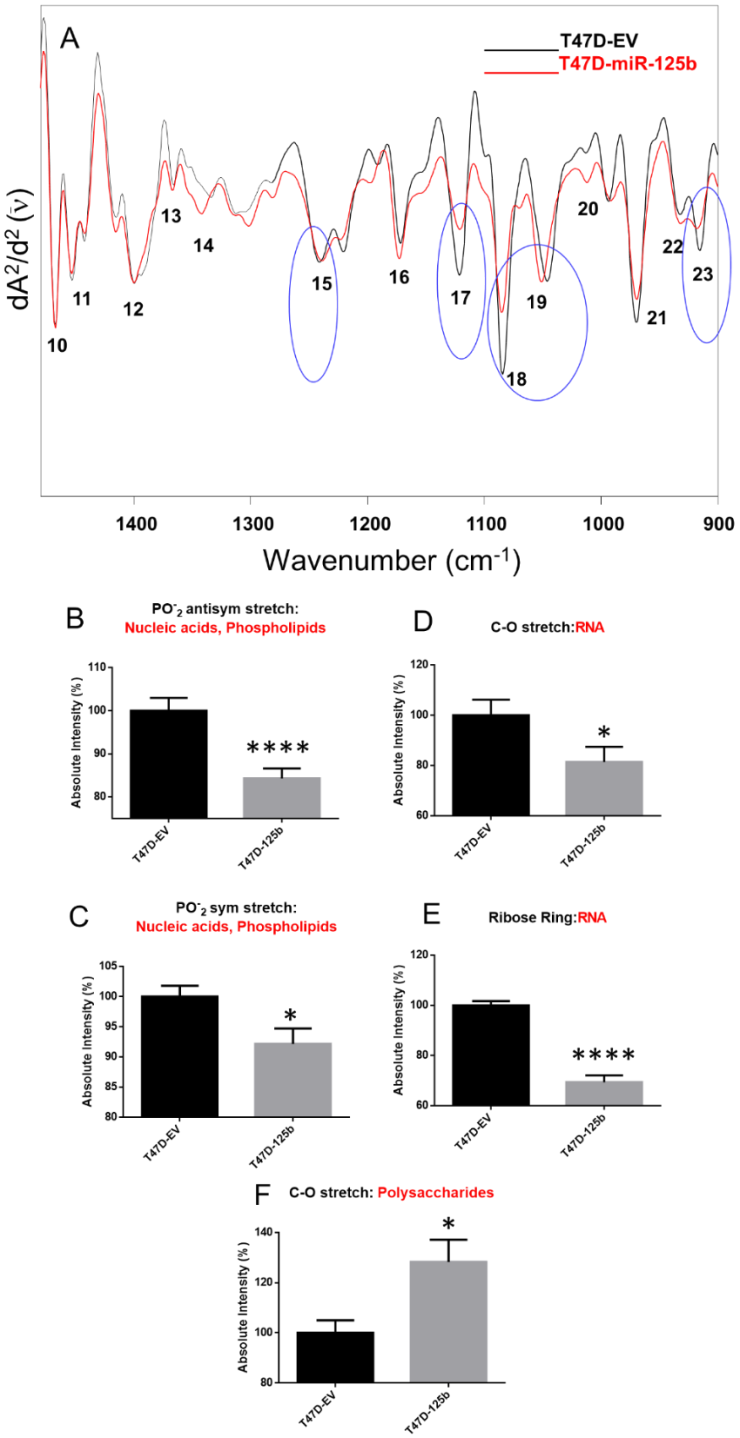

Figure 34 Representative second derivative spectra of EV and miR-125b transfected T47D cells in the 1480-900 cm^{-1} region. The absolute intensities of B and C) PO^{-}_2 antisymmetric and symmetric bands, respectively, D) Ribose Ring, E) C-O stretching:RNAand F) C-O stretching:Polysachharides bands in these cells.

3.1.1.1.4 Proliferation, Transcription and Metabolic Status

To determine miR-125b reexpresion induced alteration in the proliferation rate breast cancer cells, the intensity ratio of RNA (1120 cm^{-1}) and lipid (2921cm^{-1}) bands was analyzed. (Mourant et al., 2003). The intensity ratio of RNA/lipid was significantly decreased in MCF7-125b cells but was insignificant for T47D-125b cells. This decrease implies a decrease in the growth rate of the MCF7-125b cells. Moreover this decrease was more profound for MCF7 cells compared to T47D cells. The significant decreased proliferation rate in MCF7-125b cells with respect to the MCF7-EV cells was also confirmed by trypan blue exclusion and MTT assay results (Ozek et al., 2010, Akhavantabasi, 2012). On the other hand, no decreased proliferation rate in T47D-125b cells in comparison to the T47D-EV cells was also demonstrated by MTT assay (Akman et al., 2015, Akhavantabasi, 2012). These results were in accordance with the results acquired by another study (Guo et al., 2009). The differences in the proliferation rate of miR-125b transfected MCF7 T47D cells may be explained by the differences in the level of endogenous mature miR-125 family members in these two cell lines. These differences which were also demonstrated by Shiva (2012) revealed that higher miR-125a level was observed in T47D cell with respect to the MCF7 cells. Since miR-125b and miR-125a contain similar seed structure, they can target same mRNAs. Therefore, miR-125a may target mRNA which has a regulatory role in proliferation and thus inhibits the binding of miR-125b to same mRNA in T47D cells. miR-125b transfected induced alterations in the proliferation of MCF7 and T47D cells are also due to the variations of their cellular transcriptomes, specifically the protein expressions which have roles in cellular proliferation. Similarly, in a previous study, Aka and Lin (2012) revealed that proteins implicated in cell proliferation stimulation seem to be more up-regulated in T47D as compared to MCF7, whereas proteins involved in cell growth regression are therein down-regulated (Adjo Aka et al., 2012).

To screen the changes in transcriptional activity of the breast cancer cells with miR-125b transfection, RNA/DNA band ratio was measured by taking the ratio of intensity values of the RNA (1121 cm^{-1}) and DNA bands (1020 cm^{-1}). (Salman et al., 2001).

The significant decline in this ratio was acquired in miR-125b transfected breast cancer cells. This indicated a reduction in the transcriptional status of these cells.

Glycogen/phosphate ratio is used to monitor the alterations in the metabolic activity of cancer cells. (Ramesh et al., 2002, Salman et al., 2001) To determine these alterations in breast cancer cells with miR-125b transfection, this band ratio was calculated from the ratio of the intensity values of the glycogen and phosphate bands which were located at 1045 cm^{-1} and 1084 cm^{-1}, respectively. Accordingly, the significant increase in the glycogen/phosphate ratio ($p < 0.05$) was found in MCF7-125b and T47D-125b cells, implying the decline in metabolism of miR-125b transfected cells. Moreover, the decreased this ratio were shown in cancer cells with respect to the normal cells by other FTIR studies. (Ramesh et al., 2002, Salman et al., 2001).

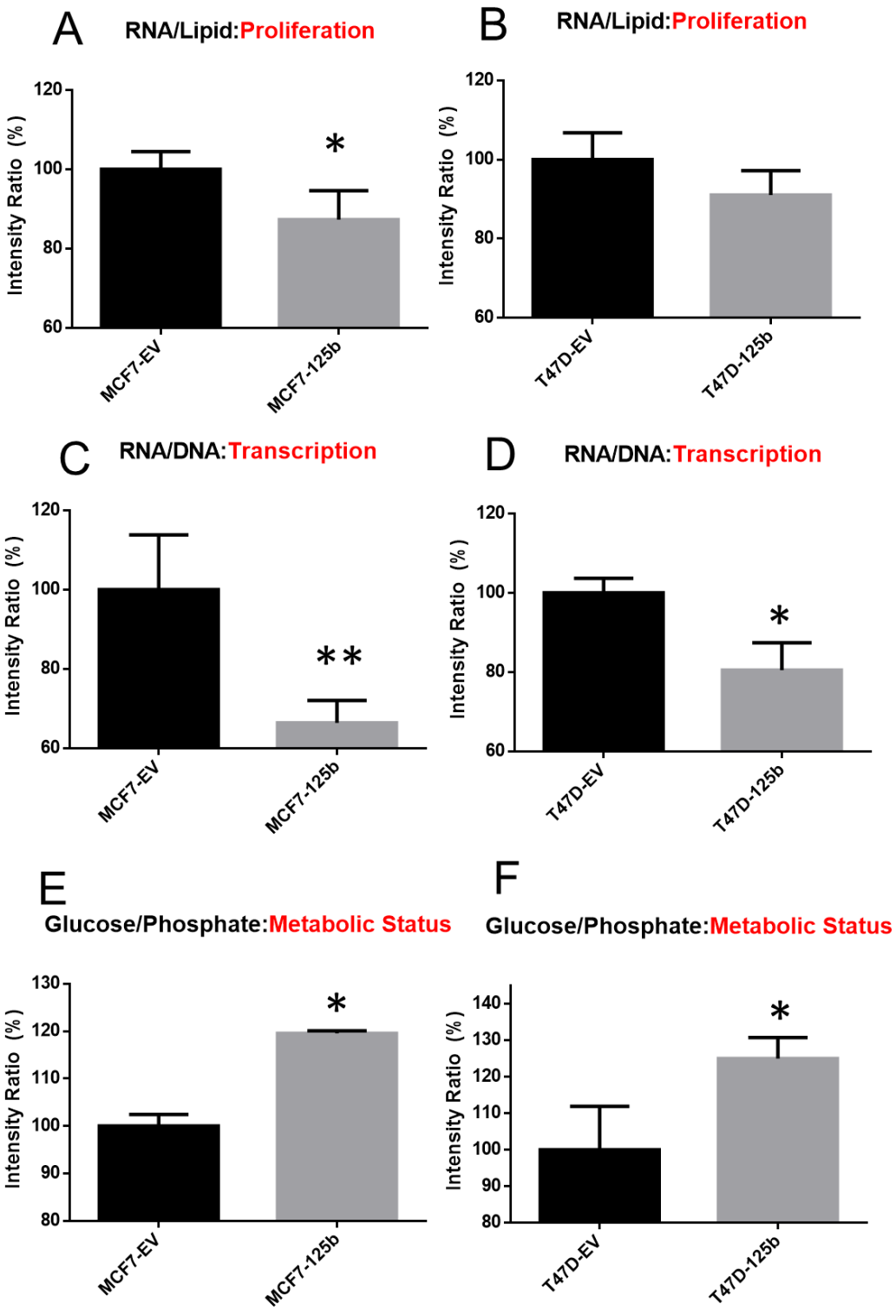

Figure 35 (A,B) Proliferation, transcription (C,D) and metabolic (E,F) status of EV and miR-125b transfected MCF7 and T47D cells (Figure 35A, C and E are adapted from Ozek et. al.,2010).

3.1.1.2 Chemometric Analysis

To identify whether there is a discrimination between EV and miR-125b transfected breast cancer cells, we performed unsupervised chemometric analysis such as PCA and HCA are directly applied to the spectra of MCF7 and T47D cells without doing any characterization studies such as mentioned above.

3.1.1.2.1 Principal Component Analysis (PCA)

PCA is a powerful multivariate analysis approach for the analysis of large spectral data sets. It enables to determine spectral variabilities among studied groups, thus to identify and differentiate different spectral groups using score plots. Therefore, it is widely used to discriminate the different biological systems such as microorganisms, cell, membranes, even tissues. Spectral variabilities are explained by principal components (PCs). The first PC describes the most variance within the data set. The second PC describes the most of the remaining variance so on. Each PC has associated with it a component score vector and loading vector. Score plots are plotted based on a pair of two score vectors. These plots used to demonstrate the relationships between studied groups of samples. In our study, the score plots for EV and miR-125b transfected MCF7 and T47D cells were demonstrated in Figure 36 A and B, respectively. As can be seen from the Figure 36A, 31% of the total data variances between EV and miR-125b transfected MCF7 cells were explained by PC2. However, 94% of data variances between EV and miR-125b transfected T47D cells were described by PC1 and PC2. (Figure 36B). The score plots of both cells indicated that transfected cells were successfully discriminated from each other for both MCF7 and T47 D cells, implying that the biochemical profiles of the studied groups in both cell lines were significantly different from each other.

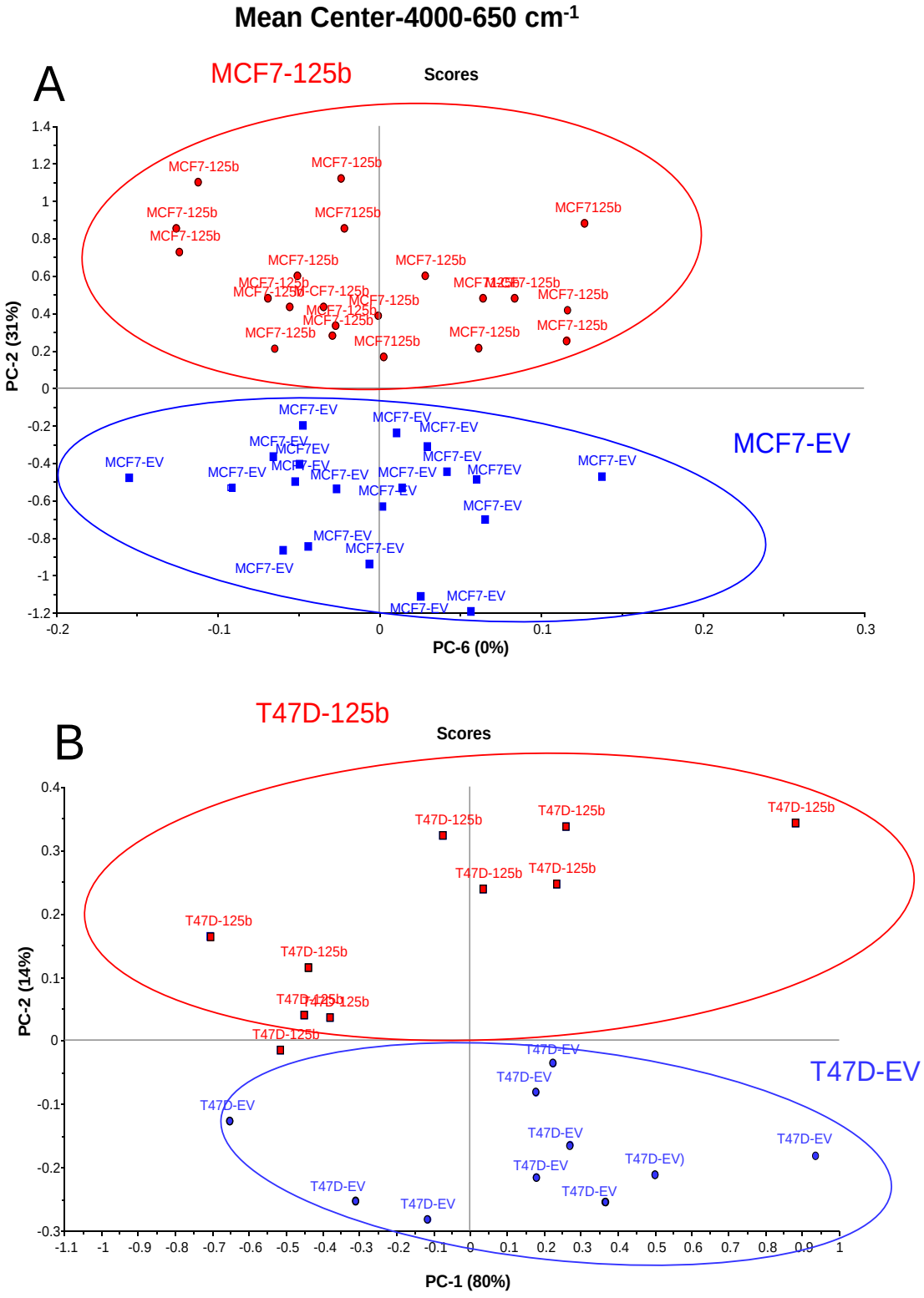

Figure 36 PCA score plots for EV and miR-125b transfected MCF7 (A) T47D (B) cancer cells in the 4000-650 cm^{-1} spectral region.

In PCA, loading plots of PC score values demonstrate the spectral origin of the variations which differentiate the data groupings according to the wavenumbers. This plots have a spectral dimension, where positive and negative peaks can be observed. If the original spectrum is assigned to positive score values, positive peaks in the loadings indicate increased contribution of IR of the respective signals in the measured IR spectra. In contrast, negative loading bands denote a reduced contribution of the respective signals in the measured IR spectra. The loading plots for MCF7 and T47D cells were shown in Figure 37A and B respectively. As can be inferred from these plots, high loading values for C-H stretching (3000-2800 cm^{-1}) and fingerprint region (1800-650 cm^{-1}) figures was obtained, indicating the changes in the intensity of spectral bands in these regions. These changes were due to miR-125b reexpression in MCF7 and T47D cells and these alterations enabled to distinct the studied groups.

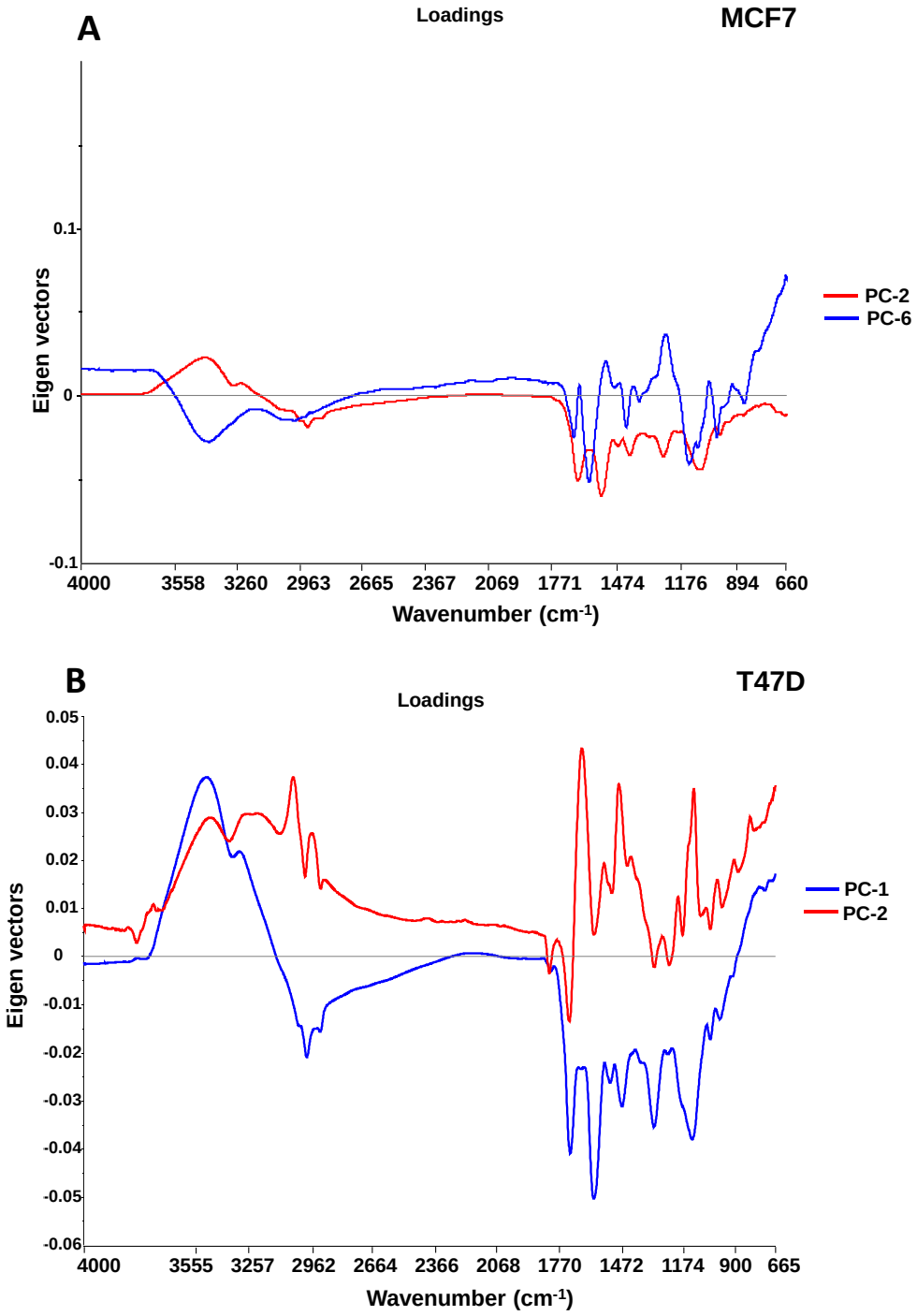

Figure 37 PCA loading plots for EV and miR-125b transfected A) MCF7 B) T47D cancer cells in the 4000-650 cm^{-1} spectral region.

3.1.1.2.2 Hierarchical Cluster Analysis (HCA)

In addition to PCA analysis, cluster analysis was employed to differentiate the EV and miR-125b transfected breast cancer cells based on the spectral differences. A combination of PCA and HCA approach enables the efficient and accurate spectral data analysis. In HCA, groups are clustered and demonstrated as dendrograms. Figure 38A and B demonstrated the dendrograms for MCF7 and T47D cells, respectively. In both cell lines, EV and miR-125b transfected cells were efficiently clustered as a separate group. We obtained higher heterogeneity values in both EV and miR-125b transfected MCF7 and T47D cell lines. This indicated that there were significant alteration in molecular content and structure between both EV and miR-125b cells.

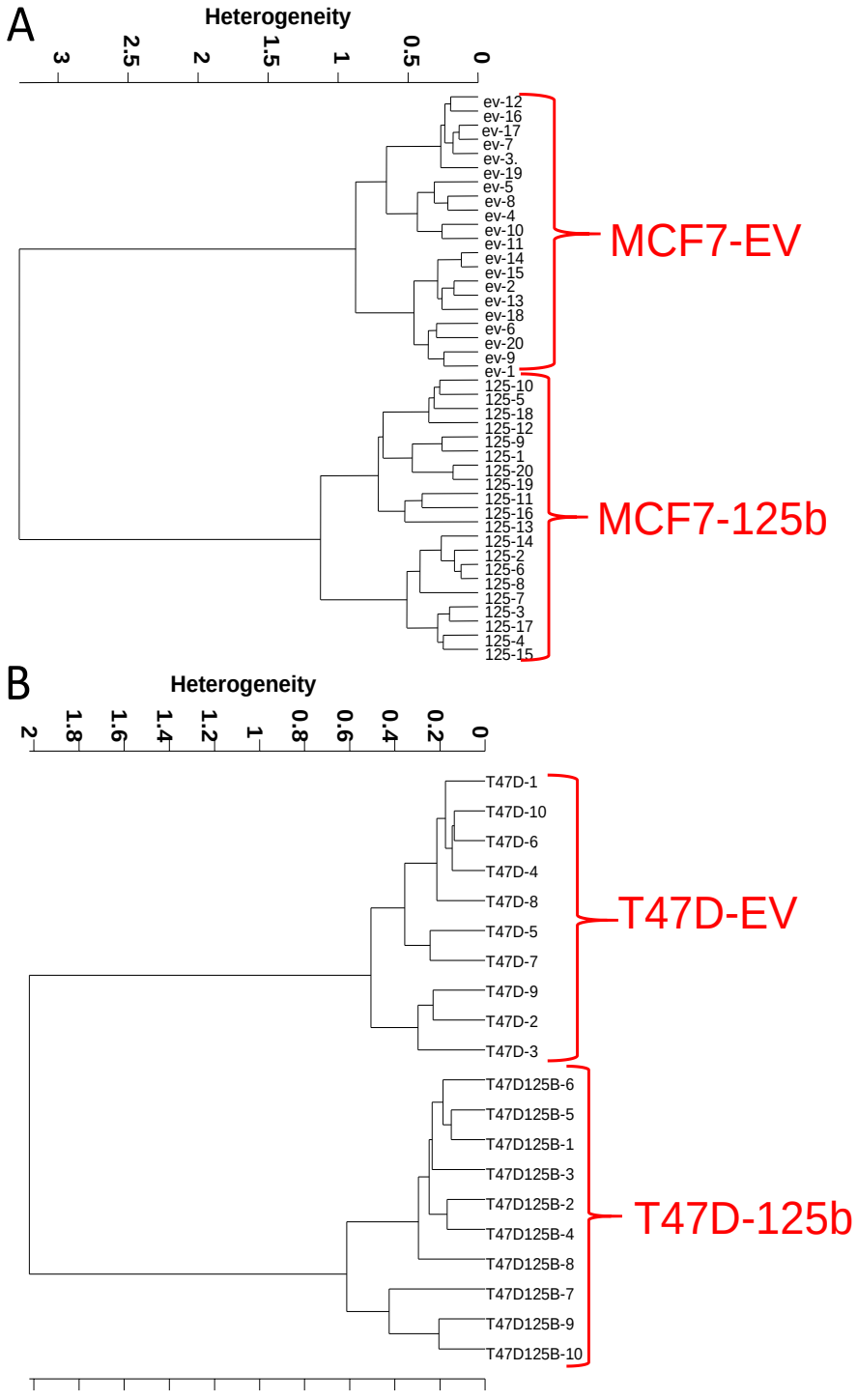

Figure 38 Cluster analysis of EV and miR-125b transfected MCF7 (A) and T47D (B) cells in the 3050-2800 cm^{-1} and 3800-800 cm^{-1} spectral regions, respectively (Figure38A is taken from Ozek et. al.,2010).

3.2 Elucidation of miR-125b reexpression induced alterations in the type and content of breast cancer cell lipids

Deregulation of metabolism is known as one of the hallmark of cancer cells (Cairns et al., 2011). Specifically, alteration of lipid metabolism has been increasingly recognized as a hallmark of cancer cells (Santos and Schulze, 2012). This metabolism is regulated by oncogenic signals and important for the etiopathogenesis of the cancers (Cantor and Sabatini, 2012, Santos and Schulze, 2012). It has been documented that tumors such as breast, colon etc. are characterized by the high rate of lipid metabolism (Li et al., 2000, Yoon et al., 2007). In recent years, the regulatory role of miRNAs in metabolism of cancer cell has also been reported (Wen and Friedman, 2012). However, it is not clear how these micromanagers regulate the lipid metabolism of cancer cells. Specifically, the role of miR-125b in breast cancer lipid metabolism has not been demonstrated yet. Furthermore, the predicted target genes of this miRNA were analyzed through miRNA target prediction databases. It has been found that several targets of this miRNA have roles in lipid metabolism and these targets were given in Table 5.

Table 5 Examples of putative gene targets of miR-125b which have roles in lipid metabolism.

Target Gene	Gene Name	Function
ELOVL6	ELOVL fatty acid elongase 6	First and rate-limiting step of fatty acid elongation
ELOVL4	ELOVL fatty acid elongase 4	Biosynthesis of fatty acids
ELOVL1	ELOVL fatty acid elongase 1	Elongation of very-long-chain-fatty acids
SCD	Stearoyl-CoA desaturase (delta-9-desaturase)	Fatty acid biosynthesis, primarily the synthesis of oleic acid.
SLC27A4	Solute carrier family 27 (fatty acid transporter), member 4	Translocation of long-chain fatty acids cross the plasma membrane.
PCTP	Phosphatidylcholine transfer protein	Transfer of phosphatidylcholine
LIPA	Lipase A, lysosomal acid, cholesterol esterase	Catalysis of the hydrolysis of cholesteryl esters and triglycerides
LPCAT4	Lysophosphatidylcholine acyltransferase 4	Catalysis of the conversion of lysophosphatidic acid (LPA) to phosphatidic acid (PA), a precursor in the biosynthesis of all glycerolipids
DGAT1	Diacylglycerol O-acyltransferase 1	Catalysis of the conversion of diacylglycerol and fatty acyl CoA to triacylglycerol.

The spectral analysis in the current study revealed that lipid metabolism in breast cancer cells was profoundly affected from miR-125b reexpression. Therefore, this part of study was performed to clarify the miR-125b reexpression-induced alterations in the lipid constituents of breast cancer cells. To achieve this aim, first, lipids of these cells were extracted and their IR spectra were collected by an ATR-FTIR spectrometer. Then, the spectra were analyzed in a qualitative and quantitative manner. We used this technique since the robustness and suitability of this method in the determination of tissue and cell lipids have been demonstrated in several studies (Derenne et al., 2014, Dreissig et al., 2009).

3.2.1 ATR-FTIR Spectroscopy for lipid extracts

3.2.1.1 Spectral Analysis

In this context, we analyzed the spectral bands in different IR regions originating from different lipids. Figure 39A, B and C represented the extracted lipid spectra of EV transfected MCF7 and T47Dbreast cancer cells at 3050-2800 cm^{-1}, 1800-1500 cm^{-1} and 1500-700 cm^{-1} spectral regions, respectively.

The major spectral bands were labeled. The frequency values and definition of these were given in Table 5. The assignment of these bands were based on IR spectra of pure lipids collected in Derenne (2013) (Appendix A) (Derenne, 2013). As evidenced by Figure 39 and Table 5, IR spectra of the lipids of MCF7 and T47D cells contained many spectral bands due to the presence of various types of lipids. In the lipid spectra, there are two main spectral regions. The first region is called C-H stretching region located between 3100-2800 cm^{-1}. This region includes spectral bands, mainly originating from the hydrocarbon chains of lipids. For example, the olefinic band is originated from =CH stretching of unsaturated fatty acids and located around 3008-3020 cm^{-1}. The second region is called fingerprint region, which is below 1800 cm^{-1}. That region contains spectral bands arising from the polar head groups of the lipids. In this region, the peak with highest intensity arises from ester C=O stretching of phospholipids and cholesterol esters. Different polar head groups have distinct IR spectra. Thus each lipid class corresponds to unique FTIR spectra. This enables to identify and quantify lipids even from the complex mixture (lipid extracts).

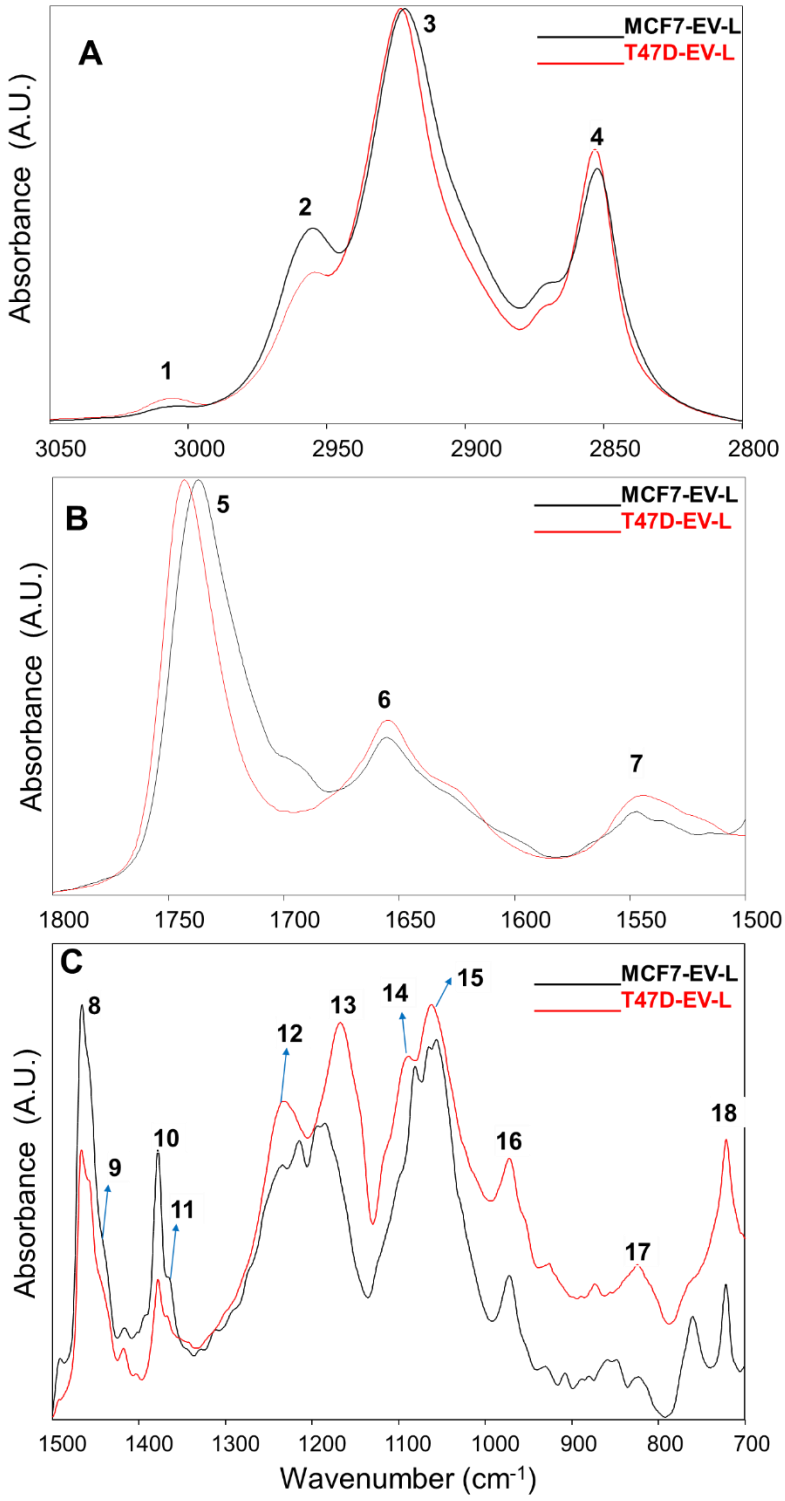

Figure 39 The extracted lipid spectra of EV and miR-125b transfected MCF7 cells in the A) 3050-2800 cm^{-1}, B) 1800-1500 cm^{-1} and C) 1500-700 cm^{-1} regions .

Table 6 Band assignments of major absorptions in IR spectra of breast cancer cell lipids in 3030–700 cm^{-1} region based on literature (Derenne et al., 2014, Dreissig et al., 2009).

Peak no.	Wavenumber (cm^{-1})	Definition of the spectral assignment
1	3008	Olefinic=CH stretching vibration: Unsaturated lipids
2	2958	CH_3 antisymmetric stretching: Saturated lipids
3	2921	CH_2 antisymmetric stretching: Saturated lipids
4	2851	CH_2 symmetric stretching: Saturated lipids
5	1738-40	Ester C=O stretch: Phospholipids, cholesterol esters
6	1640-1652	C=O stretching, N-H stretching:Sphingolipids
7	1545-1549	C=O stretching, N-H stretching:Sphingolipids
8	1465-1467	CH_2 deformation:Fatty acids
9	1443	CH_2 cyclic deformation:Cholesterol, cholesterol esters
10	1378–1381	CH_3 deformation:Fatty acids
11	1365	CH_2 deformation:Fatty acids
12	1225–1234	PO_2 antisymmetric: Phospholipids
13	1174-1179	C-O antisymmetric : Phospholipids, cholesterol esters
14	1084-1090	PO_2 symmetric: Phospholipids
15	1055-1070	C-O-H vibration: Sphingolipids, cholesterol
16	970/971	$N+–(CH_3)_3$: Phosphatidyl choline,Sphingomyelin
17	822/823	P–O antisymmetric:Phospholipids
18	718-722	CH_2 rocking: Fatty acids

To detect the miR-125b transfection induced variation in unsaturated and saturated fatty acid contents of cancer cells, the C-H stretching region was analyzed since this region contains spectral bands originating from =CH, CH_3 and CH_2 antisymmetric and symmetric stretching vibrations of these fatty acids (Derenne et al., 2014, Dreissig et al., 2009). The IR spectra of extracted lipids of EV and miR-125b transfected MCF7 cells in the 3050-2800 cm^{-1} region are shown in Figure 40 A while the same region for T47D cells it is demonstrated in Figure 41A.

The olefinic band located at 3008 cm^{-1} originates from =CH stretching of unsaturated lipids .As noted in the Figures 40B and 41B, the band area of this band (band number: 1) significantly decreased in miR-125b transfected cells. To support this data, the unsaturation ratio was calculated by taking the band area ratio of olefinic and CH_2 antisymmetric stretching bands. The significant decline in this ratio was also obtained for both miR-125b transfected cell lines (Figures 40 C and 41 C). As mentioned in part 3.1.1., this decrease implies an increased in lipid peroxidation that was induced by miR-125b reexpression which also supports the result of olefinic band obtained from the analysis of cell spectra. The recent studies have demonstrated that desaturation of lipids and monounsaturated fatty acids are required for the cancer cell proliferation and survival (Igal, 2010). Among the desaturation of lipids, Stearoyl-CoA Desaturase 1 has important role in cancers. An increase in the expression of this enzyme has been implicated in several cancers. For instance, Guo and his colleagues have indicated that the significant elevated level of monounsaturated fatty acids and monounsaturated phosphatidylcholines relative to polyunsaturated fatty acids and polyunsaturated phosphatidylcholines were observed in the microenvironment of different cancers (breast, lung, colorectal, esophageal, gastric, and thyroid cancer) compared with the healthy tissue (Guo et al., 2014). Moreover the increased amount of different unsaturated fatty acids such as palmitoleate (16:1), oleate (18:1), arachinodate (20:4) was found in Aggressive and Indolent CLL (Tili et al., 2012). In these patients, miR-125b expression was downregulated as compared to the healthy ones. They also showed that normal level of these lipids except arachinodate was obtained in MEC2 cells, induced by miR-125b overexpression. In the same study, overexpression of miR-125b in MEC2 cells diminished the level of Stearoyl-Coenzyme A desaturase 1 (SCD1) which catalyzes a rate-limiting step in the synthesis of unsaturated fatty acids

(Tili et al., 2012). These results support our findings as we reported here a decreased unsaturated lipid content of miR-125b transfected in breast cancer cells.

The changes in saturated fatty acid contents was determined through the analysis of CH_3 (band number: 2) and CH_2 antisymmetric (band number: 3) bands. The band area of these bands for MCF7 and T47D cells were represented in Figures 40 and 41D, E respectively. Both of these values were significantly diminished in miR-125b transfected cells in comparison to the EV ones, implying the decrease in saturated fatty acid content due to this miRNA expression. The elevated level of saturated fatty acids such as essential, medium and long chain fatty acids in indolent and aggressive CLL has been indicated. Moreover, these patients had down-regulated miR-125b levels with respect to the healthy ones (Tili et al., 2012) In the same study, the overexpression of this miRNA induced a decrease in these fatty acids in MEC2 cells. They also implicated that the miR-125b overexpression significantly affected the expression of transcripts encoding metabolic enzymes and regulators including fatty acid elongase 6 (ELOVL6) which uses malonyl-CoA as a 2-carbon donor in the first and rate-limiting step of fatty acid elongation. These results implied that miR-125b has important role in lipid synthesis and elongation, which is in agreement with our results.

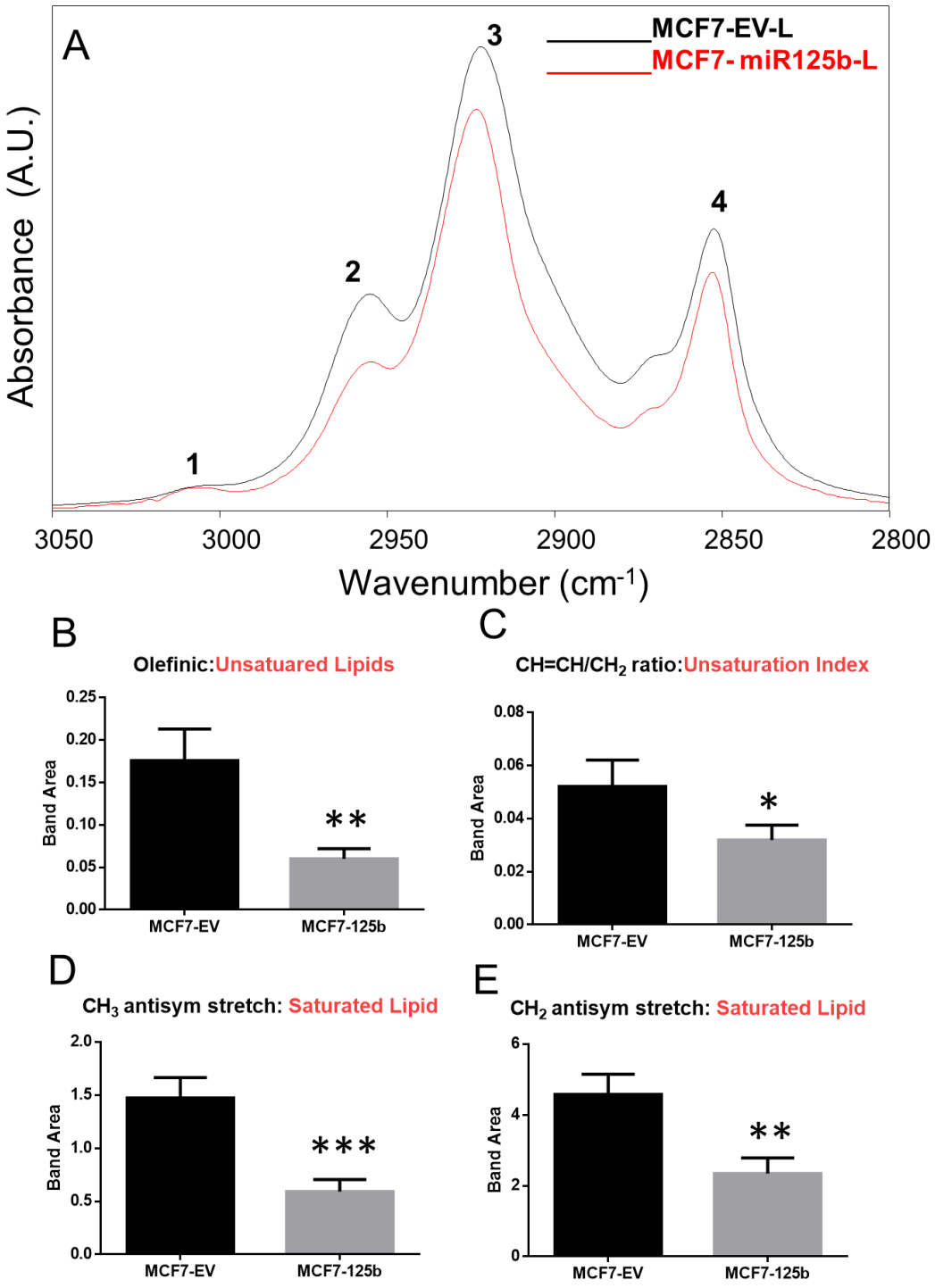

Figure 40 A) The extracted lipid spectra of EV and miR-125b transfected MCF7cells in the 3050-2800 cm-1 region B) the band area of olefinic, C) the area ratio of CH=CH/CH2, D) the band area of CH_3 and E) CH_2 antisymmetric stretching bands in EV and miR-125b transfected MCF7cells.

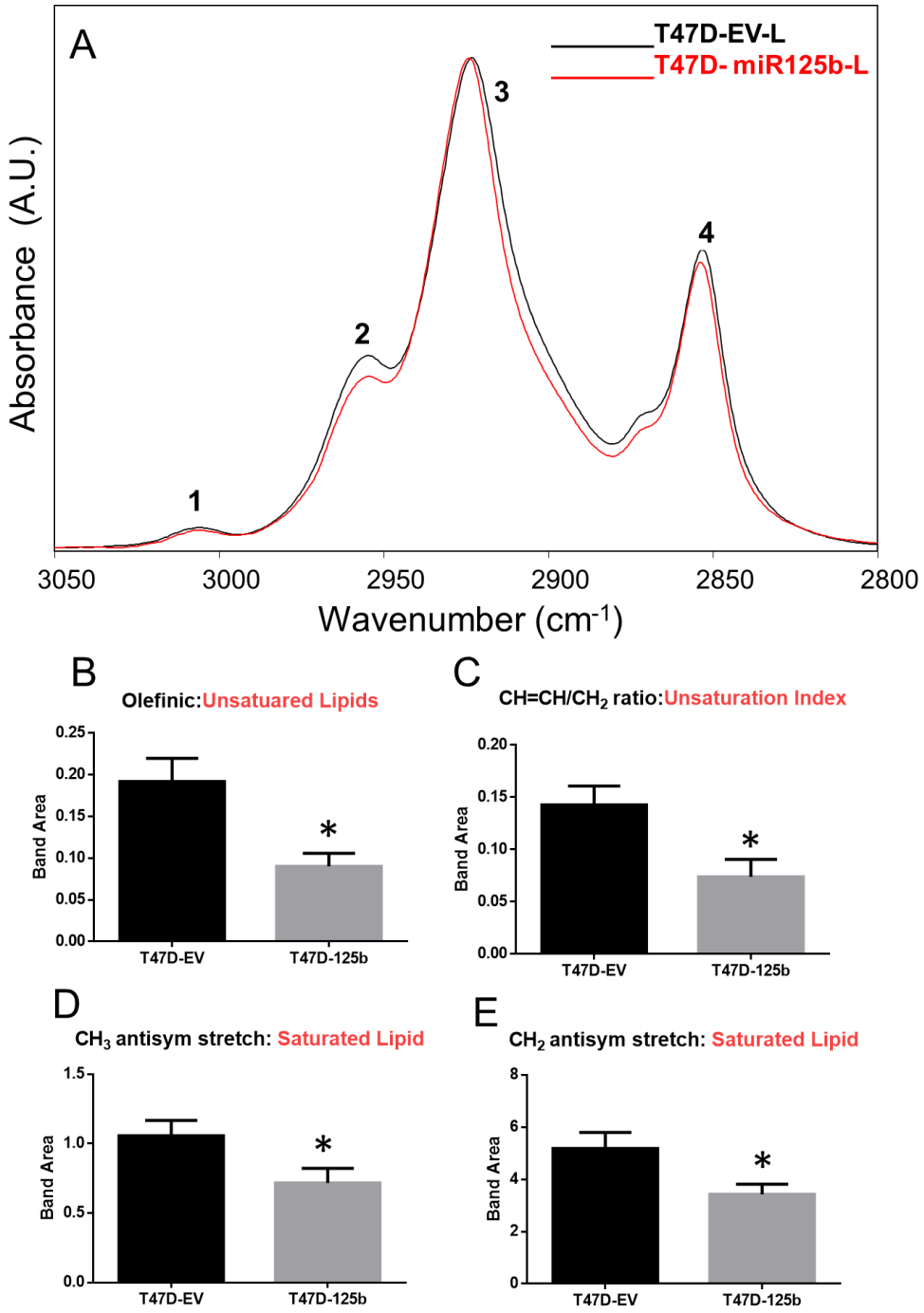

Figure 41 The extracted lipid spectra of EV and miR-125b transfected T47D- cells in the 3050-2800 cm^{-1} region B) the band area of olefinic, C) the area ratio of CH=CH/CH2 , D) the band area of CH_3 and E) CH_2 antisymmetric stretching bands in T47D-EV and T47D-125b cells.

In our study, the fingerprint region (1800-700 cm^{-1}) was analyzed as two distinct regions; namely, 1800-1500 and 1500-700 cm^{-1} spectral regions. The first region for lipid spectra of MCF7 and T47D cells was illustrated in Figures 42A and 43 A, respectively and the major lipid bands were labeled in these spectra. The ester C=O stretching band located at 1740 cm^{-1} (band number: 5) originates from phospholipids and cholesterol esters (Derenne et al., 2014, Dreissig et al., 2009). The band area of this band for both breast cancer cell lines was given in Figures 42B and 43 B. As can be inferred from these figures, the phospholipid and cholesterol ester content were significantly diminished in MCF7 cells while an increased was observed in T47D cells due to miR-125b reexpression. Since we found a decline in the phospholipid amount of T47D-125b cells by the analysis of PO_2 symmetric band, we can infer that only the cholesterol ester content of miR-125b transfected cell was increased. Alteration in phospholipid metabolism of the cells is observed when cell gains tumorigenic property. It has been reported that physical and functional interaction between membrane proteins and phospholipids (PL) affects survival, cell adhesion, and, consequently, migration and invasion of cells (Escribá et al., 2008). In 2012, Doria and her colleagues have reported that the PL alteration was associated with malignant, metastatic, and/or morphological characteristics of mammary epithelial and breast cancer cells. Specifically, they found that the highest amount in phosphatidylethanolamine (PE) content was found in non-malignant cells while the highest level of phosphatidic acid was observed in metastatic cells. In addition, the concentration of alkyl acyl PCs and phosphatidylinositol were higher in migratory cells whereas, PI was found to be lowest in non-malignant cells compared to cancer cells (Dória et al., 2013). Tili et. al (2012) have also demonstrated the elevated amount of PE in miR-125b downregulated CLL patients while normal level of PE was found in MEC2 cells following miR-125b overexpression (Tili et al., 2012). These results imply that the downregulation of miR-125b leads to the deregulation of phospholipid metabolism in breast cancer cells. However, to define the exact regulatory role of this miRNA in the phospholipid metabolism of breast cancer cells, miR-125b reexpression-induced alterations in the specific types of phospholipids such as PE, PI, PS and PC should be determined.

The bands located at 1640-1652 and 1545-1549 cm^{-1} originates from C=O and N-H stretching of sphingolipids (Derenne et al., 2014, Dreissig et al., 2009). The band area of Amide I band for MCF7 and T47D cells was shown in Figures 42C and 43 C, respectively. The significant decline in the sphingolipid content of both miR-125b transfected cells as comparison to the EV ones was acquired. This decrease was supported by the diminished content of sphingomyelin in miR-125b transfected cells (Figures 44 E and 45 E). It has been known that sphingolipids and their metabolites have important regulatory roles in cellular structural integrity and functions in fluidity, growth, differentiation, apoptosis and autophagy. Therefore, dysregulated sphingolipid metabolism contributes to the tumor pathogenesis. Tumorigenic and tumor suppressor roles of sphingolipid metabolites have been reported (Ségui et al., 2006). For example, gangliosides, and sphingosine 1-phosphate (S1P) have tumorigenic effects while ceramide, sphingosine etc. have tumor suppressor roles. (Cuvillier et al., 1996).The studies on sphingolipid metabolism and breast cancers have indicated the elevated level of S1P and increased expression of sphingosine kinase 1 in breast cancer (Ruckhäberle et al., 2008, Nagahashi et al., 2012). The lower level of sphingomyelin in malignant breast cancer was stated (Hendrich and Michalak, 2003), while the high level of the same lipid was also demonstrated in drug resistant breast cancer cells (Vijayaraghavalu et al., 2012). However, the decreased sphingolipid and sphingomyelin content of miR-125b transfected breast cancer cells may be due to two reasons. The first one is that this miRNA induced suppression of genes which transcribe enzymes play role in the synthesis of these lipids. The second reason is that miR-125b induced upregulation of genes which encode enzymes have roles in the degradation of these lipids.

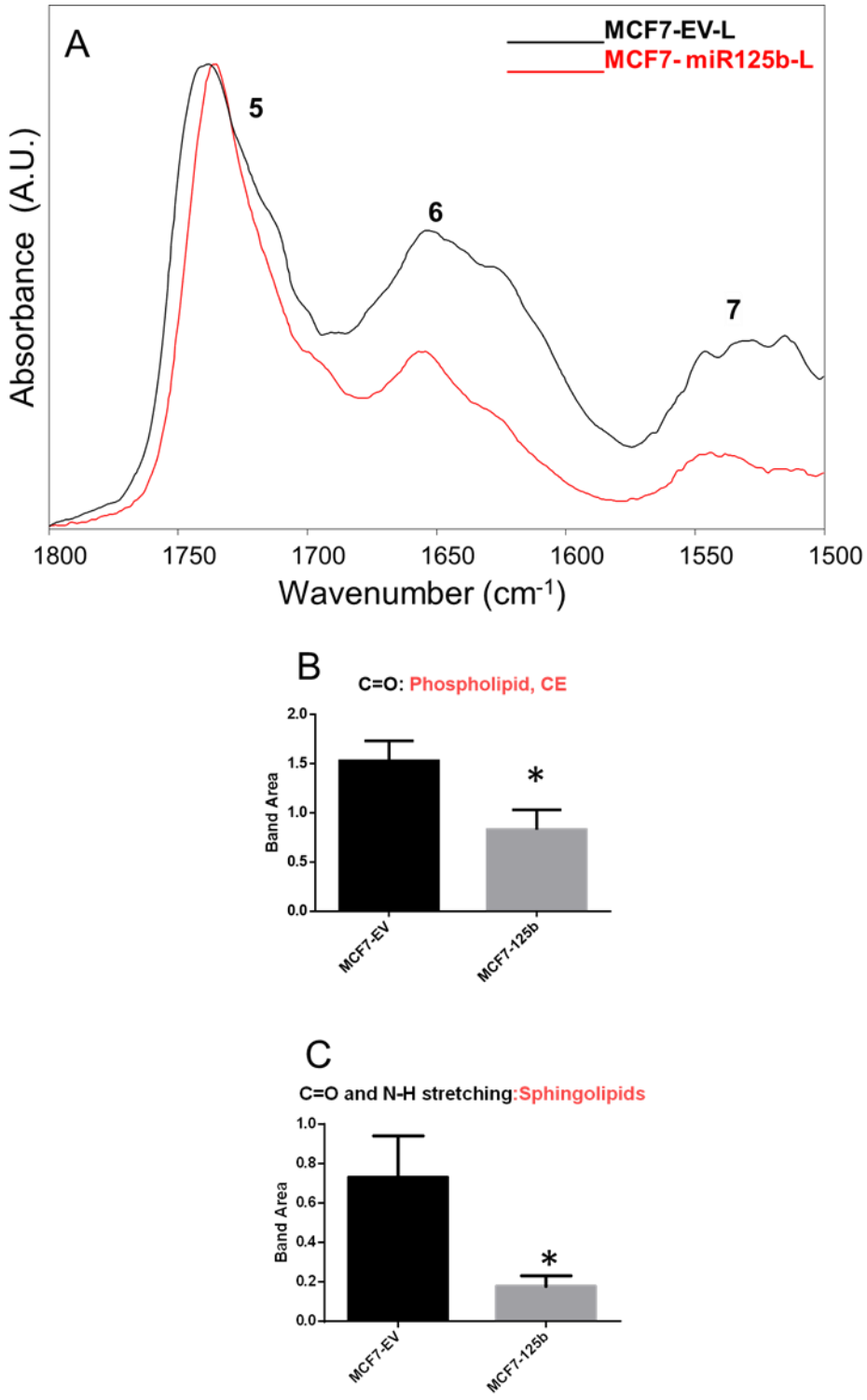

Figure 42 The extracted lipid spectra of EV and miR-125b transfected MCF7 cells in the 1800-1500 cm^{-1} region (A). The band area of C=O ester (B) and C=O and N-H stretching (C) bands in the EV and miR-125b transfected MCF7cells.

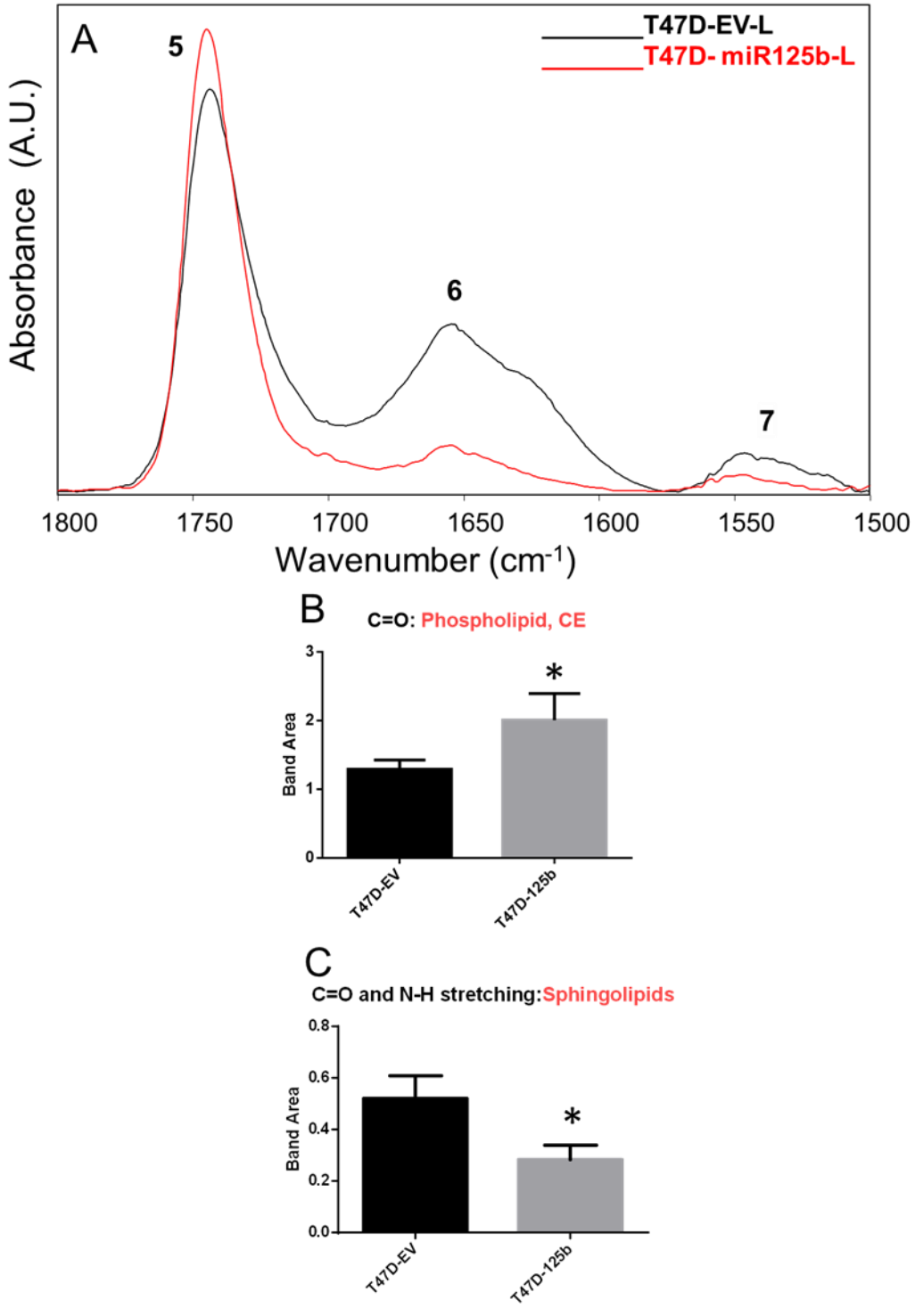

Figure 43 The extracted lipid spectra of T47D-EV and T47D-125b cells in the 1800-1500 cm^{-1} region (A). The band area of C=O ester (B) and Amide I (C) bands in the EV and miR-125b transfected T47D cells.

The second part of the fingerprint region is placed between 1500-700 cm^{-1}. Figures 44A and 45A demonstrated EV and miR-125b transfected MCF7 and T47D cells, in this region, respectively. The band areas of fatty acid related CH_2 deformation (band number: 8) bands for both these cell lines were illustrated in Figures 44B and 45B, indicating the significant decrease in fatty acid amount due to the miR-125b reexpression (Dreissig et al., 2009). This supported that the miR-125b upregulation that led to the decline in saturated and unsaturated fatty acid contents of breast cancer cells and targets of this miRNA have role in fatty acids metabolism of breast cancer cells.

The band located at 1443 cm^{-1}(band number: 9) is due to the CH_2 cyclic deformation of cholesterol, and cholesterol esters (Dreissig et al., 2009). The band areas of this band for both breast cancer cells were demonstrated in Figures 44C and 45C. As can be clearly seen from the figure, cholesterol and cholesterol ester content significantly decreased in MCF7 cells but significantly increased for T47D cells induced by miR-125b reexpression. Previous studies have demonstrated that elevated cholesterol levels are observed in cancer cells and tissues and it has role in cell proliferation, tumor progression and even in drug resistance (Luu et al., 2013, Gorin et al., 2012). Among cancers, increase in cholesterol amount of breast cancer has been reported. Moreover, the proliferative property of 27-hydroxycholesterol (27HC) was indicated in estrogen receptor (ER)-positive breast cancer cells (Nelson et al., 2013).The increased level of cholesteryl ester in breast cancer tumors has been also shown recently (de Gonzalo-Calvo et al., 2015). Although, several miRNAs, which have regulatory role in cholesterol metabolism, have been reported (Rotllan and Fernández-Hernando, 2012). However, Tili and his colleagues have performed a study on miR-125b expression and metabolon levels in CLL (Tili et al., 2012). They indicated that cholesterol and their derivative level remains unchanged in miR-125b downregulation and overexpression. On the other hand, Chen et. al. reported that the inhibition of miR-125-5p increased total cholesterol in human monocytic leukemia (THP-1) (Chen et al., 2009) that supports our findings. In our study, the decreased and increased cholesterol and cholesterol ester levels in MCF7-125b and T47D-125b cells have implied that the deregulation of miR-125b expression lead to the alterations of these lipid metabolism of breast cancer cells without the direct activity of their targets.

Figures 44Dand 45D demonstrated the areas of PO_2 symmetric stretching band for both EV and miR-125b transfected MCF7 and T47D cells, separately. This band is arisen from phospholipids and the area of this band significantly decreased in both miR-125b transfected cell lines, implying diminished phospholipid content because of miRNA reexpression, which proves the role of miR-125b reexpression in the alteration of phospholipid constituents of breast cancer cells (Dreissig et al., 2009, Mantsch and Chapman, 1996).

To determine the alterations in phosphatidyl choline and sphingomyelin content, the band located at 970-971 cm^{-1}, due to the $N+–(CH_3)_3$ vibrations (band number:16) can be used (Dreissig et al., 2009, Mantsch and Chapman, 1996). As illustrated in Figures 44E and 45E, the area of this band significanly reduced in miR-125b transfected breast cancers with respect to their EV ones. Abnormal choline metabolism, the activation of this metabolism is specifically thought to be one of the hallmark of tumor cells. This is characterized by increased phosphocholine (PCho) and total choline-containing compounds (tCho) in cancer cells that was previously demonstrated in tumors using magnetic resonance spectroscopy (Griffiths et al., 1981, Griffiths et al., 1983).Similar to other cancers, the increase in phosphatidyl choline content, glycerophosphocholine and total choline containing compounds in breast cancers have also been demonstrated in several studies (Ide et al., 2013, Gribbestad et al., 1998). The decrease in this lipid content, which is induced by miR-125b expression, indicates that the mRNA targets of miR-125b have a role in lipid metabolism. Tili and his colleagues have demonstrated the increase in choline and glycerophosphocholine content in miR-125b downregulated indolent and aggressive CLL patients (Tili et al., 2012). They also identified the 2.6 fold down regulation of phosphatidyl choline transfer protein (PCTP) in MEC2 cells following miR-125b overexpression which was one of the target of miR-125b (Tili et al., 2012).TargetScan analysis of miRNA confirms that PCTP is its target. This result supports the role of miR-125b downregulation in the abnormal choline metabolism in breast cancer cell.

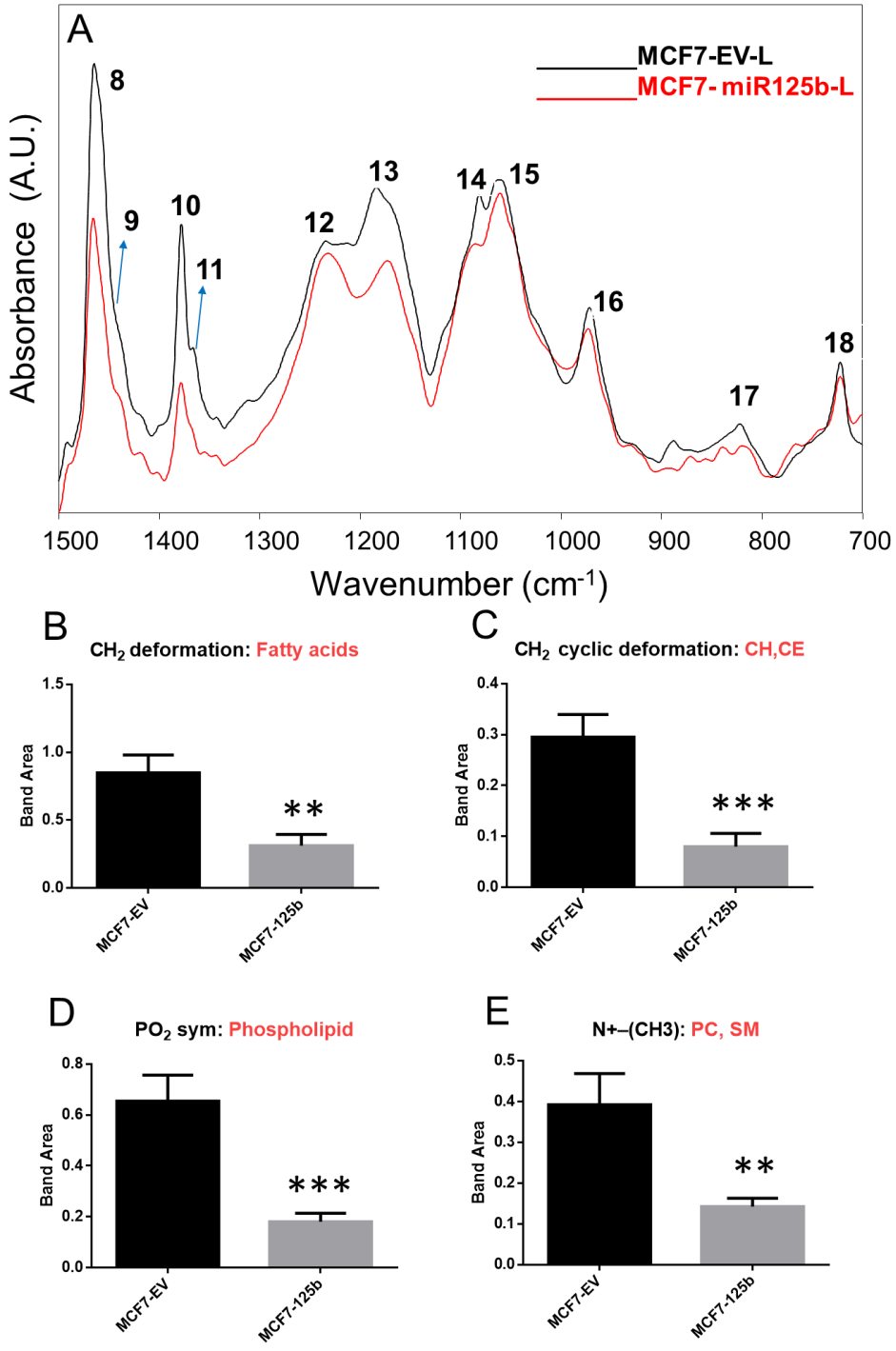

Figure 44 The extracted lipid spectra of EV and miR-125b transfected MCF7 cells in the 1500-700 cm^{-1} region (A). The band area of CH_2 deformation (B), CH_2 cylic deformation (C), PO_2 symmetric (D) and N+-(CH3) (E) stretching bands in EV and miR-125b transfected MCF7 cells.

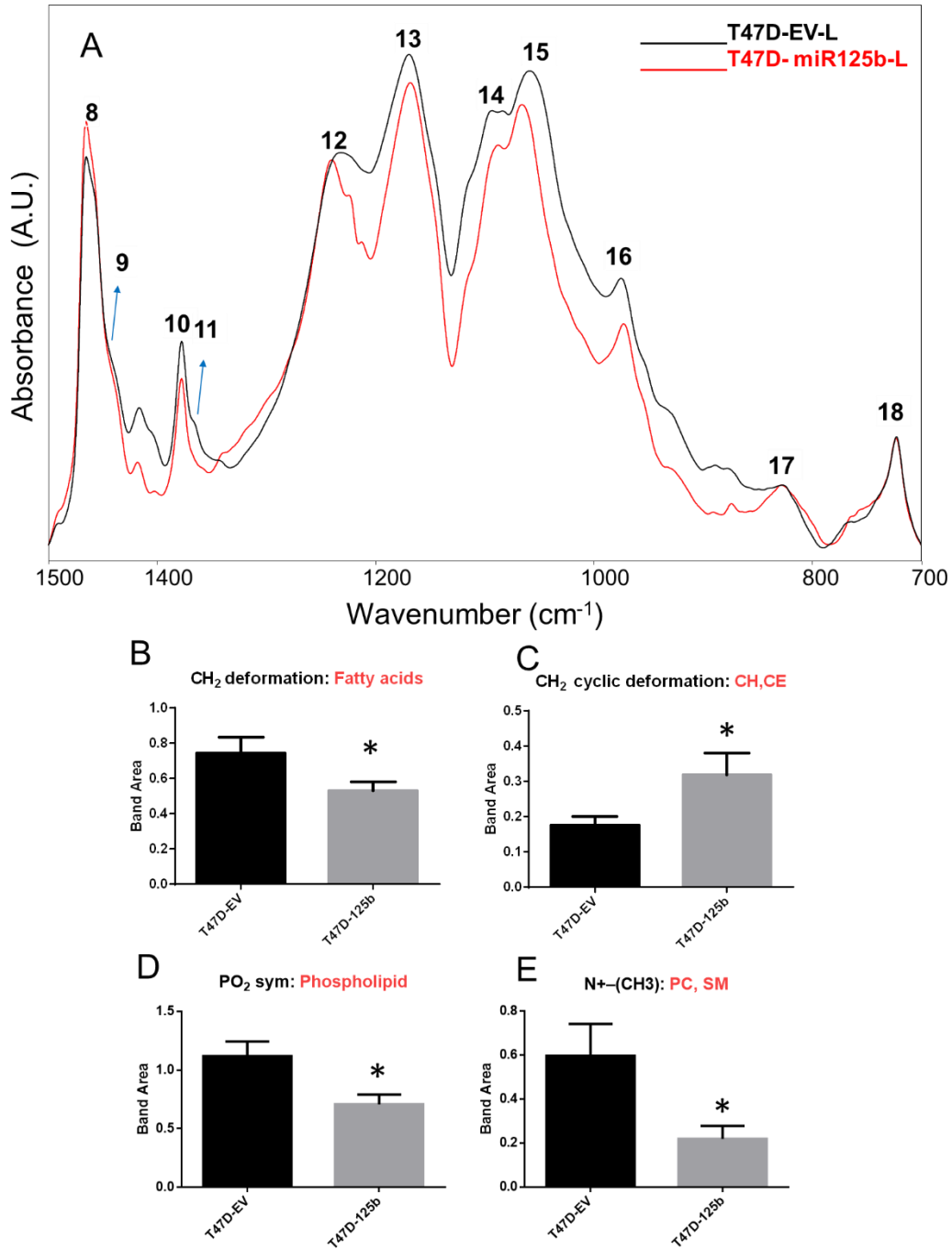

Figure 45. The extracted lipid spectra of T47D-EV and T47D-125b cells in the 1500-700 cm^{-1} region (A). The band area of CH_2 deformation (B), CH_2 cylic deformation (C), PO_2 symmetric (D) and N+-(CH3) (E) stretching bands in T47D-EV and T47D-125b cells.

3.2.1.2 Chemometric Analysis

To see whether there is a clear discrimination between EV and miR-125b transfected MCF7 and T47D cells extracted lipids, unsupervised chemometric analyses (PCA and HCA) were performed.

3.2.1.2.1 Principal Component Analysis

The score plots for extracted lipids of EV and miR-125b transfected MCF7 and T47D cells were illustrated in Figure 46A and B, respectively. As detailed in the figure, for MCF7 cells 93% of total variation (PC1+PC2) between EV and miR-125b transfected cells was transfected in the first two PCs, while for T47D cells, total variation (PC1+PC5) was found to be 88%. As can be seen from both figures, there was a clear segregation of EV and miR-125b cell lipids from each other.

Figure 47A and B, demonstrated the PCA loading plots for the extracted lipids of EV and miR-125b transfected MCF7 and T47D cells in the 4000-650 cm^{-1} spectral region, respectively. As can be deduced from these plots, the intensity of the spectral bands in C-H stretching region decreased in both miR-125b transfected cells. This region is used to obtain information about saturated and unsaturated lipids. The decreased intensity of the spectral bands supports the decline in these lipid concentration which were obtained from IR spectral analysis of both EV and miR-125b transfected cells. Moreover, most of the spectral bands in fingerprint region (1800-650 cm^{-1}) showed negative loading values, implying the decreased the amount of these bands originated molecules in miR-125b transfected breast cancer cells. These obvious differences between the loading plots in the lipids of EV and miR-125b indicated the altered lipid profiles of MCF7-125b and T47D-125b cells.

Both the score and loading plots of both cell lipids supported that miR-125b reexpression induced alterations in the lipid metabolism of breast cancer cells.

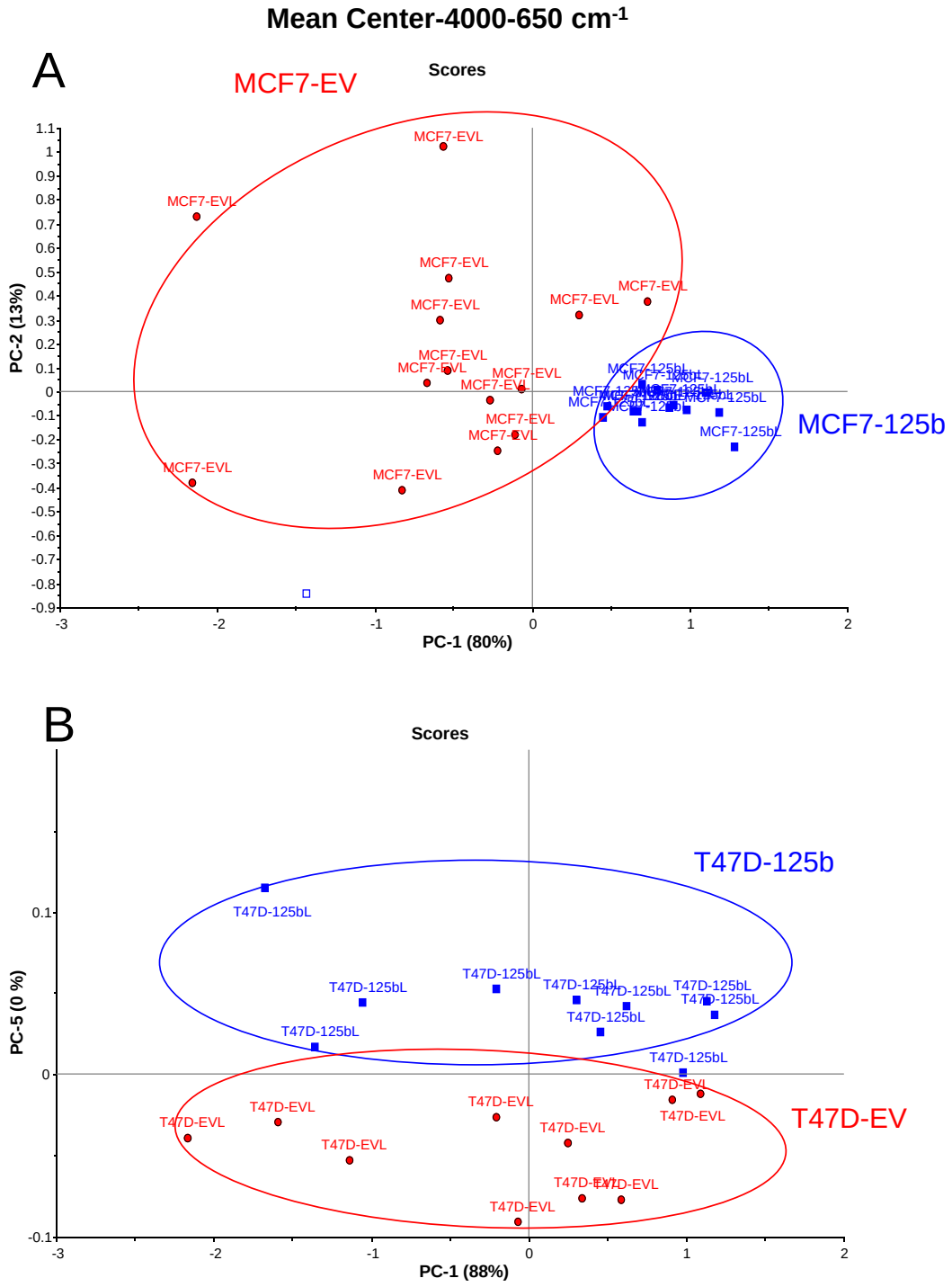

Figure 46 PCA score plots for EV and miR-125b transfected A) MCF7 B) T47D cancer cell lipids in the 4000-650 cm^{-1} spectral region.

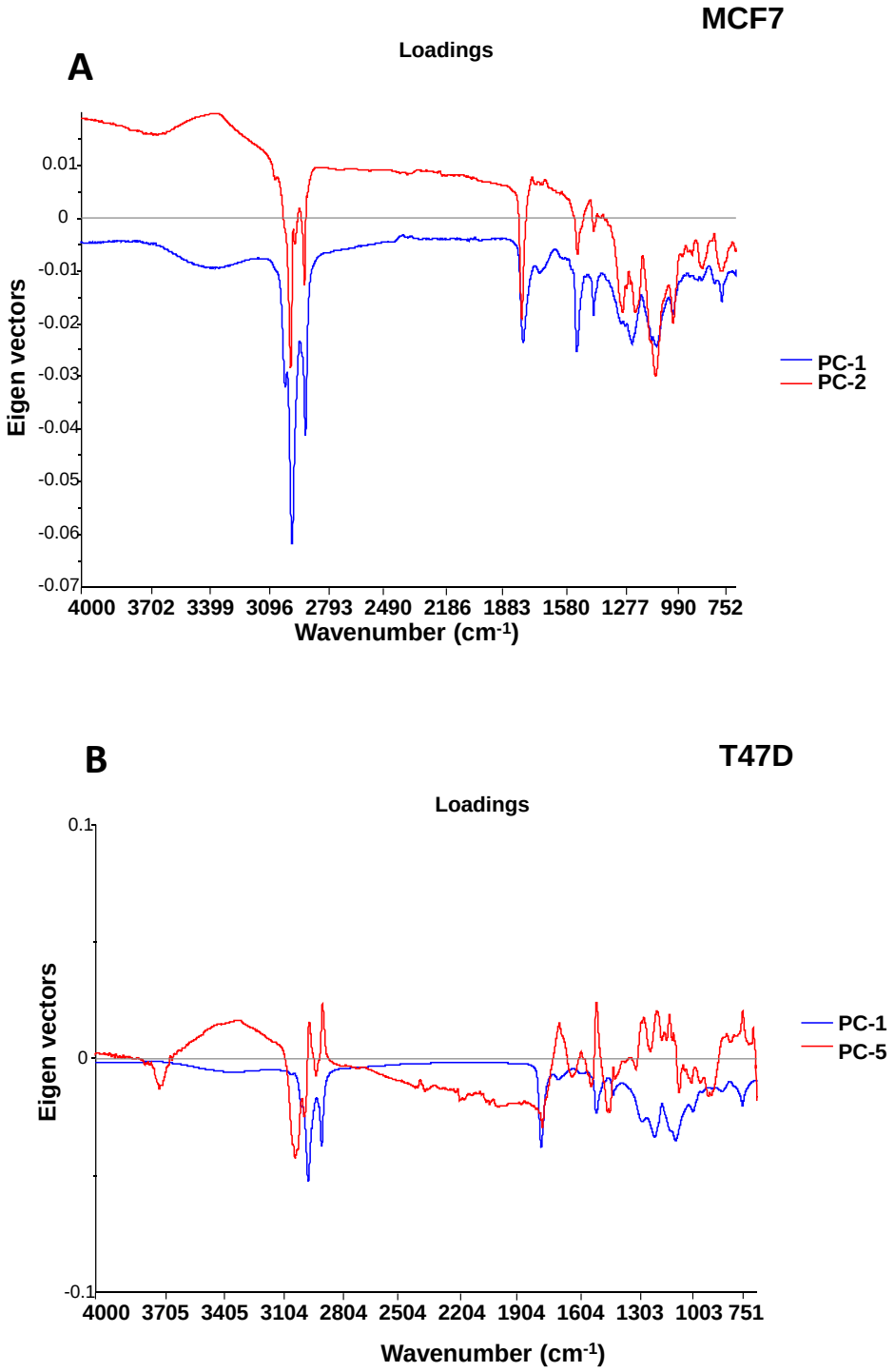

Figure 47 PCA loading plots for EV and miR-125b transfected A) MCF7 B) T47D cancer cell lipids in the 4000-650 cm^{-1} spectral region.

3.2.1.2.2 Hierarchical Cluster Analysis

Finally, HCA was employed to distinguish the extracted lipids of breast cancer cells according to the differences in their ATR-FTIR data. Figure 48A showed the HCA dendograms of extracted lipids of EV and miR-125b transfected MCF7 cells, whilst Figure 48B demonstrated the extracted lipids of T47D-EV and T47D-125b cells. As shown in figures, both cell types were successfully differentiated from control groups, indicating meaningful differences between the lipids of studied cancer cell types.

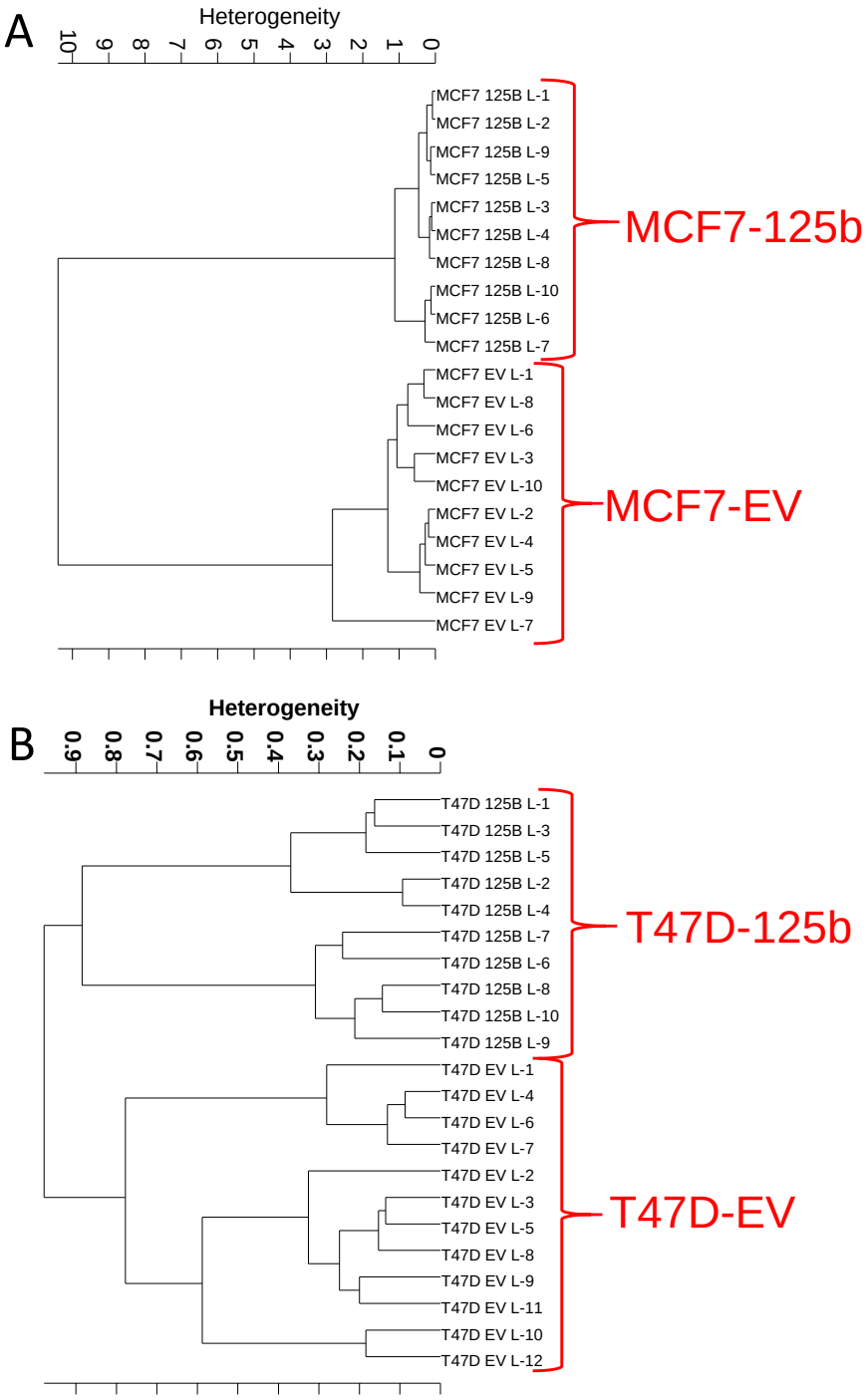

Figure 48 Cluster analysis of EV and miR-125b transfected MCF7 (A) and T47D (B) cell lipids in the 4000-650 cm^{-1} spectral regions, respectively.

CHAPTER IV

CONCLUSION

miRNAs, as being micro-regulators, have fundamental roles in many cellular functions including the metabolism of cells. Therefore, it is inevitable that the deregulation of these molecules lead to pathogenesis of cancers. Among deregulated miRNAs in breast cancer, miR-125b is one of the most downregulated miRNAs (Calin et al., 2002). Although several targets of this miRNA and their roles in main cellular properties e.g. proliferation, migration etc. have been determined in several cancers, the link between its deregulation and the consequences of this deregulation in the molecular alterations especially in the lipids of cancer cells has not been fully elucidated yet. For that reason, we performed holistic approach to reveal these changes in miR-125b transfected and empty vector transfected breast cancer cells by ATR-FTIR spectroscopy coupled with chemometric analysis methods and ESR spectroscopy.

The spectral data analysis of cell and cell lipids indicated that the decrease in the amount of saturated and unsaturated fatty acids was found in MCF7-125b and T47D-125b cells. Moreover, the shorter chains of fatty acids was observed in both cells. These changes may be due to increase in lipid peroxidation. Moreover, miR-125b reexpression lowered the membrane fluidity in MCF7-125b cells while it enhanced the same parameter in T47D-125b cells. The protein and nucleic acid amounts were significantly diminished in both cell lines which may be due to the miR-125b induced-suppression of the targets that have role in the synthesis of these molecules. Regarding cellular properties, the decline in the metabolic and transcriptional status of miR-125b transfected cells was observed. The glycogen content of MCF7 was found to be decreased whilst this parameter increased for T47D-125b cells. Furthermore, the

proliferation rate was found to be significantly lower for MCF7-125b relative to the T47D-125b cells which may be due to fact that these cells may have differences in terms of their transcriptomes and what miR-125b targets in these cells.

To define which molecular content was more profoundly altered with miR-125b transfection, lipid/protein ratio was calculated. The decrease in this ratio for MCF7 cell was obtained, implying that lipid metabolism was more profoundly altered. On the other hand, the increase in this ratio for T47D cell was attained, indicating more profound changes in protein relative to lipid metabolism. Therefore, to reveal the variations in the content and types of lipids, the extracted lipid spectra of EV and miR-125b transfected MCF7 and T47D cells were examined. The results indicated the reduction in the phospholipid, sphingolipid and sphingomyelin amount for both cell lines with miR-125b expression. The reduced cholesterol, cholesterol ester concentration was seen in MCF7 cells but opposite value was obtained for T47D cells. The differences in the alterations of cholesterol and cholesterol ester concentration may account for the dissimilarity of membrane dynamical changes between cells since the change in the relative ratio of cholesterol and sphingolipid content in membranes differently affects membrane fluidity.

Based on these contextual alterations in breast cancer cells following miR-125b transfection, to indicate whether there is a discrimination between EV and miR-125b transfected cells, PCA and HCA methods were applied to the both cell and cell lipid spectra. PCA score plots revealed the successful and separate clustering of studied groups. Loading spectra showed the alterations in different molecules that lead them to be distinguished. In addition to these analysis, HCA dendrogram results demonstrated the discrimination between miR-125b transfected and EV transfected breast cancer cells with higher heterogeneity.

Both spectral data and chemometric analysis results support deregulation of miR-125b expression which may be associated with metabolic alterations of epithelial breast cell, especially lipids, and contribute to the pathogenesis of breast cancer cells. Our results contributed to the elucidation of the global roles of miRNAs in cancer etipathogenesis. Moerover, this study proved the capability of ATR-FTIR spectroscopy in the

discrimination of cancer cells based on miRNA expression .However, to elucidate the holistic roles of this miRNA in breast cancer, further metabolic assays/arrays and genetic studies are required. Future studies will focus on these aspects.

REFERENCES

Adjo Aka J, Lin S-X, Rameshwar P (2012) Comparison of functional proteomic analyses of human breast cancer cell lines T47D and MCF7. PLoS One 7**:**e31532.

Akhavantabasi S (2012) Functional Characterization of Two Potential Breast Cancer Related Genes, in Series Functional Characterization of Two Potential Breast Cancer Related Genes, Vol. PhD, Biological Sciences, Middle East Technical University.

Akhavantabasi S, Sapmaz A, Tuna S, Erson-Bensan AE (2012) miR-125b targets ARID3B in breast cancer cells. Cell structure and function 37**:**27-38.

Akman HB, Selcuklu SD, Donoghue MTA, Akhavantabasi S, Sapmaz A, Spillane C, Yakicier MC, Erson-Bensan AE (2015) ALCAM is indirectly modulated by miR-125b in MCF7 cells. Tumor Biology 36**:**3511-3520.

Alahari S, Alahar S (2013) MicroRNA in Cancer, Springer.

Ambs S, Prueitt RL, Yi M, Hudson RS, Howe TM, Petrocca F, Wallace TA, Liu C-G, Volinia S, Calin GA (2008) Genomic profiling of microRNA and messenger RNA reveals deregulated microRNA expression in prostate cancer. Cancer research 68**:**6162-6170.

Avery-Kiejda KA, Braye SG, Forbes JF, Scott RJ (2014) The expression of Dicer and Drosha in matched normal tissues, tumours and lymph node metastases in triple negative breast cancer. BMC cancer 14**:**253.

Baker MJ, Trevisan J, Bassan P, Bhargava R, Butler HJ, Dorling KM, Fielden PR, Fogarty SW, Fullwood NJ, Heys KA (2014) Using Fourier transform IR spectroscopy to analyze biological materials. Nature protocols 9**:**1771-1791.

Banyay M, Sarkar M, Gräslund A (2003) A library of IR bands of nucleic acids in solution. Biophysical chemistry 104**:**477-488.

Banzhaf-Strathmann J, Edbauer D (2014) Good guy or bad guy: the opposing roles of microRNA 125b in cancer. Cell Communication and Signaling 12.

Blenkiron C, Goldstein LD, Thorne NP, Spiteri I, Chin S-F, Dunning MJ, Barbosa-Morais NL, Teschendorff AE, Green AR, Ellis IO (2007) MicroRNA expression profiling of human breast cancer identifies new markers of tumor subtype. Genome Biol 8**:**R214.

Bligh EG, Dyer WJ (1959) A rapid method of total lipid extraction and purification. Canadian journal of biochemistry and physiology 37**:**911-917.

Bloomston M, Frankel WL, Petrocca F, Volinia S, Alder H, Hagan JP, Liu C-G, Bhatt D, Taccioli C, Croce CM (2007) MicroRNA expression patterns to differentiate pancreatic adenocarcinoma from normal pancreas and chronic pancreatitis. Jama 297**:**1901-1908.

Boesze-Battaglia K, Schimmel R (1997) Cell membrane lipid composition and distribution: implications for cell function and lessons learned from

photoreceptors and platelets. The Journal of experimental biology 200:2927-2936.
Bousquet M, Harris MH, Zhou B, Lodish HF (2010) MicroRNA miR-125b causes leukemia. Proceedings of the National Academy of Sciences 107:21558-21563.
Brandie NR, Margarita MI, Huy XM, Joshua KS, Bradford GH, Carolyn MK (2015) Bioenergetic differences between MCF-7 and T47D breast cancer cells and their regulation by oestradiol and tamoxifen. Biochemical Journal 465:49-61.
Brereton RG (2003) Chemometrics: data analysis for the laboratory and chemical plant, John Wiley & Sons.
Cairns RA, Harris IS, Mak TW (2011) Regulation of cancer cell metabolism. Nature Reviews Cancer 11:85-95.
Cakmak G, Togan I, Severcan F (2006) 17β-Estradiol induced compositional, structural and functional changes in rainbow trout liver, revealed by FT-IR spectroscopy: a comparative study with nonylphenol. Aquatic toxicology 77:53-63.
Calin GA, Dumitru CD, Shimizu M, Bichi R, Zupo S, Noch E, Aldler H, Rattan S, Keating M, Rai K (2002) Frequent deletions and down-regulation of micro-RNA genes miR15 and miR16 at 13q14 in chronic lymphocytic leukemia. Proceedings of the National Academy of Sciences 99:15524-15529.
Calin GA, Sevignani C, Dumitru CD, Hyslop T, Noch E, Yendamuri S, Shimizu M, Rattan S, Bullrich F, Negrini M (2004) Human microRNA genes are frequently located at fragile sites and genomic regions involved in cancers. Proceedings of the National academy of Sciences of the United States of America 101:2999-3004.
Cantor JR, Sabatini DM (2012) Cancer cell metabolism: one hallmark, many faces. Cancer discovery 2:881-898.
Catto JW, Miah S, Owen HC, Bryant H, Myers K, Dudziec E, Larré S, Milo M, Rehman I, Rosario DJ (2009) Distinct microRNA alterations characterize high- and low-grade bladder cancer. Cancer research 69:8472-8481.
Chan B, Manley J, Lee J, Singh SR (2015) The emerging roles of microRNAs in cancer metabolism. Cancer letters 356:301-308.
Chen B, Li H, Zeng X, Yang P, Liu X, Zhao X, Liang S (2012) Roles of microRNA on cancer cell metabolism. J Transl Med 10:228.
Chen T, Huang Z, Wang L, Wang Y, Wu F, Meng S, Wang C (2009) MicroRNA-125a-5p partly regulates the inflammatory response, lipid uptake, and ORP9 expression in oxLDL-stimulated monocyte/macrophages. Cardiovascular research 83:131-139.
Choo LP, Mansfield J, Pizzi N, Somorjai R, Jackson M, Halliday W, Mantsch H (1995) Infrared spectra of human central nervous system tissue: Diagnosis of alzheimer's disease by multivariate analyses. Biospectroscopy 1:141-148.
Currie E, Schulze A, Zechner R, Walther TC, Farese RV (2013) Cellular fatty acid metabolism and cancer. Cell metabolism 18:153-161.
Cuvillier O, Pirianov G, Kleuser B, Vanek PG, Coso OA, Gutkind JS, Spiegel S (1996) Suppression of ceramide-mediated programmed cell death by sphingosine-1-phosphate.

Daefler S, Krueger G, Mödder B, Deliconstantinos G (1986) Cell membrane fluidity in chronic lymphocytic leukemia (CLL) lymphocytes and its relation to membrane receptor expression. Journal of experimental pathology 3**:**147-154.

Dang CV (2010) Rethinking the Warburg effect with Myc micromanaging glutamine metabolism. Cancer research 70**:**859-862.

Danzer K, Hobert H, Fischbacher C, Jagemann K-U (2013) Chemometrik: Grundlagen und Anwendungen, Springer-Verlag.

Davis-Dusenbery BN, Hata A (2010) Mechanisms of control of microRNA biogenesis. Journal of biochemistry 148**:**381-392.

Davis BN, Hilyard AC, Lagna G, Hata A (2008) SMAD proteins control DROSHA-mediated microRNA maturation. nature 454**:**56-61.

de Gonzalo-Calvo D, López-Vilaró L, Nasarre L, Perez-Olabarria M, Vázquez T, Escuin D, Badimon L, Barnadas A, Lerma E, Llorente-Cortés V (2015) Intratumor cholesteryl ester accumulation is associated with human breast cancer proliferation and aggressive potential: a molecular and clinicopathological study. BMC cancer 15**:**460.

Deo N, Somasundaran P (2002) Electron spin resonance study of phosphatidyl choline vesicles using 5-doxyl stearic acid. Colloids and Surfaces B: Biointerfaces 25**:**225-232.

Derenne A (2013) FTIR Spectra of Cancer Cells Exposed To Anticancer Drugs Reflect Their Cellular Mode of Action.

Derenne A, Gasper R, Goormaghtigh E (2011) The FTIR spectrum of prostate cancer cells allows the classification of anticancer drugs according to their mode of action. Analyst 136**:**1134-1141.

Derenne A, Vandersleyen O, Goormaghtigh E (2014) Lipid quantification method using FTIR spectroscopy applied on cancer cell extracts. Biochimica et Biophysica Acta (BBA)-Molecular and Cell Biology of Lipids 1841**:**1200-1209.

Di Giambattista L, Pozzi D, Grimaldi P, Gaudenzi S, Morrone S, Castellano AC (2011) New marker of tumor cell death revealed by ATR-FTIR spectroscopy. Analytical and bioanalytical chemistry 399**:**2771-2778.

Di Leva G, Garofalo M (2014) MicroRNAs in Solid Tumors, in MicroRNAs: Key Regulators of Oncogenesis, MicroRNAs: Key Regulators of Oncogenesis, pp 97-127, Springer.

Diem M, Boydston-White S, Chiriboga L (1999) Infrared spectroscopy of cells and tissues: shining light onto a novel subject. Applied Spectroscopy 53**:**148A-161A.

Diem M, Griffiths PR, Chalmers JM (2008) Vibrational spectroscopy for medical diagnosis, Wiley Chichester.

Dogan A, Siyakus G, Severcan F (2007) FTIR spectroscopic characterization of irradiated hazelnut (Corylus avellana L.). Food Chemistry 100**:**1106-1114.

Dória ML, Cotrim CZ, Simões C, Macedo B, Domingues P, Domingues MR, Helguero LA (2013) Lipidomic analysis of phospholipids from human mammary epithelial and breast cancer cell lines. Journal of cellular physiology 228**:**457-468.

Dreissig I, Machill S, Salzer R, Krafft C (2009) Quantification of brain lipids by FTIR spectroscopy and partial least squares regression. Spectrochimica Acta Part A: Molecular and Biomolecular Spectroscopy 71**:**2069-2075.

Ebert MS, Neilson JR, Sharp PA (2007) MicroRNA sponges: competitive inhibitors of small RNAs in mammalian cells. Nature methods 4**:**721-726.
Eichner LJ, Perry M-C, Dufour CR, Bertos N, Park M, St-Pierre J, Giguère V (2010) miR-378∗ mediates metabolic shift in breast cancer cells via the PGC-1β/ERRγ transcriptional pathway. Cell metabolism 12**:**352-361.
Erson A, Petty E (2008) MicroRNAs in development and disease. Clinical genetics 74**:**296-306.
Erson AE, Petty EM (2009) miRNAs and cancer: New research developments and potential clinical applications. Cancer biology & therapy 8**:**2317-2322.
Escribá PV, González-Ros JM, Goñi FM, Kinnunen PK, Vigh L, Sánchez-Magraner L, Fernández AM, Busquets X, Horváth I, Barceló-Coblijn G (2008) Membranes: a meeting point for lipids, proteins and therapies. Journal of cellular and molecular medicine 12**:**829-875.
Faber C, Horst D, Hlubek F, Kirchner T (2011) Overexpression of Dicer predicts poor survival in colorectal cancer. European Journal of Cancer 47**:**1414-1419.
Fang R, Xiao T, Fang Z, Sun Y, Li F, Gao Y, Feng Y, Li L, Wang Y, Liu X (2012) MicroRNA-143 (miR-143) regulates cancer glycolysis via targeting hexokinase 2 gene. Journal of Biological Chemistry 287**:**23227-23235.
Fei X, Qi M, Wu B, Song Y, Wang Y, Li T (2012) MicroRNA-195-5p suppresses glucose uptake and proliferation of human bladder cancer T24 cells by regulating GLUT3 expression. FEBS letters 586**:**392-397.
Ferracin M, Bassi C, Pedriali M, Pagotto S, D'Abundo L, Zagatti B, Corra F, Musa G, Callegari E, Lupini L, Volpato S, Querzoli P, Negrini M (2013) miR-125b targets erythropoietin and its receptor and their expression correlates with metastatic potential and ERBB2/HER2 expression. Molecular Cancer 12.
Flowers E, Froelicher ES, Aouizerat BE (2013) MicroRNA regulation of lipid metabolism. Metabolism 62**:**12-20.
Fukuda T, Yamagata K, Fujiyama S, Matsumoto T, Koshida I, Yoshimura K, Mihara M, Naitou M, Endoh H, Nakamura T (2007) DEAD-box RNA helicase subunits of the Drosha complex are required for processing of rRNA and a subset of microRNAs. Nature cell biology 9**:**604-611.
Gao P (2011) MicroRNAs and Cancer Metabolism, in MicroRNAs in Cancer Translational Research, MicroRNAs in Cancer Translational Research, pp 485-497, Springer.
Gao P, Tchernyshyov I, Chang T-C, Lee Y-S, Kita K, Ochi T, Zeller KI, De Marzo AM, Van Eyk JE, Mendell JT (2009) c-Myc suppression of miR-23a/b enhances mitochondrial glutaminase expression and glutamine metabolism. Nature 458**:**762-765.
Garzon R, Fabbri M, Cimmino A, Calin GA, Croce CM (2006) MicroRNA expression and function in cancer. Trends in molecular medicine 12**:**580-587.
Gasparri F, Muzio M (2003) Monitoring of apoptosis of HL60 cells by Fourier-transform infrared spectroscopy. Biochem. J 369**:**239-248.
Gasper R (2010) Infrared spectroscopy as a new tool for the screening of antitumoral agents inducing original therapeutic action.
Gasper R, Dewelle J, Kiss R, Mijatovic T, Goormaghtigh E (2009) IR spectroscopy as a new tool for evidencing antitumor drug signatures. Biochimica et Biophysica Acta (BBA)-Biomembranes 1788**:**1263-1270.

Gillies RJ, Robey I, Gatenby RA (2008) Causes and consequences of increased glucose metabolism of cancers. Journal of Nuclear Medicine 49:24S-42S.
Gonda K, Watanabe TM, Ohuchi N, Higuchi H (2010) In vivo nano-imaging of membrane dynamics in metastatic tumor cells using quantum dots. Journal of Biological Chemistry 285:2750-2757.
Goormaghtigh E, Raussens V, Ruysschaert J-M (1999) Attenuated total reflection infrared spectroscopy of proteins and lipids in biological membranes. Biochimica et Biophysica Acta (BBA)-Reviews on Biomembranes 1422:105-185.
Gorin A, Gabitova L, Astsaturov I (2012) Regulation of cholesterol biosynthesis and cancer signaling. Current opinion in pharmacology 12:710-716.
Gribbestad IS, Sitter B, Lundgren S, Krane J, Axelson D (1998) Metabolite composition in breast tumors examined by proton nuclear magnetic resonance spectroscopy. Anticancer research 19:1737-1746.
Griffiths J, Cady E, Edwards R, McCready V, Wilkie D, Wiltshaw E (1983) 31 P-NMR studies of a human tumour in situ. The Lancet 321:1435-1436.
Griffiths J, Stevens A, Iles R, Gordon R, Shaw D (1981) 31 P-NMR investigation of solid tumours in the living rat. Bioscience reports 1:319-325.
Guo H, Ingolia NT, Weissman JS, Bartel DP (2010) Mammalian microRNAs predominantly act to decrease target mRNA levels. Nature 466:835-840.
Guo S, Wang Y, Zhou D, Li Z (2014) Significantly increased monounsaturated lipids relative to polyunsaturated lipids in six types of cancer microenvironment are observed by mass spectrometry imaging. Scientific reports 4.
Guo X, Liao Q, Chen P, Li X, Xiong W, Ma J, Li X, Luo Z, Tang H, Deng M (2012) The microRNA-processing enzymes: Drosha and Dicer can predict prognosis of nasopharyngeal carcinoma. Journal of cancer research and clinical oncology 138:49-56.
Guo X, Wu Y, Hartley R (2009) MicroRNA-125a represses cell growth by targeting HuR in breast cancer. RNA biology 6:575-583.
Ha M, Kim VN (2014) Regulation of microRNA biogenesis. Nature reviews Molecular cell biology 15:509-524.
Han J, Pedersen JS, Kwon SC, Belair CD, Kim Y-K, Yeom K-H, Yang W-Y, Haussler D, Blelloch R, Kim VN (2009) Posttranscriptional crossregulation between Drosha and DGCR8. Cell 136:75-84.
Hanahan D, Weinberg RA (2011) Hallmarks of cancer: the next generation. cell 144:646-674.
Hedegaard M, Krafft C, Ditzel HJ, Johansen LE, Hassing S, Popp Jr (2010) Discriminating isogenic cancer cells and identifying altered unsaturated fatty acid content as associated with metastasis status, using k-means clustering and partial least squares-discriminant analysis of Raman maps. Analytical chemistry 82:2797-2802.
Hendrich A, Michalak K (2003) Lipids as a target for drugs modulating multidrug resistance of cancer cells. Current drug targets 4:23-30.
Heo I, Joo C, Cho J, Ha M, Han J, Kim VN (2008) Lin28 mediates the terminal uridylation of let-7 precursor MicroRNA. Molecular cell 32:276-284.
http://www.asdlib.org/onlineArticles/ecourseware/Analytical%20Chemistry%202.0/Text_Files.html. Available at:

http://www.asdlib.org/onlineArticles/ecourseware/Analytical%20Chemistry%202.0/Text_Files.html, Last accessed on October 2015.

http://www.food.imdea.org/blog/2015/microtargeting-cancer-metabolism-opening-new-therapeutic-windows-based-lipid-metabolism#sthash.6hpkQQIZ.dpuf). Available at: http://www.food.imdea.org/blog/2015/microtargeting-cancer-metabolism-opening-new-therapeutic-windows-based-lipid-metabolism#sthash.6hpkQQIZ.dpuf), Last accessed on October 2015.

http://www.proteinatlas.org/ENSG00000128059-PPAT/cancer. Available at: http://www.proteinatlas.org/ENSG00000128059-PPAT/cancer, Last accessed on October 2015.

http://zebu.uoregon.edu. Available at: http://zebu.uoregon.edu, Last accessed on Ocotber 2015.

Hu W, Chan CS, Wu R, Zhang C, Sun Y, Song JS, Tang LH, Levine AJ, Feng Z (2010) Negative regulation of tumor suppressor p53 by microRNA miR-504. Molecular cell 38**:**689-699.

Ide Y, Waki M, Hayasaka T, Nishio T, Morita Y, Tanaka H, Sasaki T, Koizumi K, Matsunuma R, Hosokawa Y (2013) Human breast cancer tissues contain abundant phosphatidylcholine (36**:** 1) with high stearoyl-CoA desaturase-1 expression.

Igal RA (2010) Stearoyl-CoA desaturase-1: a novel key player in the mechanisms of cell proliferation, programmed cell death and transformation to cancer. Carcinogenesis 31**:**1509-1515.

Iorio MV, Ferracin M, Liu CG, Veronese A, Spizzo R, Sabbioni S, Magri E, Pedriali M, Fabbri M, Campiglio M, Menard S, Palazzo JP, Rosenberg A, Musiani P, Volinia S, Nenci I, Calin GA, Querzoli P, Negrini M, Croce CM (2005) MicroRNA gene expression deregulation in human breast cancer. Cancer Research 65**:**7065-7070.

Jackowski S, Wang J, Baburina I (2000) Activity of the phosphatidylcholine biosynthetic pathway modulates the distribution of fatty acids into glycerolipids in proliferating cells. Biochimica et Biophysica Acta (BBA)-Molecular and Cell Biology of Lipids 1483**:**301-315.

Jackson M, Ramjiawan B, Hewko M, Mantsch HH (1998) Infrared microscopic functional group mapping and spectral clustering analysis of hypercholesterolemic rabbit liver. Cellular and molecular biology (Noisy-le-Grand, France) 44**:**89-98.

Jakymiw A, Patel RS, Deming N, Bhattacharyya I, Shah P, Lamont RJ, Stewart CM, Cohen DM, Chan EK (2010) Overexpression of dicer as a result of reduced let-7 MicroRNA levels contributes to increased cell proliferation of oral cancer cells. Genes, Chromosomes and Cancer 49**:**549-559.

Jiang S, Zhang LF, Zhang HW, Hu S, Lu MH, Liang S, Li B, Li Y, Li D, Wang ED (2012) A novel miR-155/miR-143 cascade controls glycolysis by regulating hexokinase 2 in breast cancer cells. The EMBO journal 31**:**1985-1998.

Johanning GL (1996) Modulation of breast cancer cell adhesion by unsaturated fatty acids. Nutrition 12**:**810-816.

Kasayama S, Koga M, Kouhara H, Sumitani S, Wada K, Kishimoto T, Sato B (1994) Unsaturated fatty acids are required for continuous proliferation of transformed androgen-dependent cells by fibroblast growth factor family proteins. Cancer research 54**:**6441-6445.

Kazarian S, Chan K (2006) Applications of ATR-FTIR spectroscopic imaging to biomedical samples. Biochimica et Biophysica Acta (BBA)-Biomembranes 1758:858-867.

Kim VN, Han J, Siomi MC (2009) Biogenesis of small RNAs in animals. Nature reviews Molecular cell biology 10:126-139.

Kinder CZ, JM Wessels R (1997) Gamma-irradiation and UV-C light-induced lipid peroxidation: a Fourier transform-infrared absorption spectroscopic study. International journal of radiation biology 71:561-571.

Krishnakumar N, Manoharan S, Palaniappan PR, Venkatachalam P, Manohar MA (2009) Chemopreventive efficacy of piperine in 7, 12-dimethyl benz [a] anthracene (DMBA)-induced hamster buccal pouch carcinogenesis: an FT-IR study. Food and chemical toxicology 47:2813-2820.

Krol J, Loedige I, Filipowicz W (2010) The widespread regulation of microRNA biogenesis, function and decay. Nature Reviews Genetics 11:597.

Lavine BK (2000) Chemometrics. Analytical Chemistry 72:91-98.

Le MT, Teh C, Shyh-Chang N, Xie H, Zhou B, Korzh V, Lodish HF, Lim B (2009) MicroRNA-125b is a novel negative regulator of p53. Genes & development 23:862-876.

Levin IW, Bhargava R (2005) Fourier Transform Infrared Vibrational Spectroscopic Imaging: Integrating Microscopy and Molecular Recognition. Annu. Rev. Phys. Chem. 56:429-474.

Li JN, Mahmoud MA, Han WF, Ripple M, Pizer ES (2000) Sterol regulatory element-binding protein-1 participates in the regulation of fatty acid synthase expression in colorectal neoplasia. Experimental cell research 261:159-165.

Li Z, Rana TM (2014) Therapeutic targeting of microRNAs: current status and future challenges. Nature reviews Drug discovery 13:622-638.

Liang L, Wong CM, Ying Q, Fan DNY, Huang S, Ding J, Yao J, Yan M, Li J, Yao M (2010) MicroRNA-125b suppressesed human liver cancer cell proliferation and metastasis by directly targeting oncogene LIN28B2. Hepatology 52:1731-1740.

Liu K-Z, Jackson M, Sowa MG, Ju H, Dixon IM, Mantsch HH (1996) Modification of the extracellular matrix following myocardial infarction monitored by FTIR spectroscopy. Biochimica et Biophysica Acta (BBA)-Molecular Basis of Disease 1315:73-77.

Liu W, Le A, Hancock C, Lane AN, Dang CV, Fan TW-M, Phang JM (2012) Reprogramming of proline and glutamine metabolism contributes to the proliferative and metabolic responses regulated by oncogenic transcription factor c-MYC. Proceedings of the National Academy of Sciences 109:8983-8988.

Luu W, Sharpe LJ, Gelissen IC, Brown AJ (2013) The role of signalling in cellular cholesterol homeostasis. IUBMB life 65:675-684.

Mantsch HH, Chapman D (1996) Infrared spectroscopy of biomolecules, Wiley-Liss.

Marcelli A, Cricenti A, Kwiatek WM, Petibois C (2012) Biological applications of synchrotron radiation infrared spectromicroscopy. Biotechnology advances 30:1390-1404.

Massart D, Vandeginste B, Deming S, Michotte Y, Kaufman L (2003) Evaluation of precision and accuracy. Comparison of two procedures. Chemometrics: a textbook. Elsevier Science, BV, Amsterdam, The Netherlands:33-57.

Mattson MP (2005) Membrane microdomain signaling: lipid rafts in biology and medicine, Springer Science & Business Media.
Moore DJ, Sills RH, Mendelsohn R (1997) Conformational order of specific phospholipids in human erythrocytes: correlations with changes in cell shape. Biochemistry 36**:**660-664.
Morisaki N, Sprecher H, Milo G, Cornwell D (1982) Fatty acid specificity in the inhibition of cell proliferation and its relationship to lipid peroxidation and prostaglandin biosynthesis. Lipids 17**:**893-899.
Mourant J, Yamada Y, Carpenter S, Dominique L, Freyer J (2003) FTIR spectroscopy demonstrates biochemical differences in mammalian cell cultures at different growth stages. Biophysical journal 85**:**1938-1947.
Movasaghi Z, Rehman S, ur Rehman DI (2008) Fourier transform infrared (FTIR) spectroscopy of biological tissues. Applied Spectroscopy Reviews 43**:**134-179.
Muralidhar B, Winder D, Murray M, Palmer R, Barbosa-Morais N, Saini H, Roberts I, Pett M, Coleman N (2011) Functional evidence that Drosha overexpression in cervical squamous cell carcinoma affects cell phenotype and microRNA profiles. The Journal of pathology 224**:**496-507.
Nagahashi M, Ramachandran S, Kim EY, Allegood JC, Rashid OM, Yamada A, Zhao R, Milstien S, Zhou H, Spiegel S (2012) Sphingosine-1-phosphate produced by sphingosine kinase 1 promotes breast cancer progression by stimulating angiogenesis and lymphangiogenesis. Cancer research 72**:**726-735.
Nara M, Okazaki M, Kagi H (2002) Infrared study of human serum very-low-density and low-density lipoproteins. Implication of esterified lipid C・O stretching bands for characterizing lipoproteins. Chemistry and physics of lipids 117**:**1-6.
Navarro A, Diaz T, Martinez A, Gaya A, Pons A, Gel B, Codony C, Ferrer G, Martinez C, Montserrat E (2009) Regulation of JAK2 by miR-135a: prognostic impact in classic Hodgkin lymphoma. Blood 114**:**2945-2951.
Nelson ER, Wardell SE, Jasper JS, Park S, Suchindran S, Howe MK, Carver NJ, Pillai RV, Sullivan PM, Sondhi V (2013) 27-Hydroxycholesterol links hypercholesterolemia and breast cancer pathophysiology. Science 342**:**1094-1098.
Nishida N, Mimori K, Fabbri M, Yokobori T, Sudo T, Tanaka F, Shibata K, Ishii H, Doki Y, Mori M (2011) MicroRNA-125a-5p is an independent prognostic factor in gastric cancer and inhibits the proliferation of human gastric cancer cells in combination with trastuzumab. Clinical Cancer Research 17**:**2725-2733.
Ogura R, Sugiyama M, Sakanashi T, Ninomiya T (1988) ESR Spin-labeling method of determining membrane fluidity in biological materials. Tissue culture cells, cardiac mtiochondria, erythrocytes and epidermal cells. The Kurume medical journal 35**:**171-182.
Ozek NS, Bal IB, Sara Y, Onur R, Severcan F (2014) Structural and functional characterization of simvastatin-induced myotoxicity in different skeletal muscles. Biochimica et Biophysica Acta (BBA)-General Subjects 1840**:**406-415.

Ozek NS, Tuna S, Erson-Bensan AE, Severcan F (2010) Characterization of microRNA-125b expression in MCF7 breast cancer cells by ATR-FTIR spectroscopy. Analyst 135**:**3094-3102.

Ozen M, Creighton C, Ozdemir M, Ittmann M (2008) Widespread deregulation of microRNA expression in human prostate cancer. Oncogene 27**:**1788-1793.

Ozsolak F, Poling LL, Wang Z, Liu H, Liu XS, Roeder RG, Zhang X, Song JS, Fisher DE (2008) Chromatin structure analyses identify miRNA promoters. Genes & development 22**:**3172-3183.

Papachristou DJ, Sklirou E, Corradi D, Grassani C, Kontogeorgakos V, Rao UN (2012) Immunohistochemical analysis of the endoribonucleases Drosha, Dicer and Ago2 in smooth muscle tumours of soft tissues. Histopathology 60**:**E28-E36.

Passon N, Gerometta A, Puppin C, Lavarone E, Puglisi F, Tell G, Di Loreto C, Damante G (2012) Expression of Dicer and Drosha in triple-negative breast cancer. Journal of clinical pathology**:**jclinpath-2011-200496.

Pichler M, Calin G (2015) MicroRNAs in cancer: from developmental genes in worms to their clinical application in patients. British journal of cancer 113**:**569-573.

Ramesh J, Argov S, Salman A, Yuzhelevski M, Sinelnikov I, Goldstein J, Erukhimovitch V, Mordechai S (2002) Spectroscopic evidence for site-specific cellular activity in the tubular gland in human intestine. European Biophysics Journal 30**:**612-616.

Ramu A, Glaubiger D, Magrath I, Joshi A (1983) Plasma membrane lipid structural order in doxorubicin-sensitive and-resistant P388 cells. Cancer research 43**:**5533-5537.

Rose DP, Connolly JM (1990) Effects of fatty acids and inhibitors of eicosanoid synthesis on the growth of a human breast cancer cell line in culture. Cancer research 50**:**7139-7144.

Rossi S, Giuntini A, Balzi M, Becciolini A, Martini G (1999) Nitroxides and malignant human tissues: electron spin resonance in colorectal neoplastic and healthy tissues. Biochimica et Biophysica Acta (BBA)-General Subjects 1472**:**1-12.

Rothschild SI (2014) microRNA therapies in cancer. Molecular and Cellular Therapies 2**:**7.

Rotllan N, Fernández-Hernando C (2012) MicroRNA regulation of cholesterol metabolism. Cholesterol 2012.

Ruckhäberle E, Rody A, Engels K, Gaetje R, von Minckwitz G, Schiffmann S, Grösch S, Geisslinger G, Holtrich U, Karn T (2008) Microarray analysis of altered sphingolipid metabolism reveals prognostic significance of sphingosine kinase 1 in breast cancer. Breast cancer research and treatment 112**:**41-52.

Rüdel S, Wang Y, Lenobel R, Körner R, Hsiao H-H, Urlaub H, Patel D, Meister G (2010) Phosphorylation of human Argonaute proteins affects small RNA binding. Nucleic acids research**:**gkq1032.

Sachdeva M, Zhu S, Wu F, Wu H, Walia V, Kumar S, Elble R, Watabe K, Mo Y-Y (2009) p53 represses c-Myc through induction of the tumor suppressor miR-145. Proceedings of the National Academy of Sciences 106**:**3207-3212.

Salman A, Argov S, Ramesh J, Goldstein J, Sinelnikov I, Guterman H, Mordechai S (2001) FTIR microscopic characterization of normal and malignant human colonic tissues. Cell. Mol. Biol 47**:**159-166.

Sand M, Gambichler T, Skrygan M, Sand D, Scola N, Altmeyer P, Bechara FG (2010) Expression levels of the microRNA processing enzymes Drosha and dicer in epithelial skin cancer. Cancer investigation 28**:**649-653.

Sand M, Skrygan M, Georgas D, Arenz C, Gambichler T, Sand D, Altmeyer P, Bechara FG (2012) Expression levels of the microRNA maturing microprocessor complex component DGCR8 and the RNA-induced silencing complex (RISC) components argonaute-1, argonaute-2, PACT, TARBP1, and TARBP2 in epithelial skin cancer. Molecular carcinogenesis 51**:**916-922.

Santini MT, Romano R, Rainaldi G, Filippini P, Bravo E, Porcu L, Motta A, Calcabrini A, Meschini S, Indovina PL (2001) The relationship between 1 H-NMR mobile lipid intensity and cholesterol in two human tumor multidrug resistant cell lines (MCF-7 and LoVo). Biochimica et Biophysica Acta (BBA)-Molecular and Cell Biology of Lipids 1531**:**111-131.

Santos CR, Schulze A (2012) Lipid metabolism in cancer. Febs Journal 279**:**2610-2623.

Schetter AJ, Okayama H, Harris CC (2012) The role of microRNAs in colorectal cancer. Cancer journal (Sudbury, Mass.) 18**:**244.

Scholl V, Hassan R, Zalcberg IR (2012) miRNA-451: A putative predictor marker of Imatinib therapy response in chronic myeloid leukemia. Leukemia research 36**:**119-121.

Scott GK, Goga A, Bhaumik D, Berger CE, Sullivan CS, Benz CC (2007) Coordinate suppression of ERBB2 and ERBB3 by enforced expression of micro-RNA miR-125a or miR-125b. Journal of Biological Chemistry 282**:**1479-1486.

Ségui B, Andrieu-Abadie N, Jaffrézou J-P, Benoist H, Levade T (2006) Sphingolipids as modulators of cancer cell death: potential therapeutic targets. Biochimica et Biophysica Acta (BBA)-Biomembranes 1758**:**2104-2120.

Sen I, Bozkurt O, Aras E, Heise S, Brockmann GA, Severcan F (2015) Lipid Profiles of Adipose and Muscle Tissues in Mouse Models of Juvenile Onset of Obesity Without High Fat Diet Induction: A Fourier Transform Infrared (FT-IR) Spectroscopic Study. Applied spectroscopy 69**:**679-688.

Severcan F (1997) Vitamin E decreases the order of the phospholipid model membranes in the gel phase: an FTIR study. Bioscience reports 17**:**231-235.

Severcan F, Bozkurt O, Gurbanov R, Gorgulu G (2010) FT-IR spectroscopy in diagnosis of diabetes in rat animal model. Journal of biophotonics 3**:**621-631.

Severcan F, Cannistraro S (1988) Direct electron spin resonance evidence for α-tocopherol-induced phase separation in model membranes. Chemistry and physics of lipids 47**:**129-133.

Severcan F, Cannistraro S (1990) A spin label ESR and saturation transfer ESR study of α-tocopherol containing model membranes. Chemistry and physics of lipids 53**:**17-26.

Severcan F, Gorgulu G, Gorgulu ST, Guray T (2005) Rapid monitoring of diabetes-induced lipid peroxidation by Fourier transform infrared spectroscopy: evidence from rat liver microsomal membranes. Analytical biochemistry 339**:**36-40.

Severcan F, Haris PI (2012) Vibrational spectroscopy in diagnosis and screening, IOS Press.

Shim H, Dolde C, Lewis BC, Wu C-S, Dang G, Jungmann RA, Dalla-Favera R, Dang CV (1997) c-Myc transactivation of LDH-A: implications for tumor

metabolism and growth. Proceedings of the National Academy of Sciences 94:6658-6663.
Siomi H, Siomi MC (2010) Posttranscriptional regulation of microRNA biogenesis in animals. Molecular cell 38:323-332.
Smith BC (1998) Infrared spectral interpretation: a systematic approach, CRC press.
Spector AA, Yorek MA (1985) Membrane lipid composition and cellular function. Journal of lipid research 26:1015-1035.
Stuart B (1997) Biological applications of infrared spectroscopy,, Wiley, UK
Sugito N, Ishiguro H, Kuwabara Y, Kimura M, Mitsui A, Kurehara H, Ando T, Mori R, Takashima N, Ogawa R (2006) RNASEN regulates cell proliferation and affects survival in esophageal cancer patients. Clinical cancer research 12:7322-7328.
Tanaka H, Sasayama T, Tanaka K, Nakamizo S, Nishihara M, Mizukawa K, Kohta M, Koyama J, Miyake S, Taniguchi M (2013) MicroRNA-183 upregulates HIF-1α by targeting isocitrate dehydrogenase 2 (IDH2) in glioma cells. Journal of neuro-oncology 111:273-283.
Taraboletti G, Perin L, Bottazzi B, Mantovani A, Giavazzi R, Salmona M (1989) Membrane fluidity affects tumor-cell motility, invasion and lung-colonizing potential. International Journal of Cancer 44:707-713.
Tchernitsa O, Kasajima A, Schäfer R, Kuban RJ, Ungethüm U, Györffy B, Neumann U, Simon E, Weichert W, Ebert M (2010) Systematic evaluation of the miRNA-ome and its downstream effects on mRNA expression identifies gastric cancer progression. The Journal of pathology 222:310-319.
Thomann H, Dalton LR, Dalton LA (1984) Biological applications of time domain ESR, in Biological magnetic resonance, Biological magnetic resonance, pp 143-186, Springer.
Thorsen SB, Obad S, Jensen NF, Stenvang J, Kauppinen S (2012) The therapeutic potential of microRNAs in cancer. The Cancer Journal 18:275-284.
Tili E, Michaille J-J, Luo Z, Volinia S, Rassenti LZ, Kipps TJ, Croce CM (2012) The down-regulation of miR-125b in chronic lymphocytic leukemias leads to metabolic adaptation of cells to a transformed state. Blood 120:2631-2638.
Tomasetti M, Neuzil J, Dong L (2014) MicroRNAs as regulators of mitochondrial function: role in cancer suppression. Biochimica et Biophysica Acta (BBA)-General Subjects 1840:1441-1453.
Torres A, Torres K, Paszkowski T, Jodłowska-Jędrych B, Radomański T, Książek A, Maciejewski R (2011) Major regulators of microRNAs biogenesis Dicer and Drosha are down-regulated in endometrial cancer. Tumor Biology 32:769-776.
Tsang H-c (2010) MicroRNA-125b inhibits tumorigenic properties of hepatocellular carcinoma cells through suppression of eukaryotic translationinitiation factor 5A2 (elF5A2). 香港大學學位論文:1-0.
Tuna S (2010) Functional Characterization of Microrna-125b Expression In MCF7 Breast Cancer Cell Line, in Series Functional Characterization of Microrna-125b Expression In MCF7 Breast Cancer Cell Line, Vol. MSc, Biology, Middle East Technical University.
Turker S, Ilbay G, Severcan M, Severcan F (2014a) Investigation of compositional, structural, and dynamical changes of pentylenetetrazol-induced seizures on a rat brain by FT-IR spectroscopy. Analytical chemistry 86:1395-1403.

Turker S, Severcan M, Ilbay G, Severcan F (2014b) Epileptic seizures induce structural and functional alterations on brain tissue membranes. Biochimica et Biophysica Acta (BBA)-Biomembranes 1838**:**3088-3096.
Vaksman O, Hetland TE, Trope CG, Reich R, Davidson B (2012) Argonaute, Dicer, and Drosha are up-regulated along tumor progression in serous ovarian carcinoma. Human pathology 43**:**2062-2069.
Vijayaraghavalu S, Peetla C, Lu S, Labhasetwar V (2012) Epigenetic modulation of the biophysical properties of drug-resistant cell lipids to restore drug transport and endocytic functions. Molecular pharmaceutics 9**:**2730-2742.
Vitols S, Gunvén P, Gruber A, Larsson O (1996) Expression of the low-density lipoprotein receptor, HMG-CoA reductase, and multidrug resistance (Mdr1) genes in colorectal carcinomas. Biochemical pharmacology 52**:**127-131.
Volinia S, Calin GA, Liu C-G, Ambs S, Cimmino A, Petrocca F, Visone R, Iorio M, Roldo C, Ferracin M (2006) A microRNA expression signature of human solid tumors defines cancer gene targets. Proceedings of the National academy of Sciences of the United States of America 103**:**2257-2261.
Vriens MR, Weng J, Suh I, Huynh N, Guerrero MA, Shen WT, Duh QY, Clark OH, Kebebew E (2012) MicroRNA expression profiling is a potential diagnostic tool for thyroid cancer. Cancer 118**:**3426-3432.
Wada T, Kikuchi J, Furukawa Y (2012) Histone deacetylase 1 enhances microRNA processing via deacetylation of DGCR8. EMBO reports 13**:**142-149.
Wang Q, Sanad W, Miller LM, Voigt A, Klingel K, Kandolf R, Stangl K, Baumann G (2005) Infrared imaging of compositional changes in inflammatory cardiomyopathy. Vibrational spectroscopy 38**:**217-222.
Wang V, Wu W (2009) MicroRNA-based therapeutics for cancer. BioDrugs 23**:**15-23.
Warburg O (1956) On the origin of cancer cells. Science 123**:**309-314.
Wen J, Friedman JR (2012) miR-122 regulates hepatic lipid metabolism and tumor suppression. The Journal of clinical investigation 122**:**2773-2776.
Wiggins JF, Ruffino L, Kelnar K, Omotola M, Patrawala L, Brown D, Bader AG (2010) Development of a lung cancer therapeutic based on the tumor suppressor microRNA-34. Cancer research 70**:**5923-5930.
Wu L, Belasco JG (2005) Micro-RNA regulation of the mammalian lin-28 gene during neuronal differentiation of embryonal carcinoma cells. Molecular and cellular biology 25**:**9198-9208.
www.microRNA.org. Available at: www.microRNA.org, Last accessed on October 2015.
www.targetscan.org. Available at: ww.targetscan.org, Last accessed on September 2015.
Xie B, Ding Q, Han H, Wu D (2013) miRCancer: a microRNA–cancer association database constructed by text mining on literature. Bioinformatics**:**btt014.
Yan M, Huang H-Y, Wang T, Wan Y, Cui S-D, Liu Z-z, Fan Q-X (2012) Dysregulated expression of dicer and drosha in breast cancer. Pathology & Oncology Research 18**:**343-348.
Yekta S, Shih I-h, Bartel DP (2004) MicroRNA-directed cleavage of HOXB8 mRNA. Science 304**:**594-596.
Yoon S, Lee M-Y, Park SW, Moon J-S, Koh Y-K, Ahn Y-H, Park B-W, Kim K-S (2007) Up-regulation of acetyl-CoA carboxylase α and fatty acid synthase by

human epidermal growth factor receptor 2 at the translational level in breast cancer cells. Journal of Biological Chemistry 282**:**26122-26131.

Zeisig R, Koklič T, Wiesner B, Fichtner I, Sentjurč M (2007) Increase in fluidity in the membrane of MT3 breast cancer cells correlates with enhanced cell adhesion in vitro and increased lung metastasis in NOD/SCID mice. Archives of biochemistry and biophysics 459**:**98-106.

Zeng Y, Sankala H, Zhang X, Graves P (2008) Phosphorylation of Argonaute 2 at serine-387 facilitates its localization to processing bodies. Biochem. J 413**:**429-436.

Zhang L, Huang J, Yang N, Greshock J, Megraw MS, Giannakakis A, Liang S, Naylor TL, Barchetti A, Ward MR (2006) microRNAs exhibit high frequency genomic alterations in human cancer. Proceedings of the National Academy of Sciences 103**:**9136-9141.

Zhang S-D, Ling L-Z, Zhang Q-F, Xu J-D, Cheng L (2015) Evolutionary Comparison of Two Combinatorial Regulators of SBP-Box Genes, MiR156 and MiR529, in Plants.

Zhang Y, Yan L-X, Wu Q-N, Du Z-M, Chen J, Liao D-Z, Huang M-Y, Hou J-H, Wu Q-L, Zeng M-S, Huang W-L, Zeng Y-X, Shao J-Y (2011) miR-125b Is Methylated and Functions as a Tumor Suppressor by Regulating the ETS1 Proto-oncogene in Human Invasive Breast Cancer. Cancer Research 71**:**3552-3562.

APPENDIX

A. IR spectra of pure lipids

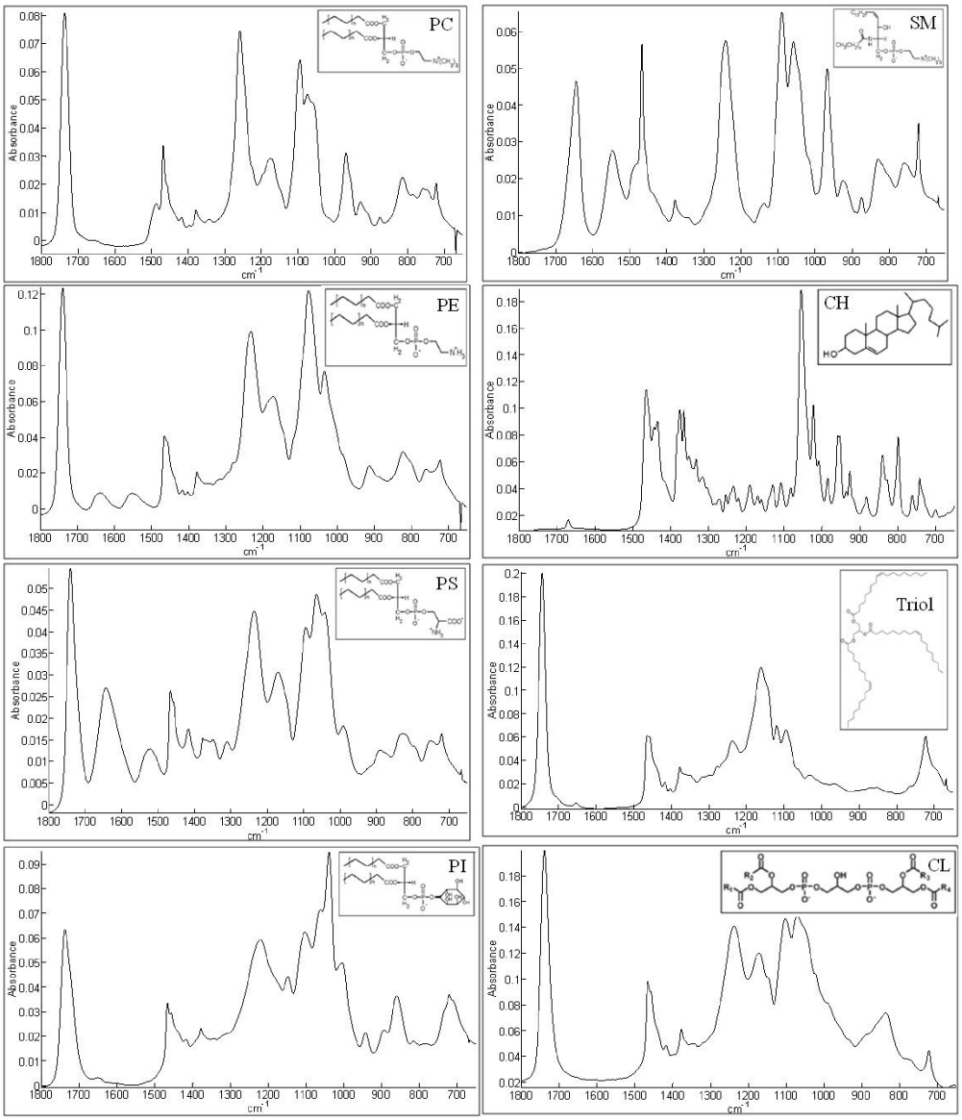

Figure A.1 IR spectra of pure lipids. Lipid structures are indicated in the top right corner of each box (Taken from Derenne 2013).

CURRICULUM VITAE

SURNAME NAME : ŞİMŞEK ÖZEK, Nihal

DATE OF BIRTH : Dec., 19, 1979

1. EDUCATION

HIGH SCHOOL 1997 Kanuni High School, Ankara, Turkey

BS 2001 Ankara University, Dept. of Biology Ankara, Turkey

MA 2007 Middle East Technical Univ. Ankara, Turkey,. Dept of Biological Sciences

PH.D 2007-2015 Middle East Technical Univ. Ankara, Turkey,. Dept. of Biological Sciences

2. SCHOLARSHIPS and AWARDS:

1. Graduation from High School with highest score.

2. Graduation from Ankara University with high honors (Cumulative Grade: 3.89 over 4)

3. ACADEMIC WORK

TEACHING ASSISTANT 2003- Middle East Technical Univ. Ankara, Turkey, Dept. of Biological Sciences

4. FIELDS OF ACADEMIC INTEREST

-Molecular Investigation of normal and pathological diseases such as cancer

-Drug-Tissue interactions

-Biological spectroscopy (FTIR, UV/Visible) and calorimetry in biological systems

- Molecular and Cellular Biophysics using biophysical techniques

- Interaction Between Biological Macromolecules

- Structure and Function of Biological Membranes

5. PUBLICATIONS

5.1. Book Chapters

Ozek NS, Afnan A., Bueno J., Mclaughlin G., Ralbovsky M., Sikirzhytskaya A., Sikirzhytski V., SevercanF,Lednev IK."Forensic Applications of Vibrational Spectroscopy on Screening and Characterization of Tissues"in Vibrational spectroscopy in diagnosis and screening" Eds: Severcan F and Haris PI, IOS press, 2012, PP:350-385, ISBN: 978-1-61499-058-1.

5.2. Articles in refereed (SCI) and other refereed Journals

Gurbanov, R., Simsek Ozek, N., Gozen, A. G., & Severcan, F. Quick Discrimination of Heavy Metal Resistant Bacterial Populations Using Infrared Spectroscopy coupled with Chemometrics. Analytical Chemistry, 2015

Elibol B., Ozek-Simsek N, Dogru E, Severcan M, Severcan F, Vitamin A Deficiency Induces Structural and Functional Alterations in the Molecular Constituents of the Rat Hippocampus, British Journal Nutrition, 113(1), 45-55, 2015

Ozek N.S., Bal B., Sara Y., Onur R, Severcan F, "Structural and functional characterization of simvastatin-induced myotoxicity in different skeletal muscles" Biochim. Biophysic. Acta, (General Subject) 1840, 406-415, 2014

Severcan F., Haris P., Aksoy C., Ozek NS., "Progress of Vibrational Spectroscopic Applications in Diagnosis and Screening". *Biomedical Spectroscopy and Imaging*, vol. 2, no. 1, pp. 73-81, 2013.

Ozek NS, Tuna S, Erson-Bensan AE, Severcan F., Characterization of microRNA-125b expression in MCF7 breast cancer cells by ATR-FTIR spectroscopy, Analyst, 135(12):3094-102, 2010.

Garip S, Yapici E, Ozek NS, Severcan M, Severcan F., Evaluation and discrimination of simvastatin-induced structural alterations in proteins of different rat tissues by FTIR spectroscopy and neural network analysis., Analyst, 135(12):3233-41, 2010.

Ozek NS, Sara Y, Onur R, Severcan F, Low dose Simvastatin induces compositional structural and dynamical changes on rat skeletal extensor digitorum longus muscle tissue, Bioscience Reports, 30 :41-50 2010

5.3. Articles in the Refereed Journals (Not covered by SCI), International Conference Proceeding and in Books

Severcan F, Ozek NS, Aksoy C.,Görgülü ST "Biomedical Applications of FTIR Spectroscopy", 14. National Meeting of Biomedical Engineering, BİYOMUT 2009, May 20-24, 2009, İzmir, Turkey, 6B1, 108.

5.4. Abstracts in refereed journals (SCI)

Severcan F., Simsek Ozek N., Gok S., "Fourier Transform Infrared Spectroscopy and Imaging in Cancer Diagnosis and Characterization", Biophysical Journal, 108(2), Supplement 1, p479a–480a, 2015.

Ozek, N S., Gok, S., Banerjee S., Severcan F. "FTIR microspectroscopic analysis of sodium butyrate induced differentiation in colon cancer cells in a time-dependent manner", Joint Annual Meeting of the ASPET/BPS at Experimental Biology, FASEB J., Volume: 27 Meeting Abstract: 1006.4 APR 2013.

Severcan F., Gocmen, S. U., Ozek, N. S. Severcan M., "Characterization of simvastatin-induced structural and functional alterations in the molecules of kidney brush border membrane by ATR-FTIR spectroscopy and chemometric approaches FASEB J. Volume: 27 Meeting Abstract: 1033.8 2013.

Ozek, N.S., Sade, A., Banerjee, S., Severcan F., "Characterization of Sodium Butyrate Induced Differentiation in Colon Cancer Cells by Fourier Transform Infrared Spectroscopy and Microscopy", 57th Annual Meeting of the Biophysical-Society, BIOPHYSICAL J.,Volume: 104 Issue: 2 Supplement: 1 Pages: 339A, 2013.

Ozgun K,Simsek Ozek N, Severcan M., Severcan F.," High Dose Simvastatin Administration induces changes in the structure and concentration of liver microsomal

membranes." Amino Acids, 2011 Vol: 41, Page: 26. 12th International Congress on Amino Acids, Peptides and Proteins, China.

Ozgun K., Ozek N.S., Severcan F., Determination of Simvastatin Induced Variations in Sciatic Nerve by ATR-FTIR Spectroscopy, ***Biophysical Journal***, Volume 96, Issue 3, Pages 312a-312a (2009)

Ozek N.S., Severcan F., Bal I.B., Esen E., Sara Y., Onur R., Yilmaz O., (2008) The Investigation of the Effects of Simvastatin on Rat Skeletal Muscle by Spectroscopic and Electrophysiological Techniques, Biophysical Society Meeting Abstracts, Biophysical Journal, Volume 94, Supplement, pp.290-291, Abstract, 856-Pos.

Ozek NS, Sara Y, Onur R, Severcan F.,The investigation of the possible effects of cholesterol reducing agent simvastatin on rat testis tissue, Biophysical Journal : 336A-336A Suppl. S JAN 2007

5.5. Presentations at International Meetings

Ozgun K, Simsek Ozek N, Severcan M., Severcan F High Dose Simvastatin Administration induces changes in the structure and concentration of liver microsomal membranes. 12th International Congress on Amino Acids, Peptides and Proteins, 2011, Abstract Book, page S26,1st - 5th August 2011, China, (Oral Presentation)

Garip S., Yapici E., Ozek N.S., Severcan M., Severcan F., Discrimination of simvastatin-induced structural alterations in proteins of different rat tissues by FTIR spectroscopy and neural network analysis, SPEC2010 "Shedding Light on Disease: Diagnostic Applications for the New Millennium" June 26-July 1, 2010, Manchester, UK, Abstract book, pp: 163. (Poster Presentation)

Simsek Ozek N., Tuna S., Erson A.E., Severcan F., "Characterization of microRNA-125b expression in MCF7 breast cancer cells determined by ATR-FTIR spectroscopy, SPEC2010 "Shedding Light on Disease: Diagnostic Applications for the New Millennium" June 26-July 1 2010, Manchester, UK, Abstract book, pp: 189 (Poster Presentation)

Bal İB, Esen E, Özek N, Sara Y, Yılmaz Ö, Severcan F, Onur R "Investigation of the Effects of Simvastatin on Rat Skeletal Muscle by Spectroscopic and Electrophysiological Techniques - Workshop on Drug Treatment of Psychiatric and NeurologicalDisorders" November , 26-29, 2007 - Bad Honnef, Germany . (Poster and Oral Presentation).

Simsek Ozek N., Ozgun K., Severcan M., Severcan F., "Application of FTIR Spectroscopy As A Novel Bioinformatic Method To Determine Simvastatin-Induced Protein Secondary Structure Alterations In Rat Liver Microsomal Membranes", 2nd International Biophysics Congress and Biotechnology at GAP & 21st National Biophysics Congress, October , 5-9 2009, Diyarbakır, Turkey, Abstract book, pp: 109-110 (Poster Presentation).

Simsek Ozek, N., Akhavan Tabasi, S., Erson, A.E., Severcan, F., "An ATR-FTIR Spectroscopy Analysis of Metastatic and Nonmetastatic Breast Cancer Cell Lines", 2nd International Biophysics Congress and Biotechnology at GAP & 21st National Biophysics Congress, October , 5-9 2009, Diyarbakır, Turkey, Abstract book, pp: 110 (Poster Presentation- Second Best Poster Award).

5.6. Presentations at National Meetings

Ozgun K, Simsek Ozek N, Severcan F. "Determination of High Dose Simvastatin Induced Variations in Rat Sciatic Nerve by ATR-FTIR Spectrosccopy" International Symposium On New Approaches in Cardiovascular Disorders: From Genes & Molecules To Clinical Applications Abstract Book, pp: 48, May, 4-8, 2011 Ankara, Turkey, (Poster Presentation).

Garip S., Yapici E., Simsek Ozek N., Severcan M., Severcan F., "Evaluation and discrimination of simvastatin-induced structural alterations in proteins of different rat tissues by FTIR spectroscopy and neural network analysis", International Symposium On New Approaches in Cardiovascular Disorders: From Genes & Molecules To Clinical Applications Abstract Book, pp:,50, May, 4-8, 2011 Ankara, Turkey, (Poster Presentation).

Simsek Ozek N., Bal I. B., Sara Y., Onur R., Severcan F., "Chronic Simvastatin Treatment induces functional and Structural Changes in a fiber type dependent manner in Rat Skeletal Muscles", International Symposium On New Approaches in Cardiovascular Disorders: From Genes & Molecules To Clinical Applications Abstract Book, pp:51, May, 4-8, 2011 Ankara, Turkey, (Poster Presentation).

Şimşek Özek N., Tuna S., Bensan Erson A.E., Severcan F. Characterization of microrna-125b expression in MCF7 cells by ATR-FTIR spectroscopy, 23rd International Biophysics Congress ,Abstract Book, pp:53, September , 13-16, 2011, Edirne, Turkey (Poster Presentation).

Ergun S., Ozek N. S., Severcan F., "Investigation of the Effects of Different Cooking Conditions on Chicken by ATR FTIR Spectroscopy at Molecular Level" XII. Spectroscopy Congress With International Participation, Abstract Book, pp:127 May 12-22, 2011, Antalya, Turkey, (Poster Presentation).

Çakmak, G. Togan İ, Şimşek Özek N, Severcan F, " Determination of nonylphenol induced Structural and Functional Changes in trout liver macromolecules by Fourier Transform Infrared (FTIR) Spectroscopy" 1st . National Palandöken Toxicology Symposium Abstract Book, pp:81 May, 28-30 2010,Erzurum, Turkey, (Poster Presentation).

Şimşek Özek N, Özgün K., Severcan M., Severcan F.,Determination of Simvastatin induced structural and contextual alterations in liver microsomal membrane proteins by FTIR Spectroscopy" Proteomics Workshop with International Participation, Abstract book pp:77,July, 12-17,2010, İstanbul,Turkey. (Poster Presentation).

Şimşek Özek N., Tabasi S.A., Erson A.E., Severcan F.,"Macromolecular Level Differences in Metastatic and Nonmetastatic Breast Cancer Cell Lines"., 3rd Muitidisiplinery Cancer Research Symposium, , No:9, March, 14-17, 2010, Uludağ, Bursa, Turkey (Oral Presentation).

Simsek Özek N, Severcan F, "Evaluation of the effects of Simvastatin on the protein conformation in different tissues", 20th National Biophysics Congress , Abstract book: pp:11, October, 22-25, 2008, Mersin, Turkey (Oral Presentation).

Özgün K., Simsek Özek N., Severcan F., Analysis of Simvastatin-induced moleculer alterations in rat sciatic nerve by ATR-FTIR Spectroscopy , 20th National Biophysics Congress, October, 22-25 2008, , Abstract book: pp:43 (Poster Presentation).

Özek N.Ş., Bal İ.B., Esen E., Sara Y., Onur R., Yilmaz Ö., Severcan F. "Investigation of the effects of simvastatin on different rat skeletal muscles by Spectroscopic and Electrophysiological methods,Simvastatinin Farklı Sıçan İskelet Kasları Üzerine Olan Etkilerinin Spektroskopik ve Elektrofizyolojik Yöntemlerle Araştırılması, 19th National Biophysics Congress, Abstract book: pp:61, September ,, . 5-7 2007, Konya, Turkey, (Poster Presentation).

Bal İB, Esen E, Özek N, Sara Y, Yılmaz Ö, Severcan F, Onur R - The effects of simvastatin on skeletal muscle - Turkish Society of Pharmacology,19th National Pharmacology Congress, October, 24-27,2007, Trabzon, Turkey, (Poster Presentation).

Simşek Özek N., Sara Y., Onur R., Severcan F. "Investigation of Possible Effects of Cholesterol-lowering drug, simvastatin, on testis by FTIR Spectroscopy" 18th National Biophysics Congress , Abstract book: pp:63, September , 6-9, 2006 Ankara, Turkey, (Poster Presentation)

5.7 Thesis

Ozek Simsek N. "The Molecular Investigation of the Effects of Cholesterol Reducing Drug-Simvastatin On Different Rat Skeletal Muscle Tissues" Middle East Technical University. Msc Thesis 2007.

One part of this thesis are reproduced from a published manuscript (Ozek et. al. 2010) with permission from the Royal Society of Chemistry

(Ozek NS, Tuna S, Erson-Bensan AE, Severcan F., Characterization of microRNA-125b expression in MCF7 breast cancer cells by ATR-FTIR spectroscopy, Analyst, 135(12):3094-102, 2010)